USGS
science for a changing world

Prepared in cooperation with Nisqually Indian Tribe, U.S. Fish and Wildlife Service, Billy Frank Jr. Nisqually National Wildlife Refuge, and Washington Department of Fish and Wildlife Estuary and Salmon Restoration Program

Assessment of Vulnerabilities and Opportunities to Restore Marsh Sediment Supply at Nisqually River Delta, West-Central Washington

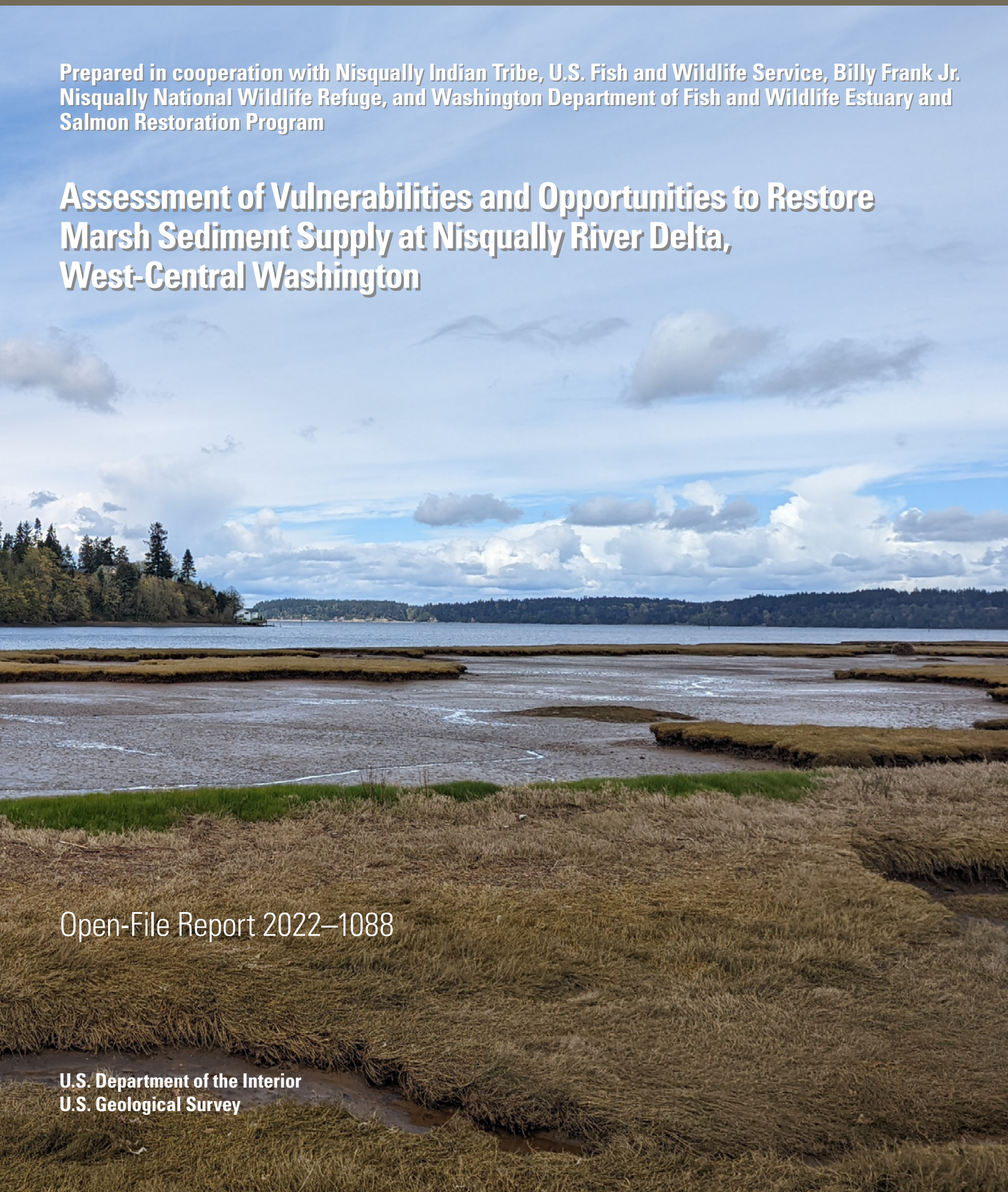

Open-File Report 2022–1088

U.S. Department of the Interior
U.S. Geological Survey

Cover. Photograph taken looking northwest from Nisqually Estuary Boardwalk Trail along McAllister Creek by Kathryn Pauls, used with permission.

Assessment of Vulnerabilities and Opportunities to Restore Marsh Sediment Supply at Nisqually River Delta, West-Central Washington

By Eric E. Grossman, Sean C. Crosby, Andrew W. Stevens, Daniel J. Nowacki, Nathan R. vanArendonk, and Christopher A. Curran

Prepared in cooperation with Nisqually Indian Tribe, U.S. Fish and Wildlife Service, Billy Frank Jr. Nisqually National Wildlife Refuge, and Washington Department of Fish and Wildlife Estuary and Salmon Restoration Program

Open-File Report 2022–1088

U.S. Department of the Interior
U.S. Geological Survey

U.S. Geological Survey, Reston, Virginia: 2022

Suggested citation:
Grossman, E.E., Crosby, S.C., Stevens, A.W., Nowacki, D.J., vanAredonk, N.R., and Curran, C.A., 2022, Assessment of vulnerabilities and opportunities to restore marsh sediment supply at Nisqually River Delta, west-central Washington: U.S. Geological Survey Open-File Report 2022–1088, 50 p., https://doi.org/10.3133/ofr20221088.

Associated data for this publication:
Tyler, D.J., Danielson, J.J., Grossman, E.E., and Hockenberry, R.J., 2020, Topobathymetric Model of Puget Sound, Washington, 1887 to 2017: U.S. Geological Survey data release, https://doi.org/10.5066/P95N6CIT.

Opatz, C.C., Curran, C.A., Tecca, A.E., and Grossman, E.E., 2019, Stage, water velocity and water quality data collected in the Lower Nisqually River, McAllister Creek and tidal channels of the Nisqually River Delta, Thurston County, Washington, February 11, 2016 to September 18, 2017 (ver. 1.1, December, 2019): U.S. Geological Survey data release, https://doi.org/10.5066/F7GF0SG7.

ISSN 2331-1258 (online)

Acknowledgments

This study was funded by the Washington Department of Fish and Wildlife Estuary and Salmon Restoration Program and the U.S. Geological Survey (USGS) Coastal and Marine Hazards and Resource Program as part of the Coastal Habitats in Puget Sound Project. This effort benefitted from numerous discussions with the Nisqually Indian Tribe, U.S. Fish and Wildlife Service, and Estuary and Salmon Restoration Program about estuary information needs and lessons learned from the decades of planning and initial implementation of estuary restoration in the Nisqually River Delta. We thank Edwin Elias of Deltares-USA and Guy Gelfenbaum (USGS) for their guidance on the project, and we would like to also thank Stefan R.P.M. Pluis of Utrecht University in the Netherlands for his efforts in helping to configure and carry out exploratory schematized model simulations as part of an internship with USGS. We acknowledge Chad Opatz of the USGS Washington Water Science Center and Dan Hull of the Nisqually Reach Nature Center for their help in the field, often during inclement weather along with the logistical and student assistantship support of the Geology Department of Western Washington University. This study benefitted from constructive peer reviews by Li Erikson and Kai Parker.

Contents

Figures

Tables

Conversion Factors

International System of Units to U.S. customary units

Multiply	By	To obtain
	Length	
centimeter (cm)	0.3937	inch (in.)
centimeter per year (cm/yr)	0.3937	inch per year (in/yr)
millimeter (mm)	0.03937	inch (in.)
millimeter per year (mm/yr)	0.03937	inch per year (in/yr)
meter (m)	3.281	foot (ft)
meter per year	3.281	foot per year (ft/yr)
kilometer (km)	0.6214	mile (mi)
	Area	
square meter (m^2)	0.0002471	acre
hectare (ha)	2.471	acre
square kilometer (km^2)	0.3861	square mile (mi^2)
	Volume	
cubic meter (m^3)	264.2	gallon (gal)
cubic meter (m^3)	35.31	cubic foot (ft^3)
	Flow rate	
cubic meter per year (m^3/yr)	0.000811	acre-foot per year (acre-ft/yr)
meter per second (m/s)	3.281	foot per second (ft/s)
meter per day (m/d)	3.281	foot per day (ft/d)
meter per year (m/yr)	3.281	foot per year ft/yr)
cubic meter per second (m^3/s)	35.31	cubic foot per second (ft^3/s)
	Mass	
gram (g)	0.03527	ounce, avoirdupois (oz)
kilogram (kg)	2.205	pound avoirdupois (lb)
metric ton (t)	1.102	ton, short [2,000 lb]
metric ton (t)	0.9842	ton, long [2,240 lb]
	Density	
kilogram per cubic meter (kg/m^3)	0.06242	pound per cubic foot (lb/ft^3)

Datum

Vertical coordinate information is referenced to the North American Vertical Datum of 1988 (NAVD 88).

Horizontal coordinate information is referenced to the North American Datum of 1983 (NAD 83).

Elevation, as used in this report, refers to distance above the vertical datum.

Abbreviations

ADVM	acoustic Doppler velocity meter
ADCP	acoustic Doppler current profiler
EPA	U.S. Environmental Protection Agency
ESRP	Estuary and Salmon Restoration Program
HRDPS	high resolution deterministic prediction system
IS	initial sediment on the bed
NEP	National Estuary Program
NIS	no sediment on the bed
NNWR	Billy Frank Jr. Nisqually National Wildlife Refuge
NOAA	National Oceanic and Atmospheric Administration
NWIS	National Water Information System
PSNERP	Puget Sound Nearshore Ecosystem Restoration Project
PSP	Puget Sound Partnership
RMSE-br	bias-removed root mean square error
SSC	suspended-sediment concentration
SSL	suspended-sediment load
USFWS	U.S. Fish and Wildlife Service
USGS	U.S. Geological Survey
WDFW	Washington Department of Fish and Wildlife

Assessment of Vulnerabilities and Opportunities to Restore Marsh Sediment Supply at Nisqually River Delta, West-Central Washington

By Eric E. Grossman, Sean C. Crosby, Andrew W. Stevens, Daniel J. Nowacki, Nathan R. vanArendonk, and Christopher A. Curran

Abstract

A cascading set of hazards to coastal environments is intimately tied to sediment transport and includes the flooding and erosion of shorelines and habitats that support communities, industry, infrastructure, and ecosystem functions (for example, habitats critical to fisheries). This report summarizes modeling and measurement data used to evaluate the sediment budget of the Nisqually River Delta, the vulnerability of the largest estuary restoration project in Puget Sound at the Billy Frank Jr. Nisqually National Wildlife Refuge, and the role of coastal hydrodynamics and potential restoration alternatives for recovering sediment delivery to its marshes. The 2009 Brown's Farm Restoration area reconnected tidal connectivity to 308 hectares of historical wetlands that had been modified for grazing since the mid-1800s. The restoration achieved many goals toward recovering salmon habitat, but understanding of the delta and restoration area sediment budgets remain poorly quantified. Specifically, quantitative estimates of the amount of sediment delivered to the delta and restored marsh areas, which had subsided in response to historical diking and draining for grazing, were identified as important information needs. Forecasts of potential outcomes of proposed adaptive distributary channel restoration actions were also prioritized to inform potential solutions. These estimates can be used to evaluate whether sufficient sediment is available for marsh recovery downstream from Alder Lake, which traps the majority of the Nisqually River sediment load. Additionally, quantitative sediment information was identified to help prioritize opportunities to recover and maintain the area marshes and guide ecosystem restoration investments across the delta to reduce the vulnerability of the system to drowning under projected sea level rise.

A coupled, numerical hydrodynamic-sediment transport model and measurements of the sediment load just upstream from the delta were used to evaluate the (1) availability of sediment for marsh recovery, (2) sediment transport dynamics across the estuary, and (3) potential outcomes of distributary reconnection alternatives under existing and projected conditions of streamflow and sea level. The sediment load reaching the Nisqually River Delta downstream from Alder Lake was insufficient to recover subsided grade and restore the area marshes. Alder Lake traps about 90 percent of the Nisqually River sediment load before reaching the delta. With only 10 percent of the Nisqually River sediment load available, recovery of subsided grade and marshes would require about 20 years if the entire load reaching the delta was routed into and retained within the Brown's Farm Restoration area. Modeling and measurements indicated that the volume of fluvial sediment load reaching and accumulating in the restoration area ranges from 7 to 32 percent and identified that restoration alternatives could recover about an additional 10–12 percent under current and projected sea-level rise by the year 2100. At these rates of sediment delivery, 85–200+ years may be required to fill the subsided grade required for marsh vegetation development and maintenance, leaving the system vulnerable to projected rates of sea-level rise.

The model reveals the sensitivity of sediment transport and accumulation to sediment properties, hydrodynamics, and wave conditions. The low sediment accumulation in the restoration area results from relatively low sediment delivery and retention relative to large fluxes into and out of the restored system. The model indicates that fluxes of sediment into and out of the restoration area, particularly during high streamflows when fluvial sediment delivery is high and during storms and waves that lead to resuspension of bed material can lead to more transport offshore than accumulation. The findings have implications for siting, phasing, and implementing strategies to route and retain sediment. This study shows that opportunities to recover sediment higher in the tidal prism, where a greater hydraulic gradient and gravity could promote progradation and greater sediment retention, may be more effective than alternatives lower in the tidal prism implemented to date and assessed in this study. Furthermore, the modeling indicates that distributary channel restoration also may provide additional benefits to society by reducing flood stage, and therefore, flood hazards surrounding the delta.

Introduction

Problem Statement

Extensive historical degradation and coastal change threaten coastal habitats, biodiversity, and ecosystem services important to fisheries, people, and flood protection (Barnosky and others, 2012; Steffen and others, 2015). Considerable time (for example, decades), capital expenditure, and innovative environmental engineering projects are required to recover estuary and salmon habitat across our Nation's shorelines, including Puget Sound, where an estimated 80–90 percent loss of estuaries has occurred since the mid-1800s (Bortleson and others, 1980; Fresh and others, 2011; Simensted and others, 2011). In 2009, more than 6 kilometers (km) of dikes and levees were lowered and removed to return tidal connectivity to 308 hectares (ha) of the Nisqually River Delta as part of the Billy Frank Jr. Nisqually National Wildlife Refuge (NNWR) Brown's Farm Restoration area (fig. 1). The 2009 restoration was the largest estuary restoration projects in the Pacific Northwest and, along with earlier phases of restoration in 1996, represented an important investment toward Puget Sound salmon habitat recovery (Ellings and others, 2016). Although several estuarine habitat recovery goals were achieved with the 2009 restoration, a remaining concern is whether there is sufficient sediment flux to recover the area's tidal marshes that experienced 1–2 meters (m) of subsidence during use for grazing and that remain devoid of vegetation (Ellings and others, 2016).

Ensuring estuary restoration success and resilience is limited by poor understanding of and ability to predict changes in hydrodynamics and sediment transport associated with Earth-surface processes, land-use activities, and climate change. Numerical hydrodynamic and sediment transport models provide managers with quantitative estimates of sediment availability, routing, and accumulation to better evaluate restoration strategies, measure outcomes and performance, and adaptively manage. Although the quantity of sediment needed for shorelines and marshes to keep pace with sea-level rise can be estimated with moderate confidence, the ability to predict the routing, retention, and composition of sediment to achieve ecological functions is limited. Our limited understand is in large part due to considerable variability and uncertainty in how sediment supply rate, sediment properties, bed composition and land use, including restoration, affect estuarine hydrodynamics and sediment transport processes. Additional data and numerical models help to evaluate and constrain these uncertainties and provide tools to evaluate strategies for habitat restoration actions and impending sea-level rise, climate, and land-use change.

This report summarizes the collaborative study "Restoring Sediment Supply to Sustain Delta Marsh" undertaken by the U.S. Geological Survey (USGS) in collaboration with Nisqually Indian Tribe, U.S. Fish and Wildlife Service (USFWS), and Washington Department of Fish and Wildlife (WDFW) Estuary and Salmon Restoration Program (ESRP). Measurements and modeling were used to assess the existing sediment budget and transport dynamics of the Nisqually River Delta. Additionally,

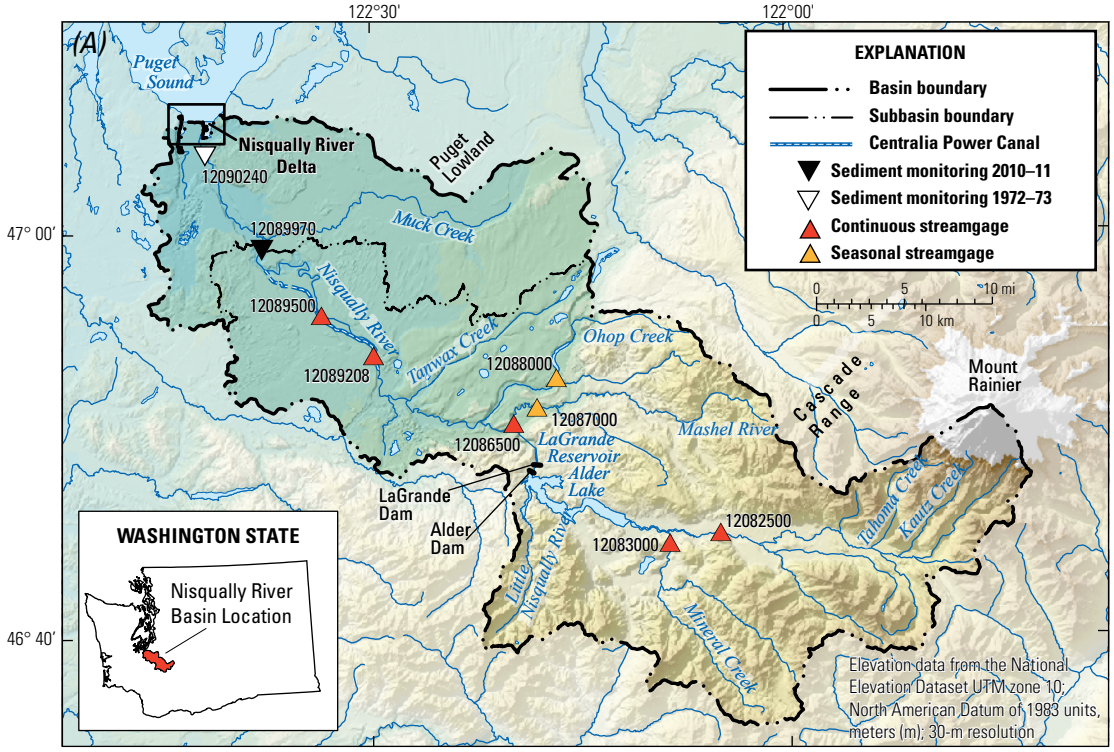

Figure 1 (pages 2 and 3). Maps showing location of the Nisqually River Delta and U.S. Geological Survey streamgages in the Nisqually River drainage basin (*A*) and estuary restoration project in the delta and Billy Frank Jr. Nisqually National Wildlife Refuge (*B*), west-central Washington. km, kilometer.

the model was used to evaluate the capacity of identified adaptive management measures to recover additional sediment supply, accounting for projected changes in streamflow and sea level. Distributary restoration design elements, including the extent of levee breaching to the channel bottom, channel depth and slope, and connectivity to fluvial and tidal processes, were evaluated to test their importance for conveying sediment. The potential for distributary channel restoration to route flood waters and reduce flood stage was examined. These results are important to establishing the extent, siting, and potential phasing of estuary channel restoration projects to achieve ecosystem recovery goals, multiple societal benefits (for example, flood exposure mitigation), especially where opportunities are constrained by competing land use and infrastructure. The knowledge gained and tools developed inform identified estuary restoration information needs to support ecosystem recovery decisions across our Nation's coasts and estuaries (U.S. Environmental Protection Agency, 2005).

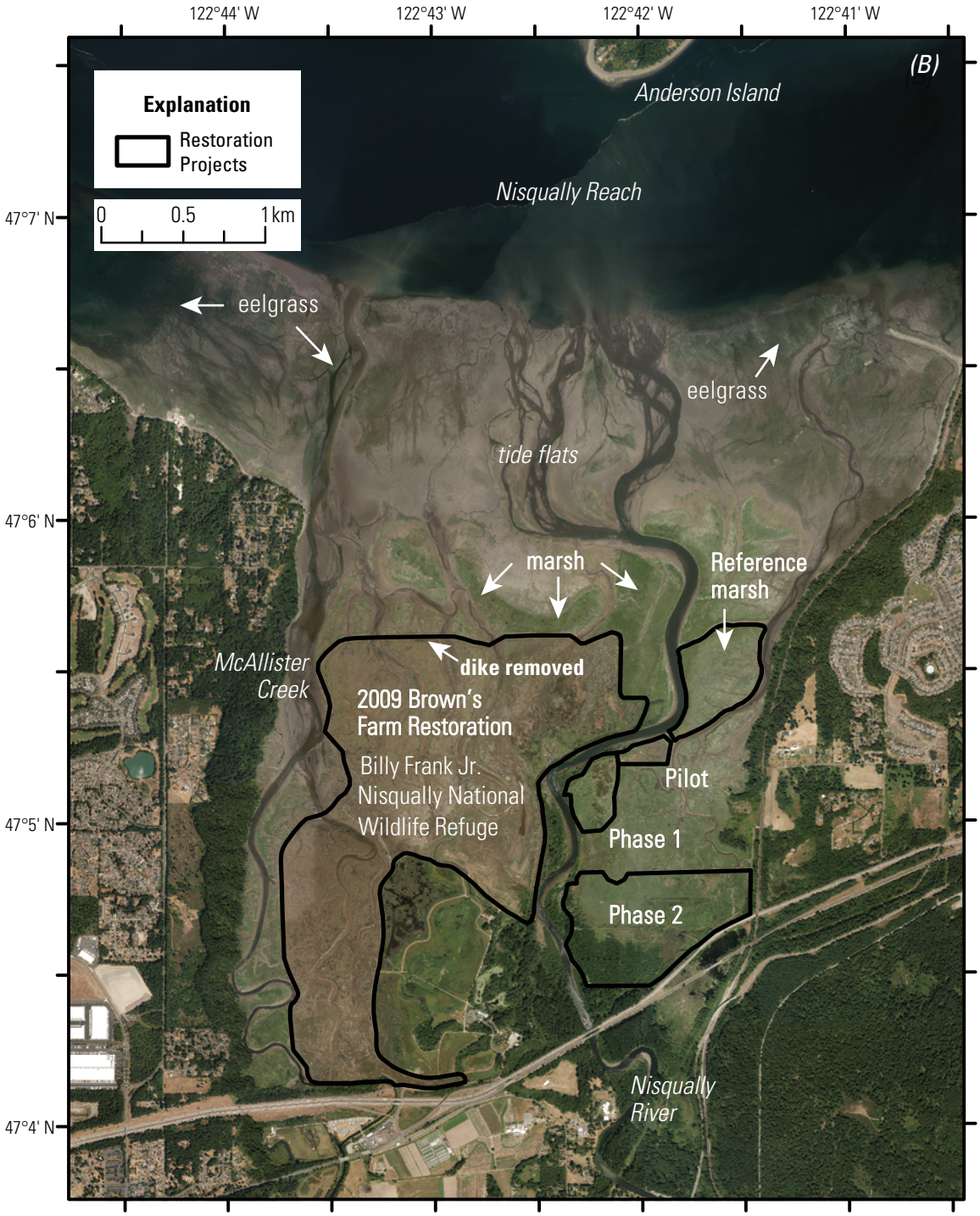

Figure 1.—Continued

Setting

The Nisqually River Delta is fed by the regulated portion of the Nisqually River downstream from Alder and La Grande Dams (fig. 1). The Nisqually River drains more than 800 square kilometers (km^2) of drainage basin area, including the partially glaciated flanks of the Cascade Range and volcanic complex of Mount Rainier, as well as the Puget Lowland composed of Pleistocene glacial till deposits and Holocene alluvium (Porter and Swanson, 1998; Collins and Montgomery, 2011). The Nisqually River Delta is formed in a drowned and filled river valley (Barnhardt and Sherrod, 2006) and is characterized by a low-sloping, about 4 km long, estuary and 1.5 km tidal flat that abruptly descends a steeply sloping delta front to 90–100 m depths in the Nisqually Reach of south Puget Sound. The area is a mesotidal environment with a mean tide range of 2.5 m and a great diurnal range of 3.5 m. It is subject to strong tidal currents and wind waves ranging 0.5–1.5 m during high wind events.

Large areas of the Nisqually River Delta wetlands were modified for agriculture beginning in the middle 1800s. Levees and dikes were constructed to restrict tidal connectivity and enable grazing. The loss of sediment delivery from the river and littoral cell, along with natural compaction from both natural processes and grazing, led to extensive subsidence relative to adjacent coastal lands outside the levees (fig. 2). In 1974, the USFWS acquired and established the Billy Frank Jr. Nisqually National Wildlife Refuge (NNWR). Since 1996, the Nisqually Indian Tribe and NNWR have restored tidal circulation to approximately 365 ha of historical estuary habitat through multiple dike and levee removal projects, the most recent consisting of the 308 ha Brown's Farm Restoration area in 2009 (Ellings and others, 2016).

Previous Work

Previous studies conducted to quantify the sediment budget of the Nisqually River Delta included estimates of the fluvial sediment load, the sedimentologic characterization of the delta and a modeling study to inform the 2009 Brown's Farm Restoration area. A comprehensive geomorphic assessment of the Nisqually River estimated that 90 percent of the sediment moving downstream has been trapped in Alder Lake since the construction of the dams in 1945, leaving about 10 percent of the total load reaching the delta (Czuba and others, 2011, 2012). A detailed study for 2010–11 indicated that the sediment load downstream from the USGS streamgage at McKenna ranged from 105,000 to 120,000 metric tons of sediment (Curran and others, 2016a) in agreement with a mean annual load of 100,000–120,000 metric tons estimated in the 1970s (Nelson, 1974). A sediment transport modeling study in 1999 conducted to assess potential outcomes of the then-proposed Brown's Farm Restoration area concluded that full tidal inundation would result with removal of the outer ring dike (ENSR International, 1999). The 1999 model indicated limited potential for sediment delivery under mean daily streamflow but sufficient to recover the system, citing more than 3 centimeters (cm) of potential accretion across the estuary under the 1996 flood of record (an extreme—about100-year event). That model evaluated potential sediment transport accounting for streamflow, sediment load, and tides but did not evaluate coastal processes like winds and waves that contribute to estuary sediment availability and exchange (Nowacki and Grossman, 2020).

Project Scope and Objectives

To address the growing need to restore and enhance estuary and tidal marsh ecosystems in the Nisqually River Delta and more generally across our Nation's coasts, the USGS, Nisqually Indian Tribe, and USFWS proposed a comprehensive study to evaluate the sediment supply and opportunities to recover additional sediment delivery to the Nisqually River Delta's vulnerable tidal marshes. The principal project goals were to (1) characterize the hydrodynamics and sediment transport processes that influence sediment delivery and (2) assess adaptive management strategies aimed to recover sediment to areas of concern. A process-based sediment transport model was identified as a priority to evaluate the sediment transport dynamics today and inform potential alternatives to recover additional sediment in the future. For this study, a numerical hydrodynamic/sediment transport model was developed, validated with local observations, and applied to examine the interactions of streamflow, tidal circulation, waves, and sediment-transport dynamics. The model also was used to evaluate potential outcomes of identified restoration alternatives, their performance under sea-level rise and their capacity to reduce flood hazards.

Research objectives included evaluating the sediment budget between Alder Lake and the Nisqually River Delta, the fraction that is transported to the 2009 restoration area, and the extent that additional sediment could be routed to the subsided marshes under current conditions and future scenarios including projected sea-level rise and increases in streamflow. Secondary objectives included evaluating the extent to which restoration could help reduce flood hazards by redirecting flood waters. An additional goal was to describe how findings of the study relate to or may inform similar large capital expenditures in estuary restoration elsewhere in the Pacific Northwest to better achieve ecosystem function and resilience.

The study set out to test the following hypotheses through the stated analyses:

1. Sediment transported by the Nisqually River downstream from the Alder Lake is sufficient to recover the delta's marshes if more is routed to them.
    - This study evaluated the fluvial sediment load of the Nisqually River reaching the delta and the proportion of that sediment that accumulates in the delta and restored estuary today, and also with potential changes under projected sea-level rise and identified restoration alternatives.
2. Delivery of sand is important to regain 1–2 m of subsided grade and promote vegetation succession at rates comparable to sea-level rise.
    - The fractions of sand and mud available and transported were evaluated to assess the recovery time required to fill subsided grade and establish mash vegetation.

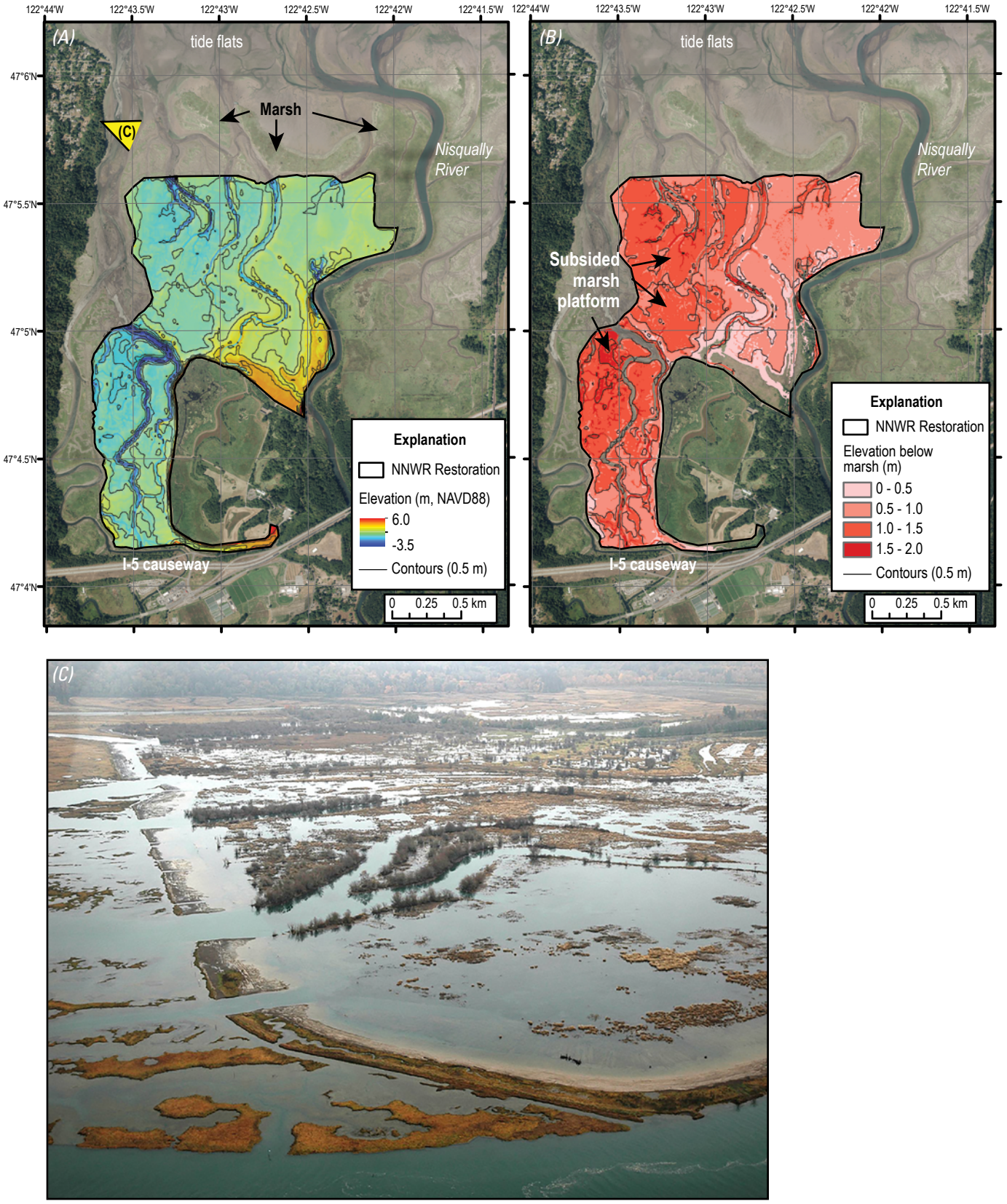

Figure 2. Maps showing elevation in meters (m) above North American Vertical Datum of 1988 (NAVD88) (*A*) and distribution of subsided areas in the 2009 Billy Frank Jr. Nisqually National Wildlife Refuge (NNRW) Brown's Farm Restoration area relative to the predominant marsh elevation of 3 meters (*B*), west-central Washington. Photograph of the dike and channel modifications along the northern restoration boundary (*C*), view shown in *A*, courtesy of Steve Liske, Ducks Unlimited, 2009. km, kilometer.

3. Full breaching of distributaries to streambed elevations rather than partial notching is required for sufficient sediment delivery to marshes.

    - The variability in sediment composition and processes contributing to sediment transport (for example, fluvial, circulation, waves) were evaluated to inform potential outcomes of distributary reconnection alternatives (for example, full breach versus partial notch).

4. Distributary restoration may benefit flood management by reducing flood risk and increasing resilience to projected climate change.

    - Many Pacific Northwest estuaries have lost historical distributaries, so the potential for habitat restoration to reduce flood hazards surrounding the project was evaluated for existing conditions and increased system resilience under climate change projections relevant to many Pacific Northwest systems where flood exposure is high and expected to increase.

5. Distributary channel and marsh restoration can benefit from more strategic siting, phasing, and designing to achieve desired outcomes.

    - The information gained from this study provides insight into how and why additional siting, phasing, and designing criteria that better account for the geomorphic context of restoration actions can achieve outcomes more effectively.

Programmatically, these activities address identified priorities among the U.S. Environmental Protection Agency (EPA) National Estuary Program (NEP) and Puget Sound Partnership (PSP), exemplified by the Puget Sound Nearshore Ecosystem Restoration Project (PSNERP) goals. These priorities include (1) quantifying sediment budgets in Nisqually River Delta systems, (2) characterizing how hydrodynamics that shape habitat and connectivity are structured today and likely to change under climate and land-use scenarios, and (3) evaluating levee breach and distributary restoration siting, designing, and phasing criteria to achieve desired outcomes. The data, models, and findings generated provide important information, tools, and a framework for informing floodplain and estuary restoration programs like the WDFW Estuary and Salmon Restoration Program, Salmon Restoration Board, Floodplains by Design, and EPA-NEP.

Methods

Study Design

The goals and application of the numerical hydrodynamic and sediment transport model were defined through an initial partner meeting in December 2016 and in response to lessons learned through research and monitoring of the initial 5-year response of Nisqually River Delta to the 2009 Brown's Farm Restoration area as summarized in Ellings and others (2016). Information needs, data availability, technical approaches, and desired outcomes identified in the partner meeting were synthesized from input of Nisqually Indian Tribe, U.S. Fish and Wildlife Service (USFWS), Billy Frank Jr. Nisqually National Wildlife Refuge (NNWR), Washington Department of Fish and Wildlife (WDFW), Estuary and Salmon Restoration Program (ESRP), and U.S. Geological Survey (USGS).

The partner meeting identified several objectives to improve understanding of sediment routing today and to assess the potential feasibility and benefits of distributary restoration alternatives. The team prioritized measuring and modeling water and sediment transport through the lower river and five principal tidal channels connecting the river to the restoration area (sites D1–D4, McAllister Creek, fig. 3) and modeling three identified adaptive management alternatives along the lower left bank for the Nisqually River (site NR2). The location and designs of the channel reconnections immediately southeast of the new "inner" ring dike built in 2009 balanced concerns for recovering sediment and protecting the remaining NNWR freshwater habitats and infrastructure. The results would help answer whether sufficient sediment exists downstream from Alder Lake and whether it can be routed efficiently to the delta marshes prior to evaluating more costly opportunities to reconnect historical distributaries upstream and through the Interstate 5 (I-5) causeway (fig. 3). Secondary outcomes of the research aimed to evaluate the performance and resilience of the alternatives and potential benefits or unforeseen feedbacks of distributary restoration actions.

Hydrodynamic and Sediment Measurements

Continuous Sampling

Continuous time-series data were collected with underwater autonomous-data logging instruments deployed at 10 sites (table 1) along the lower Nisqually River (NR1, NR2, NR3), at each of the four distributary inlets of the 2009 restored tidal marshes (D1, D2, D3, D4), and along McAllister Creek (MC1, MC2, MC3) (fig. 3). Instrument packages included acoustic Doppler current profilers (ADCP), turbidity sensors, and conductivity-temperature-depth (CTD) sensors that sampled water levels, current speeds and directions, turbidity, and water temperature and salinity at 15-min intervals. Water levels and current velocity/direction profiles were collected with either upward- or side-looking acoustic Doppler velocity meters (ADVM) that measure the transport of water following established protocols for USGS stream discharge and index velocity applications (Oberg and others, 2005; Levesque and Oberg, 2012). Turbidity was measured and used as a surrogate for suspended-sediment concentration following USGS methods for suspended-sediment monitoring (Rasmussen and others, 2009). Elevations of surveyed positions of sensors were referenced to the North American Vertical Datum (NAVD88), which reflects a uniform +1.14 meters (m) offset from the mean lower low water tidal datum of the area (available at https://vdatum.noaa.gov/). The data are published in Opatz and others (2019).

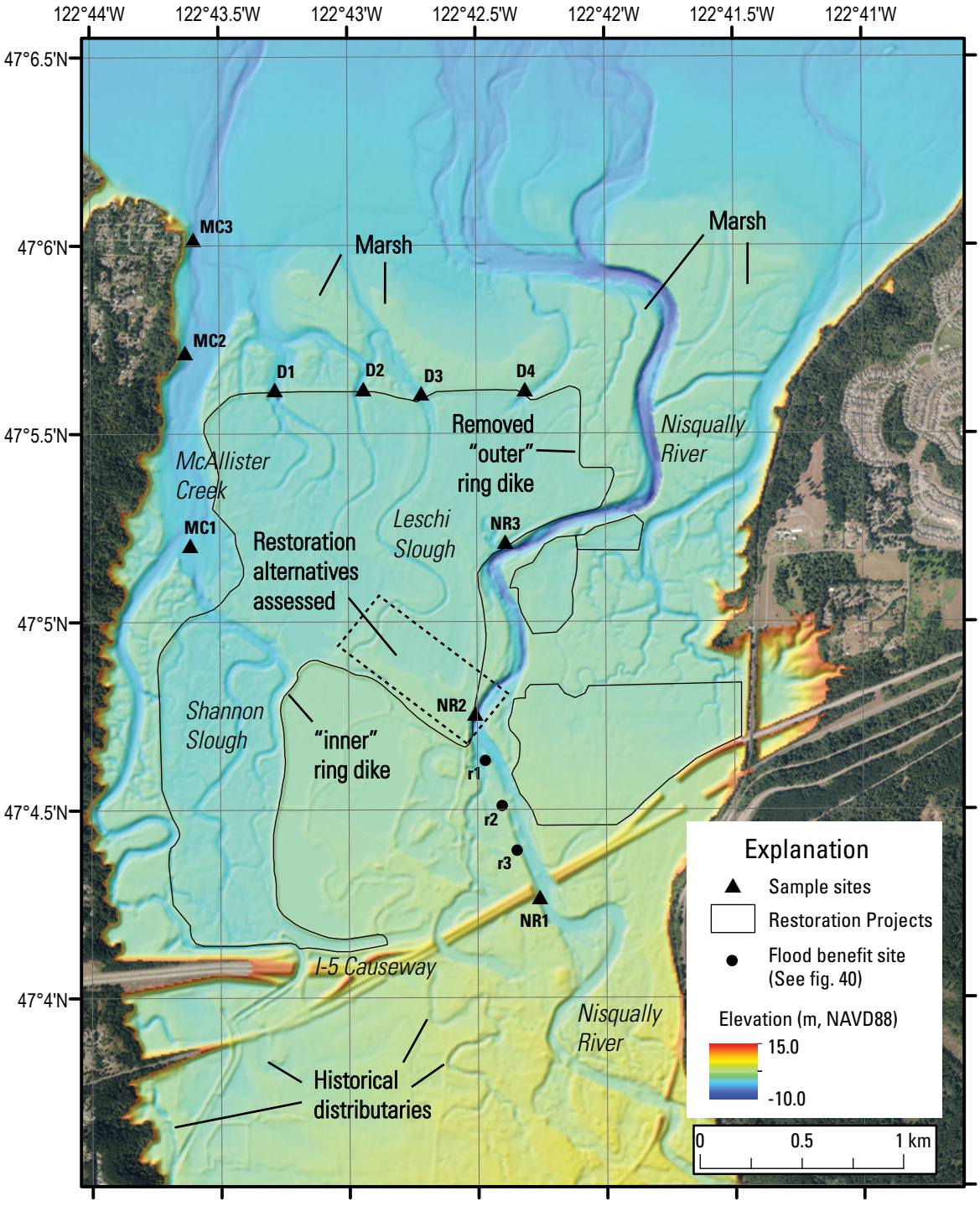

Figure 3. Map showing locations of sampling sites, restoration alternatives near site NR2 assessed in this study, and historical distributary channels that used to convey water and sediment from the river to the estuary through the Interstate 5 (I-5) freeway corridor, west-central Washington. km, kilometer; m, meter; NAVD88, North American Vertical Datum of 1988.

Table 1. Deployment information for 10 sites located across the Nisqually River estuary, west-central Washington.

[See figure 3 for location of sites. ADVM, acoustic Doppler velocity meter; CTD, conductivity-temperature-depth; NAVD88, North American Vertical Datum of 1988; NWIS, National Water Information System; WL, water level]

Site	NWIS	Latitude	Longitude	Elevation [m, NAVD88]	WL	CTD	ADVM	Turbidity
NR1	12090240	47.07114	−122.70431	−0.26	X			
NR2	12090250	47.07702	−122.70857	−0.44	X	X	X	X
NR3	12090250	47.08667	−122.70611	−0.31	X	X		
D1	12081515	47.09361	−122.72139	−0.61	X	X	X	
D2	12081520	47.09367	−122.71567	0.06	X	X	X	
D3	12081525	47.09347	−122.71192	0.47	X	X	X	
D4	12081518	47.09361	−122.70519	−0.18	X	X	X	X
MC1	12081512	47.08672	−122.72689	−1.05	X	X		
MC2	12081516	47.09528	−122.72722	−1.59	X	X	X	
MC3	1208151620	47.10028	−122.72667	−1.36	X	X	X	X

Discrete Samples

Discrete spatial measurements of cross-channel variability in hydrodynamics, elevations, and suspended-sediment concentration were collected at each study site. Boat-mounted acoustic Doppler current profiling data were collected to relate the continuous measurements at one site to the cross-channel variability in flow following standard USGS approaches (Oberg and others, 2005; Levesque and Oberg, 2012). Briefly, cross-channel velocity profile measurements were made with four replicates or until error in discharge for the replicates met acceptable USGS thresholds of less than 4 percent. The data are published in the National Water Information System (NWIS) (U.S. Geological Survey, 2022). These data also provided quantitative information for bathymetry.

Discrete samples of suspended sediment in the water column were collected over select tidal and river discharge conditions either directly with the use of standard USGS water column integrated or point depth sampler or an automated sampler following approved USGS methods in coordination with the Federal Interagency Sedimentation Program and described by (Glysson, 1987; Davis, 2005; Rasmussen and others, 2009). Typically, sediment samples were collected using the Equal Discharge Increment (EDI) method, a division of cross-channel sampling location based on equal discharge to relate variations in sediment concentration to variability in flow conditions.

Data Processing

Processing of time-series data for water levels, current velocities, temperature, salinity, and turbidity are described in Opatz and others (2019). Processing of ADCP data for discharge followed USGS methods in Mueller and others (2013) and are reported in U.S. Geological Survey (2022). Samples were processed for suspended-sediment concentration and particle size following Rasmussen and others (2009). Concentrations were reported in milligrams per liter and size fractions were split by percent coarse (sand) and fines (silt and clay) and are published in U.S. Geological Survey (2022). Suspended-sediment load was calculated as the product of suspended-sediment concentration and discharge as described by Porterfield (1972).

Hydrodynamics and Sediment Transport Modeling

Model Configuration and Set-Up

The models used for this study were constructed using Delft3D, a numerical process-based model used for the simulation of hydrodynamics and sediment transport in coastal and river systems (Lesser and others, 2004; Deltares, 2010). Delft3D solves the unsteady shallow water equations that drive hydrodynamics and their interactions with sediment transport and geomorphic change. Three different high-resolution Nisqually River Delta sediment transport models were constructed; each were two-way coupled to coarser USGS intermediate-scale models covering the south Puget Sound and Tacoma Narrows (fig. 4). Model grids were constructed with curvilinear meshes containing model cell sizes in deep water ranging from 50 to 100 m (fig. 4*A*) and finer model cells on the Nisqually River Delta of 15–30 m (fig. 4*B*). Models were georeferenced to the Universal Transverse Mercator (UTM) Zone 10 Projection and North American Vertical Datum 1988 (NAVD88) in meters.

Models shared base bathymetric and elevation data (fig. 5). The elevation data consisted of USGS swath sonar bathymetric data collected in 2009 and 2011 and a topobathymetric lidar survey collected in September 2014 by the U.S Army Corps of Engineers Joint Airborne Lidar Bathymetry Technical Center of Expertise program and published as part of the USGS Coastal National Elevation Dataset 1-m Puget Sound Digital Elevation Model (Tyler and others, 2020). Although these data cover the entire model domain, small areas of flat, bare marsh plain spanning tens of square meters were interpolated over data gaps associated with incomplete laser penetration of the turbid water column.

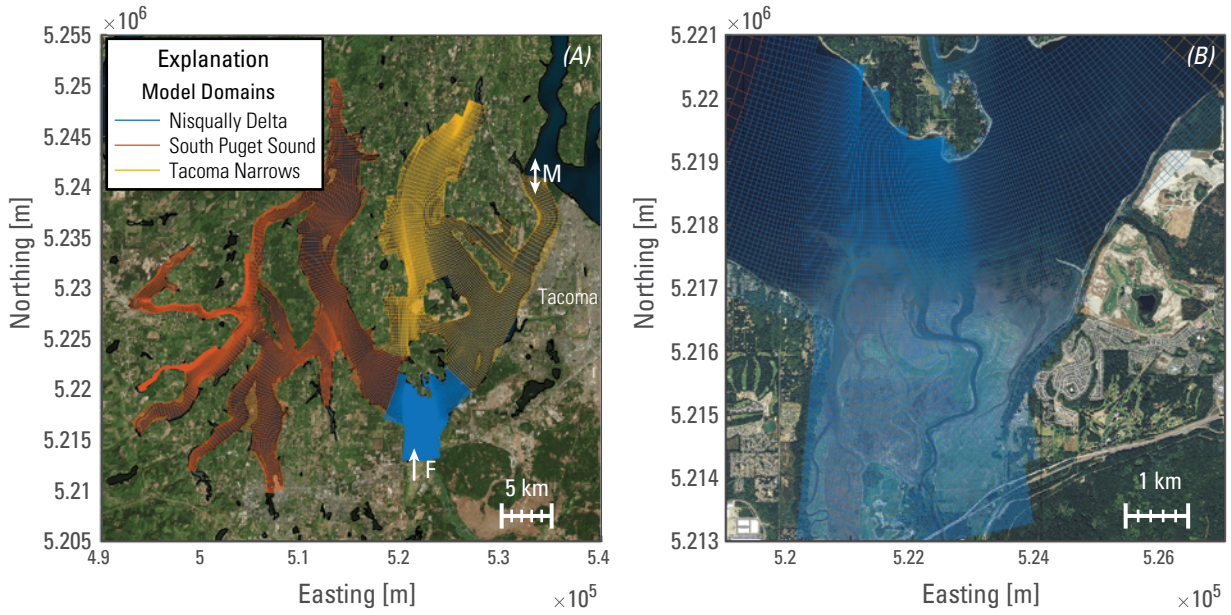

Figure 4. Maps showing hydrodynamic model grids and freshwater discharge (F) and marine (M) boundaries for the south Puget Sound and Tacoma Narrows domains (*A*) and the finer Nisqually River Delta domain (*B*), west-central Washington. km, kilometer; m, meter.

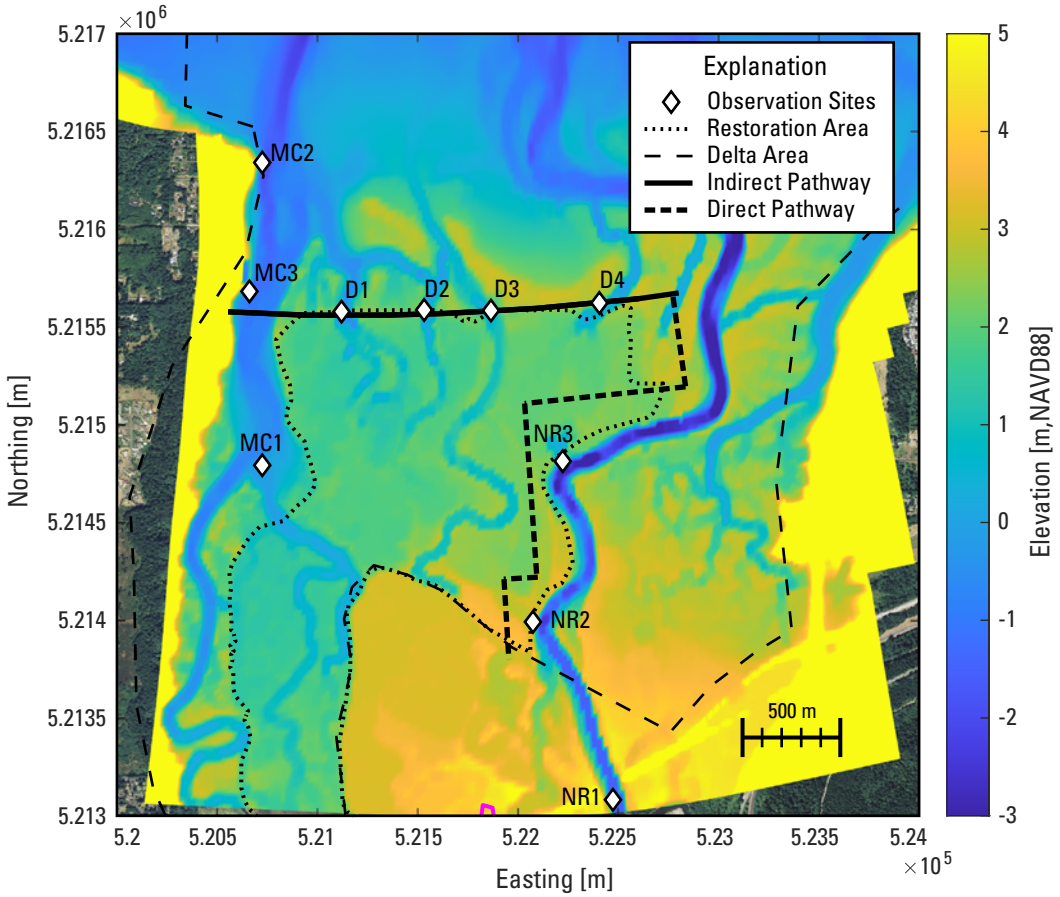

Figure 5. Map showing model bathymetry and output locations at measurement sites across the Nisqually River Delta, west-central Washington. Polygons defining the delta and restoration area are integrated to estimate sediment accumulation. Transects along the left riverbank and northern restoration boundary yield estimates of sediment flux through different pathways. m, meter; NAVD88, North American Vertical Datum of 1988.

The models were run in morphostatic mode (maintaining constant bed level) with measurement points, polygons, and transects specified in the models to track and calculate instantaneous, mean, and cumulative fluxes of sediment, pathways of transport, and accumulation of sediment in different regions of the model domain (fig. 5). The model was run in depth-averaged mode with a time-step of 0.1 min to maximize model stability. Variations in the configurations and approaches of the three sets of models included:

1. Quasi-realistic simulations of all physical processes with no initial sediment on the bed (NIS).
2. Quasi-realistic simulations of all physical processes with initial sediment on the bed (IS).
3. Schematized simulations of "restoration alternatives" under current and projected future sea level and streamflow (SCHEMA).

Quasi-Realistic Simulations with No Sediment on the Bed and Initial Sediment on the Bed

Simulations with no initial sediment on the bed (NIS) assess the routing of suspended sediment directly delivered to the delta by the river. With no initial sediment on the bed, these results constrain the fraction of fluvial delivery to the restoration site on short timescales (months). In contrast, simulations with initial sediment on the bed (IS) inform the total transport, patterns, and dynamics associated with resuspension and redistribution of sediments.

NIS and IS boundary conditions were prescribed at the ocean, river, and surface boundaries. The ocean boundary was forced by measured water levels at the National Oceanic and Atmospheric Administration (NOAA) Tacoma tide gage (NOAA #9446484). The river boundary was prescribed by the sum of discharge measurements at USGS streamgages 12089500 (Nisqually River at McKenna, WA) and 12089208 (Centralia Power Canal near McKenna, WA) (U.S. Geological Survey, 2022). The free surface was forced by meteorological forecasts of wind and pressure obtained from Environment Canada's High-Resolution Deterministic Prediction System (HRDPS). HRDPS output is available every 6 hours at 2.5 kilometers (km) spatial resolution. Archived forecasts were combined using the first 6 hours of each 48-hour forecast to provide hourly, continuous, spatially varying wind and pressure fields to the model surface boundary.

Suspended-sediment concentration (SSC) was prescribed at the upstream boundary based on the relationship of suspended-sediment load (SSL) to discharge following Curran and others (2016a). We specified SSL at the upstream boundary as follows:

$$Q\_SSL = 1.156 Q\_w^{2.68}, \quad (1)$$

where

Q_SSL is measured suspended-sediment load, in metric tons per day, and

Q_w is measured discharge, in cubic meters per second.

Sediments were simulated using three sediment classes observed in the distribution of suspended-sediment and bed-sediment samples from this study and previous studies (Curran and Grossman, 2016a). They reflect the relatively fine nature of sediment that is transported downstream from the Alder Lake, which impounds the coarse fraction (Czuba and others, 2012). The sediment classes were defined by 50 percent cohesive fines, 25 percent fine sands (d50=0.1 millimeter [mm]), and 25 percent coarse sands (d50=0.3 mm). Cohesive sediment transport was implemented in Delft3D with the Partheniades-Krone formulations (Partheniades, 1965). Because the properties of cohesive sediments can vary widely in space and time owing to size class distribution, compaction, and biotic factors, settling velocity and critical shear stress were varied across four model configurations (table 2). The values prescribed bracket the range of suspended particle sizes observed in Curran and others (2016a) and that are found across the estuary (Woo and others, 2018). Settling velocity ranging from 0.2 to 1.0 millimeters per second (mm/s) and critical bed shear stress ranging from 0.05 to 0.15 Newtons per square meter (N/m^2), applied to models in similar estuaries fall within this range (van der Vegen and others, 2011; Allen and others, 2021). In this way, our envelope of simulated sediment transport and accumulation accounts for inherent uncertainty across the system. Settling velocity was kept constant across salinity conditions.

For IS simulations, an initial bed-sediment configuration was generated following van der Wegen and others (2011). The model was run from January to February 2017 with a morphologic acceleration factor of 100, which enhances sediment transports by a factor of 100. This enhancement of sediment transport allows for a computationally tractable approach to approximate 200 months (about 8 years) of transport that, in theory, provides an estimate of a stable bed-sediment configuration. An initial bed composition of 3 m evenly distributed among mud, sand, and coarse sand was allowed to evolve over the simulation (morphostatic). During the 2-month model run, the bed composition stabilized and this final distribution of bed composition (fig. 6) was used as an initial sediment distribution in the IS simulations. Scoured regions, defined as those with less than 10 percent of the original sediment volume, were prescribed 100 percent of the coarse sand fraction in the initial IS sediment distribution. Non-scoured regions were prescribed the percent fraction of the sediment classes present.

Table 2. Model sediment specifications for simulations with no initial sediment on the bed (NIS) and with initial sediment on the bed (IS).

[N/m^2, Newtons per square meter; mm/s, millimeter per second]

Model sensitivities	Critical shear stress for erosion (N/m^2)	Settling velocity (mm/s)
R1	0.05	0.1
R2	0.05	1
R3	0.2	0.1
R4	0.2	1

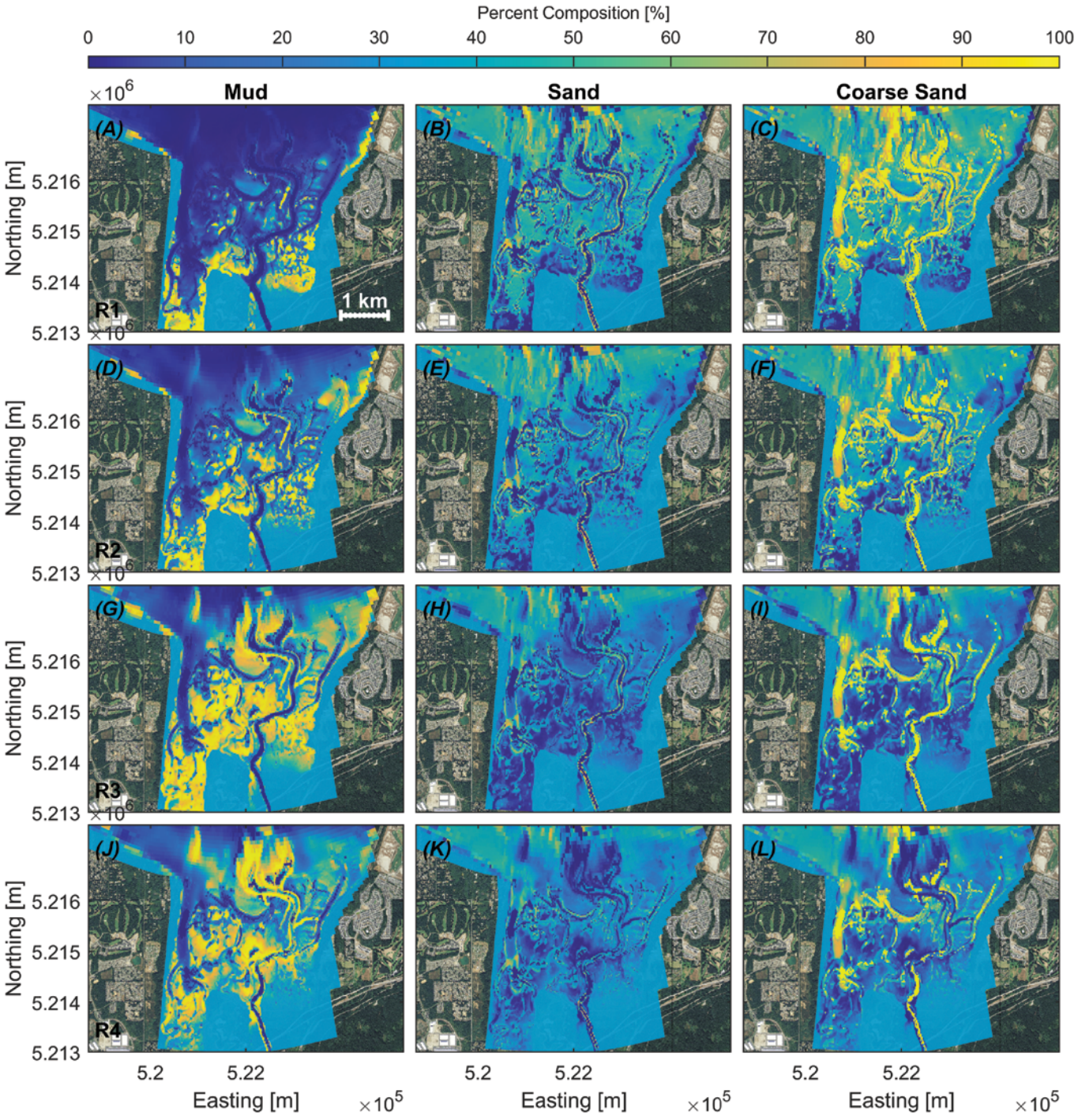

Figure 6. Spatial plots of the initial bed-sediment composition of mud (*A*,*D*,*G*,*J*), sand (*B*,*E*,*H*,*K*), and coarse sand (*C*,*F*,*I*,*L*) as a percentage for the four model sensitivities (rows) explored (table 2). km, kilometer; m, meter.

The final bed composition estimate was prescribed to be 3-m thick with the percent class by volume determined by the bed composition model run and scour analyses. This configuration was used for winter and summer model runs. This approach to summer is assumed to be conservative and provides a maximum estimate of potential mud transport as the availability of mud is suspected to be greater in winter than summer due to fluvial supply and the winnowing effects of nearshore processes (waves, currents) (Webster and others, 2013).

Annual time-series reconstructions of potential sediment delivery to the 2009 restoration area were estimated by relating modeled winter and summer direct and indirect transport to fluvial sediment delivery, wave energy, and tidal range. Modeled direct transport was correlated to the daily averaged suspended mud

and sand delivery of the Nisqually River (Curran and others, 2016a). Indirect transport was regressed against squared wave heights (proportional to wave energy) modeled offshore of the central Nisqually River Delta in water depths of 20 m. Waves were modeled using wind observations from NOAA, National Weather Service Tacoma Narrows Airport (KTIW) site. Modeled wave heights were estimated from a lookup table of pre-computed SWAN model runs for varying wind speeds (0, 5, 10, 15, 20, 25 meters per second [m/s]) and directions (0 through 360 degrees at 10-degree increments). Water-level elevation was set to mean higher high water (3.5 m NAVD88) for computational efficiency and because depth limitation on wave generation and propagation at low tides are assumed to be insignificant for estimating deep water wave heights across the steep and narrow fjordal domain surrounding the Nisqually River Delta. Indirect transport also was correlated against tidal range derived from water-level elevations measured at the Tacoma tide gage (NOAA #9446484) with data gaps filled by measured values from the Seattle tide gage (NOAA #9447130). The tidal range anomaly (η) was estimated for each day by subtracting the maximum from the minimum water-level elevation and removing the long-term mean.

Schematized Simulations of Restoration Alternatives, Future Sea Level and Streamflows

A third and computationally efficient, schematized model (SCHEMA) was used to evaluate opportunities to recover additional sediment supply with identified distributary channel restoration alternatives under current and projected future sea-level positions and streamflows. Only one site (NR2) was identified as acceptable for the alternatives analyses to balance restoration objectives and flood hazard risk and three channel restoration alternative designs were evaluated (fig. 7). The three designs varied in channel bed depth, gradient, and connectivity between

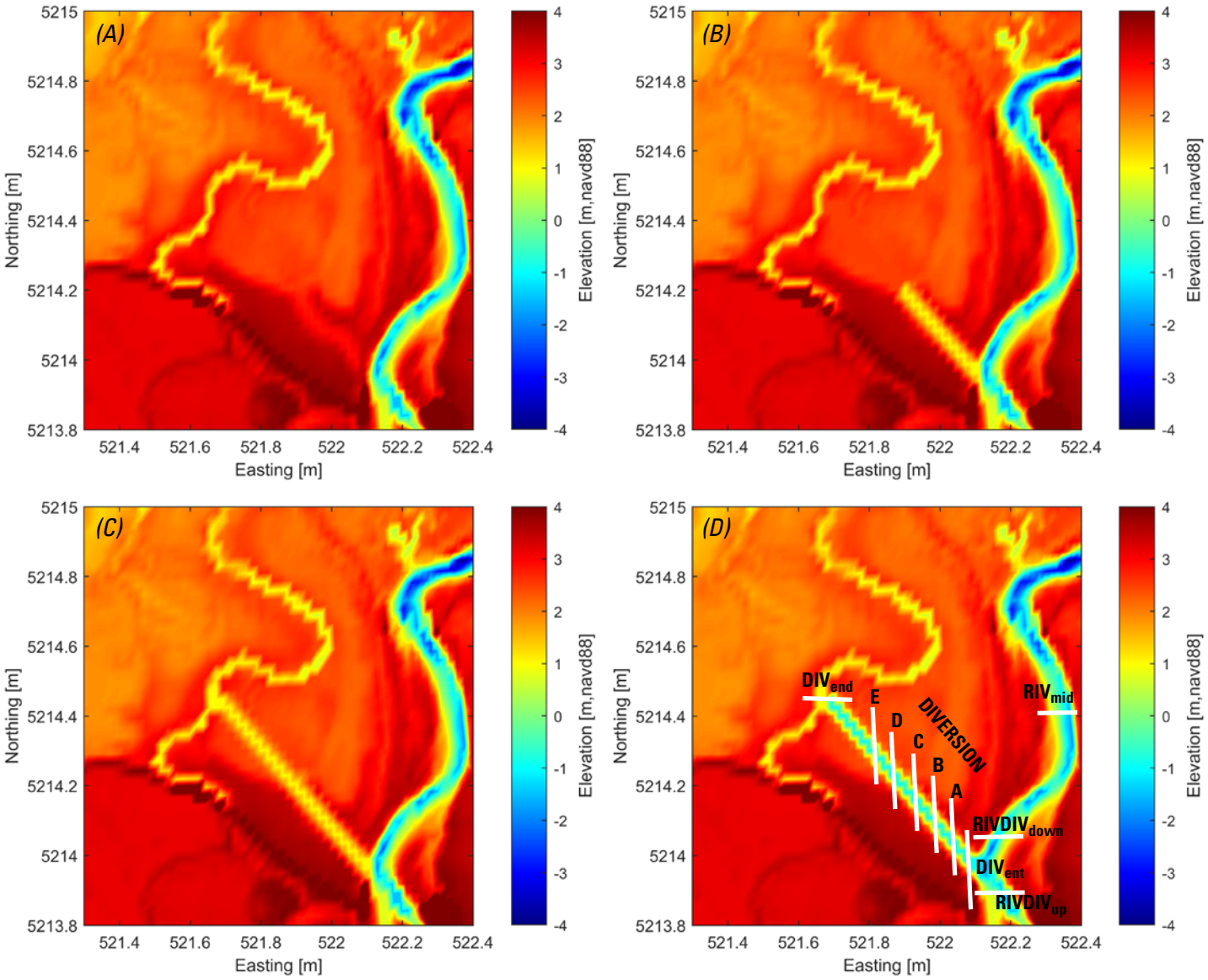

Figure 7. Maps showing geometry of the four restoration configurations, REF (*A*), A (*B*), B (*C*), C (*D*), and cross sections (shown in *D*) examined for channel sediment routing efficiency and sediment flux into the marshes. m, meter; NAVD88, North American Vertical Datum of 1988.

fluvial and tidal processes across the restoration area. In addition to the current "reference" distributary configuration (REF), the three alternative distributary channel configurations are described as follows:

A. Notched, only fluvial connectivity—uniform depth (1.5 m) extending one-half the distance to Leschi Slough in west-southwest orientation and retaining a sill (portion of levee) along the river connection.

B. Notched, partial tidal connectivity—uniform depth (1.5 m) extending to Leschi Slough in west-southwest orientation and retaining a sill (portion of levee) along the river and Leschi Slough connection.

C. Breached, full tidal connectivity—uniform depth (3.5 m) extending to Leschi Slough (full tidal connectivity) in west-southwest orientation aligned with river thalweg for full hydraulic connection.

Four stream discharge classes were simulated—(1) mean daily flow (43 cubic meters per second [m^3/s]), (2) annual 95th percentile discharge (110 m^3/s), (3) 2-year flood event (290 m^3/s), and (4) 5-year flood event (462 m^3/s). These values bracket about 95 percent of the measured flows, which are largely controlled by the hydropower operations of Alder Lake. Sediment transport was implemented using the TRANSPOR2004 equations of van Rijn and Walstra (2004) and refined by van Rijn (2007a, b). These equations allow the computation of transport of grain-size classes as non-cohesive fractions and separate total sediment transport into bedload and suspended-load components. Only suspended sediment was modeled in order to evaluate the influence of identified alternatives on direct transport and conveyance of fluvial transported material to the restoration area relative to existing conditions. Three sediment classes representing the finest fractions observed in past studies (Czuba and others, 2012; Curran and others, 2016a) were modeled. These included fine silt, medium silt, and fine sand with median grain sizes (d50) of 10, 32, and 100 micrometer (μm), respectively, with associated fractions of the fluvial load of 35, 35, and 30 percent, respectively. Modeling the finest fractions aimed to evaluate the maximum potential transport and conveyance of sediment through the alternatives given concerns of low fluvial delivery and the importance of wave resuspension processes.

Thirty-two model scenarios representing the combination of design alternatives, discharge class, and sediment fractions were simulated for present and future sea-level positions to bracket the range of marine and river discharge boundary conditions expected over this century (table 3). A future sea-level position 1 m higher than today was selected to represent a moderate to high sea-level scenario for the year 2100 (Miller and others, 2018). This value also represents the combined water level associated with moderate sea-level rise in the coming decades accompanied by storm surge that annually ranges from 0.3 to 0.6 m in winter months (Miller and others, 2019). The 32 model scenarios were simulated for a single spring-neap tide cycle (14.5 days, 14.25 tidal cycles) to derive tidally averaged metrics of flow and sediment transport for comparison among model scenarios and to scale up estimates of annual sediment delivery.

Several metrics of sediment transport, including channel routing and transport efficiency, were derived for each combination of restoration alternative, streamflow, sediment configuration, and sea-level position. Channel routing and transport efficiency help evaluate the potential performance of

Table 3. Configurations for schematized model.

[--, no data; days/yr, days per year; m, meter; m^3/s, cubic meter per second; μm, micrometer]

Configuration	Description	Units	Value
	Channel		
REF	Current condition (no action)	--	--
A	Extends 50 percent to Leschi Slough (no tidal connectivity)	Width, depth (m)	30, 1.5
B	Extends 100 percent to Leschi Slough (tidal connectivity)	Width, depth (m)	30, 1.5
C	Extends 100 percent to Leschi Slough (tidal connectivity)	Width, depth (m)	0, 3.5
	Discharge class		
1	q50 (median daily flow, occurs about 182.5 days/yr)	m^3/s	43.52
2	q5 (95th percent daily flow, occurs about 18 days/yr)	m^3/s	110.18
3	Q2-year, occurs about 0.48 days/yr)	m^3/s	290.87
4	Q5-year, occurs about 0.19 days/yr	m^3/s	462.98
	Sediment fraction		
35 percent	Fine silt	μm	10
35 percent	Medium silt	μm	32
30 percent	Fine sand	μm	100
	Sea level		
0	Current	m	+0
1	Future	m	+1

alternatives and were defined as the amount of sediment fluxed through different channel alternatives relative to either the total fluvial sediment load or the amount diverted or entering each channel as defined in (table 4). Sediment flux, accumulation, and channel routing and transport efficiency metrics from the SCHEMA models were quantified over the spring-neap period and converted to daily or annual quantities based on the frequency of occurrence of each boundary condition.

Four metrics including (1) tidally averaged sediment transport (<*S*>), (2) tidally averaged sediment transport through channel configuration entrance <$S_{Entrance}$>, (3) tidally averaged sediment transport in main stem above channel configuration entrance <$S_{Upstream}$>, and (4) tidally averaged sediment transport through channel configuration (<$S_{Transect(A-E)}$>) represent the average transport over a spring-neap tidal cycle (table 4). These values can then be used to scale up over time-periods of interest accounting for the frequency of prescribed streamflow and model boundary forcing. The three metrics that examine sediment routing or transport efficiency of the alternatives include the routing efficiency (equation 5), or the percentage of sediment routed into the configuration relative to load in stream (<$S_{Entrance}$> / <$S_{Upstream}$>, the transport efficiency relative to load in stream (equation 6), or the percentage of sediment routed through channel configuration relative to load in stream (<$S_{TransectE}$>/<$S_{Upstream}$> × 100 percent), and the transport efficiency relative to load entering the channel (equation 7) defined as the quantity fluxed through specific sections of the channel configuration relative to the amount entering the channel entrance <$S_{TransectE}$>/<$S_{Entrance}$> × 100 percent) (table 4). The first four are expressed in volume, and the last three are expressed as a percent.

Model Validation Procedure and Data

Simulated and measured water-level elevations and current velocities were validated for the 2-month period (January 1–March 1, 2017) after a 1-week model spin-up period. This winter period was characterized by a representative range of high and low streamflows, a typical range of tides, and several modest coastal storm events that elevated the sea surface with storm surge and moderate to high winds that influence waves (fig. 8). Simulated suspended-sediment concentrations were evaluated through comparisons to measured suspended-sediment concentrations for model configurations R1–R4.

Simulated sediment accumulation patterns and magnitude were compared to measured elevation change across the

Table 4. Metrics of schematized sediment transport model metrics.

[m^3, cubic meter]

Metric	Description	Equation	Equation No.
Tidally averaged sediment transport	Cumulative sediment transport averaged over a spring-neap cycle (m^3)	$\langle S \rangle = \frac{S_{cumulative}}{14.25}$	(1)
Tidally averaged sediment transport through channel configuraton entrance	Cumulative sediment transport through entrance of channel configuration averaged over a spring-neap cycle (m^3)	$\langle S_{Entrance} \rangle = \frac{S_{cumulative\ Entrance}}{14.25}$	(2)
Tidally averaged sediment transport in main stem above channel configuration entrance	Cumulative sediment transport immediately above entrance of channel configuration averaged over a spring-neap cycle (m^3)	$\langle S_{Upstream} \rangle = \frac{S_{cumulative\ Upstream}}{14.25}$	(3)
Tidally averaged sediment transport through channel configuration	Cumulative sediment transport through channel configuration and Transect E averaged over a spring-neap cycle (m^3)	$\langle S_{Transect\ E} \rangle = \frac{S_{cumulative\ Transect\ E}}{14.25}$	(4)
Routing Efficiency	Percentage of sediment routed into configuration relative to load in stream	$RE = \frac{\langle S_{Entrance} \rangle}{\langle S_{Upstream} \rangle} \times 100\%$	(5)
Transport Efficiency$_{Upstream}$	Percentage of sediment routed through channel configuration to Transect E relative to load in stream	$TE_{Upstream} = \frac{\langle S_{Transect\ E} \rangle}{\langle S_{Upstream} \rangle} \times 100\%$	(6)
Transport Efficiency$_{Entrance}$	Percentage of sediment routed through channel configuration to Transect E relative to load entering channel	$TE_{Entrance} = \frac{\langle S_{Transect\ E} \rangle}{\langle S_{Entrance} \rangle} \times 100\%$	(7)

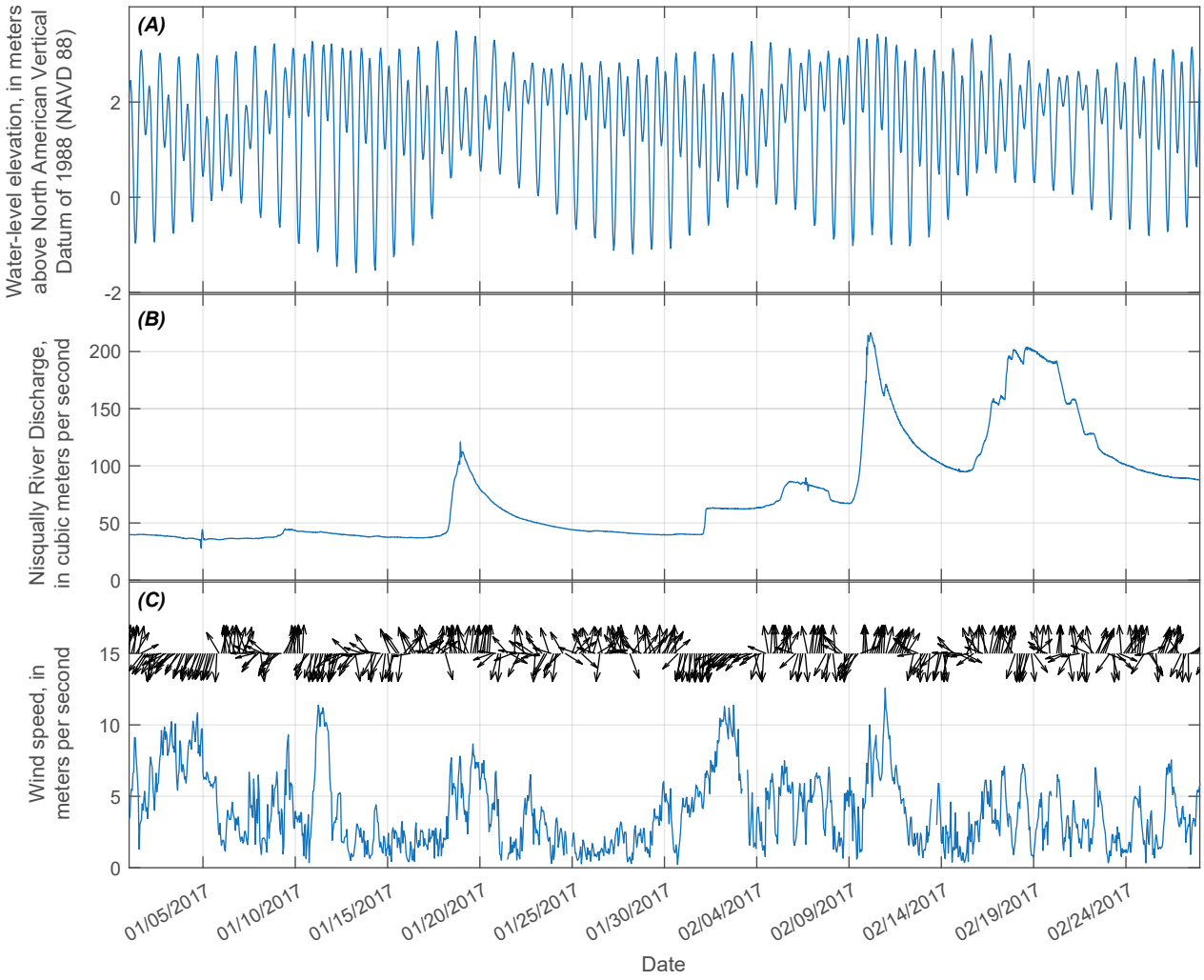

Figure 8. Graphs showing measured water-level elevations at Tacoma tide gage (*A*), measured Nisqually River discharge (*B*), and predicted wind speeds (blue and direction (black arrows) during the validated 2-month winter simulation period (*C*).

restoration area derived from repeat high-resolution lidar collected in 2011 and 2014 as well as accretion rates derived from sediment cores. Sediment accumulation accounting for elevation change was derived from differencing bare earth elevations between 2011 (Puget Sound Lidar Consortium, 2021) and 2014 (Tyler and others, 2020) in the restoration area. A systematic bias of 0.08 m was removed from the 2014 lidar data (fig. 9*A*) based on variance in elevation over broad, flat road and parking lot surfaces assumed to not change over the 3-year time frame (fig. 9*B*). An additional bias of 0.75 m representing vegetation in the 2014 lidar also was removed where it showed artifacts of marsh topography in locations where contemporaneous air photography and 2011 lidar showed bare soil (fig. 9*C*, *D*, *E*). Lastly, the elevation bias of the NNWR boardwalk installed in 2012 was removed from the 2014 lidar. This was done by removing 1.06 m from the 2014 lidar, which represents the mean elevation difference between the 2011 and 2014 lidar data within the footprint of the boardwalk.

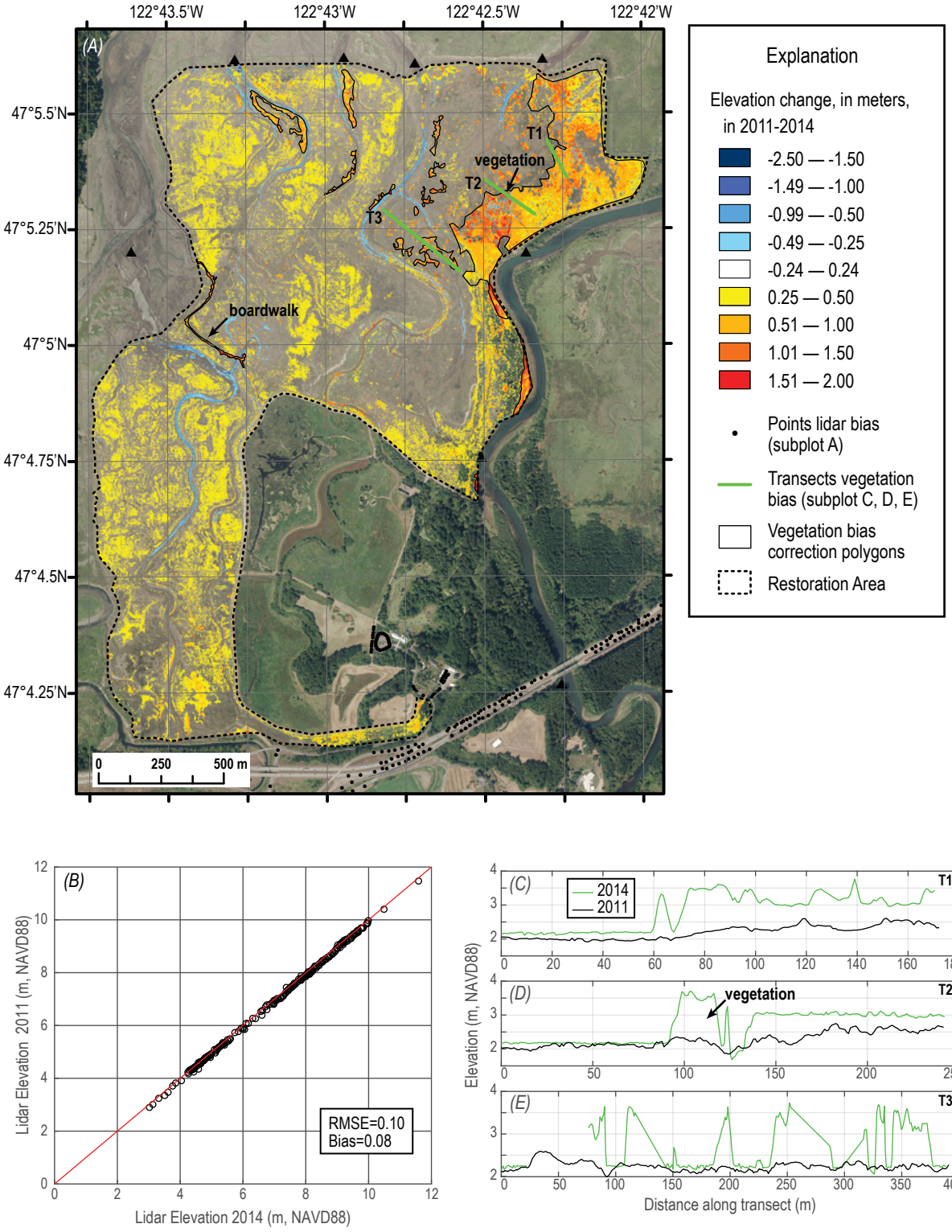

Figure 9. Map showing raw elevation change between 2011 and 2014 and locations sampled to evaluate bias in lidar and bias associated with vegetation in 2014 bare earth lidar data (*A*). Graphs showing bias in 2014 lidar relative to 2011 (*B*), and bias in 2014 lidar due to vegetation (*C*, *D*, *E*). m, meter; NAVD88, North American Vertical Datum of 1988; RMSE, root mean square error.

Results and Discussion

Data Coverage

Continuous and discrete data of hydrodynamics and water quality, including turbidity and suspended-sediment concentration, were collected in the lower Nisqually River, McAllister Creek, and tidal channels of the Nisqually River Delta from February 2016 to March 2018 (fig. 10) and published in Opatz and others (2019). Data coverage at 15-min intervals at each of the 10 sites ranged from 76 to 100 percent. Sites with less data coverage resulted from vandalism, damage from large woody debris associated with high flows, and two instances of corrosion of cable connectors. Water level, current velocity/direction, and turbidity were used for model validation. Details of data collection, processing, and variability are described in Opatz and others (2019).

Sediment Load of the Lower Nisqually River

Relations between suspended-sediment concentration and paired turbidity for material delivered to the delta in the lower river (fig. 11) and suspended-sediment load calculated in this study for the lower Nisqually River near site NR2 agreed with previously published estimates (fig. 12) downstream from Alder and La Grande Dams (Nelson, 1974; Curran and others, 2016a). A similar load of 100,000–120,000 metric tons per year (t/yr) at the delta and at Yelm during this and two previous studies indicates that the input to or loss of suspended sediment from the lower Nisqually River is negligible and has been relatively uniform since dam construction.

During water years 2016–17 (Oct. 1, 2015–Sept. 30, 2017), the cumulative suspended-sediment load of the lower Nisqually River was estimated to be about 250,000 metric tons. Nearly 30 percent more sediment (140,000 metric tons) was delivered

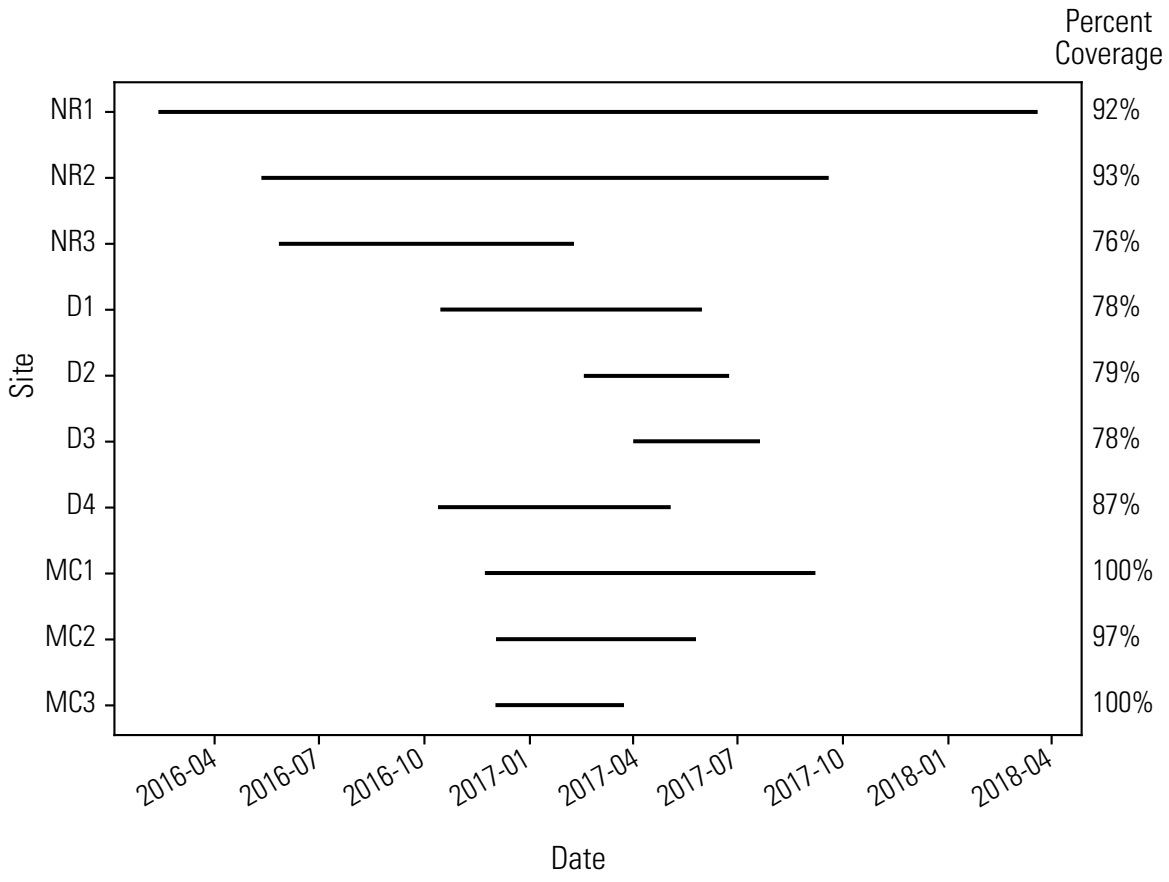

Figure 10. Graph showing data coverage, in percent coverage (to the right of the graph), for each continuous sampling site, lower Nisqually River, McAllister Creek, and tidal channels of the Nisqually River Delta, west-central Washington, February 2016–March 2018.

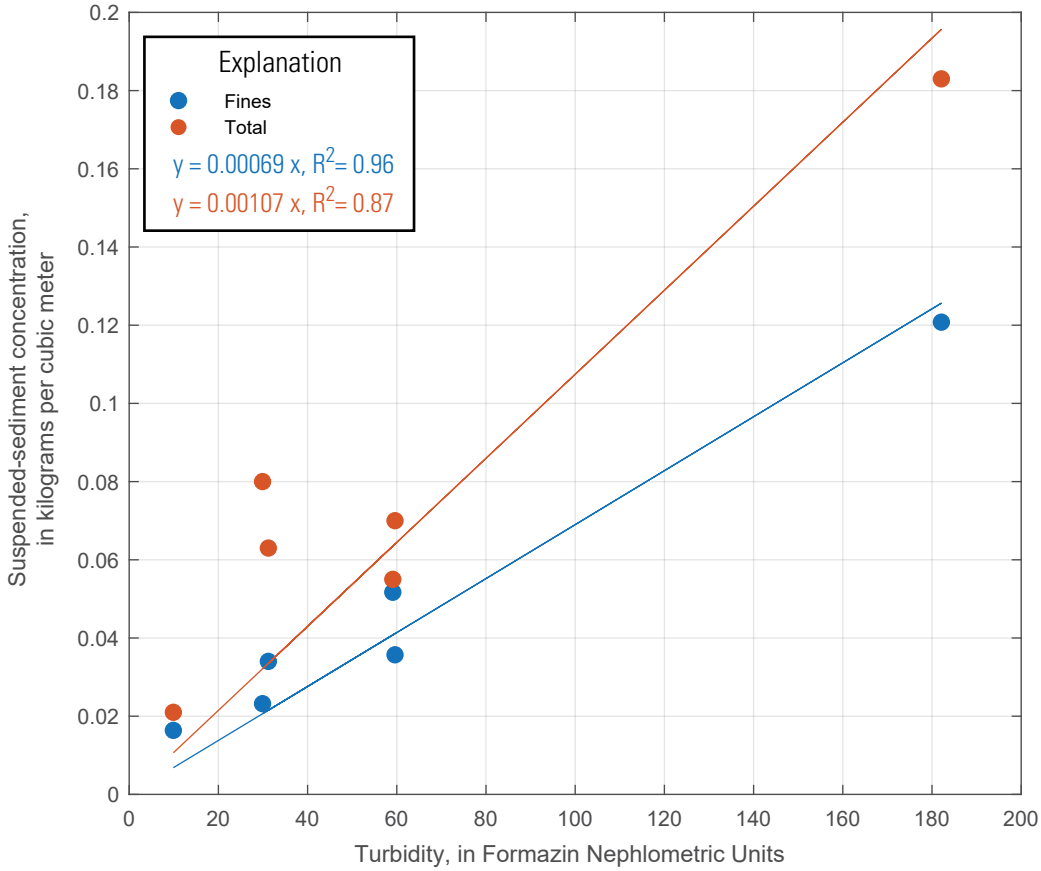

Figure 11. Graph showing relation between measured turbidity and suspended-sediment concentration (SSC) for total and fine fraction (<0.63 millimeter) at site NR2, Nisqually River Delta, west-central Washington. Regression coefficients for SSC (y) and turbidity (x) are shown with the associated R2 value.

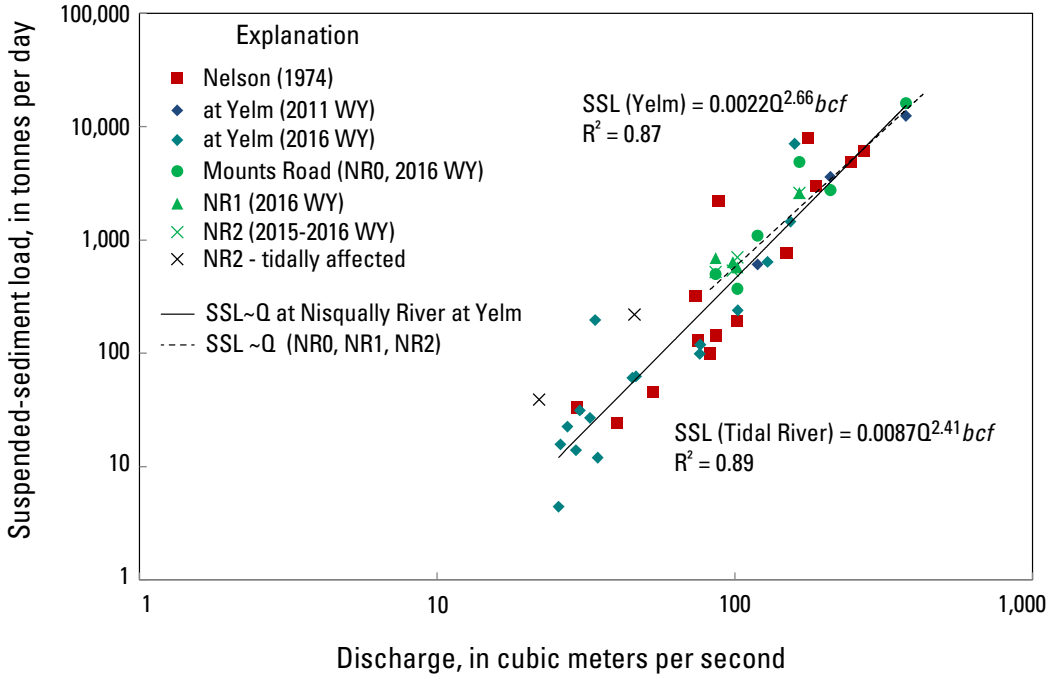

Figure 12. Rating curves for estimating suspended-sediment load (SSL) as a function of discharge (Q) in the lower Nisqually River (this study) showing agreement and potential slight increase relative to estimates upstream at Yelm from Nelson (1974) and Curran and others (2016a). bcf, bias correction factor; WY, water year.

through the lower river in water year 2016 than in water year 2017 (110,000 metric tons) in response to the flood event of December 18, 2015, that reached about 420 cubic meters per second. Most (75–90 percent) of the annual transport occurred during the two highest flows of each year (fig. 13). Flows were characterized by near-average annual flood magnitudes resulting from the modulated hydrology downstream from Alder Lake (fig. 14). The average annual sediment loads are slightly higher but generally consistent with previous estimates upstream ranging from 100,000 to 120,000 t/yr (Curran and others, 2016a).

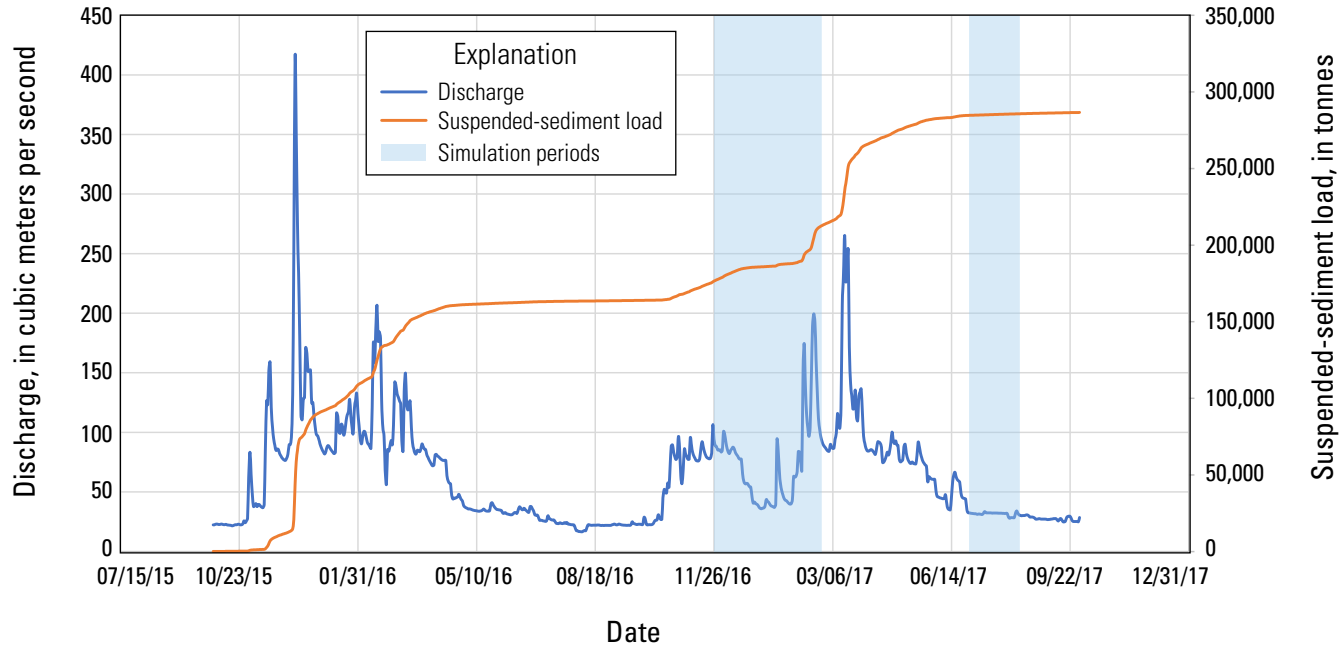

Figure 13. Graph showing discharge and cumulative suspended-sediment load in the lower Nisqually River, west-central Washington, water years 2016–17, and the winter and summer simulation period for this study.

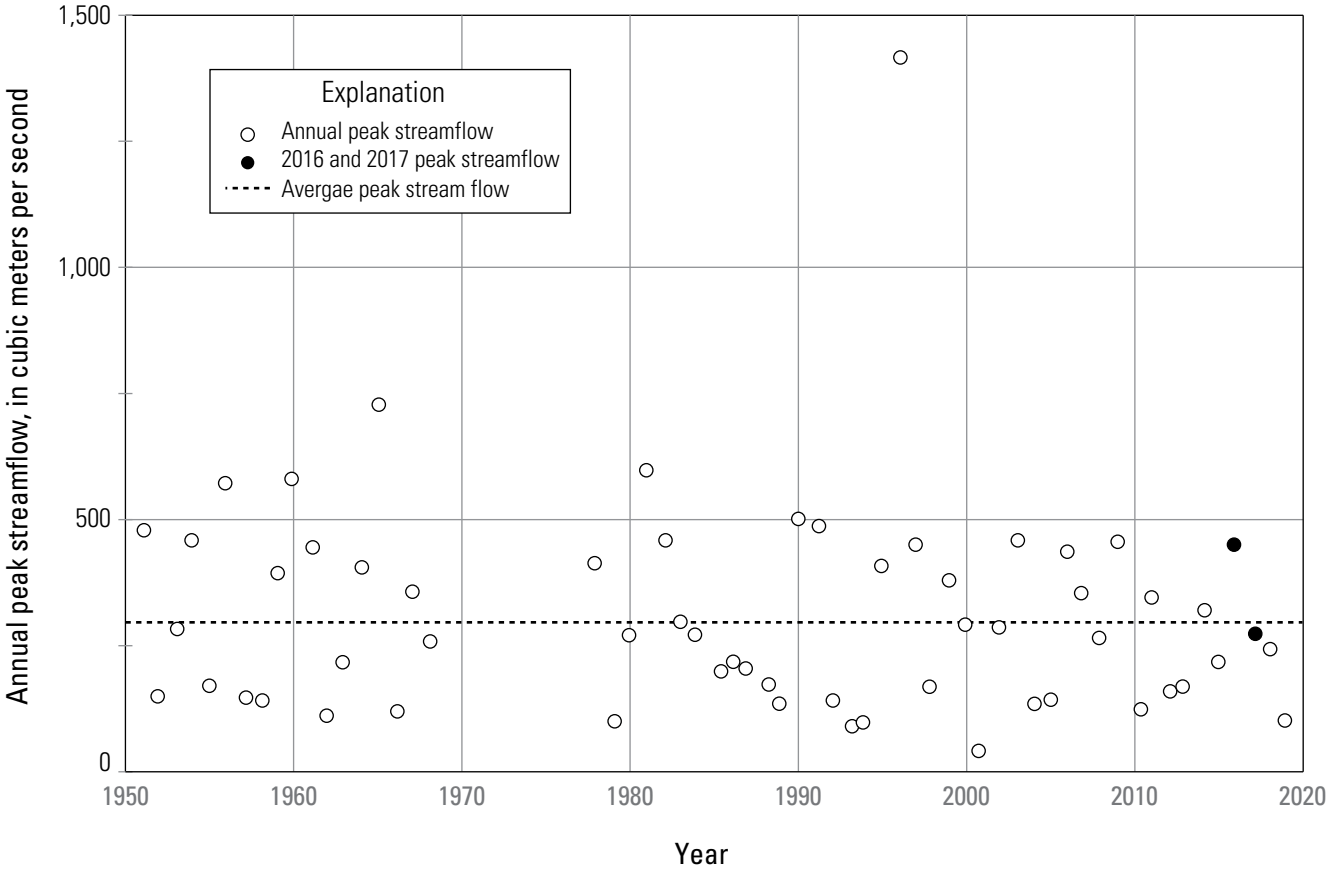

Figure 14. Graph showing annual peak streamflow at U.S. Geological Survey streamgage 12089500 Nisqually River at McKenna, Washington.

Model Validation

Water-Level Elevations

Strong agreement between simulated and measured water-level elevations (fig. 15, table 5) indicates high hydrodynamic model accuracy. Error is due likely to uncertainty in bathymetry, bed roughness, grid-cell averaging, and differences in model cell elevation and depth sensor location. Bias-removed root-mean-square-error (RMSE-br) was 16–40 centimeters (cm) for the lower river sites (NR1–NR3), 16–20 cm for the tidal channel sites (D1–D4), and 19–33 cm for the McAllister Creek sites (MC1–MC3). Uncertain bias at site MC3 is due to lack of independent survey data to quantify bias. These errors translate to simulated water-level error of about 3–5 percent of the tidal range.

Current Velocities

Accuracy of the model simulating current velocities was good (fig. 16). Despite the challenge of representing the relatively small channel widths of inlets D1–D4 in the model, the bias-removed RMSE of simulated current velocities at sites D1–D4 ranged from 14 to 21 cm/s (table 6), or on average 7–13 percent of the measured range (fig. 16). These errors are suspected to be related to the ability of the model to capture the depth averaged flow across narrow complex channel geometry, the ability of single point observations to provide reliable averages across a channel. Current velocities at site NR2 show a strongly systematic bias that is thought to be due to either incorrect surveyed sensor location or bathymetry, or effects of model grid resolution and depth averaging and affects flow conveyance. Negative model bias is likely due to insufficient model resolution to resolve

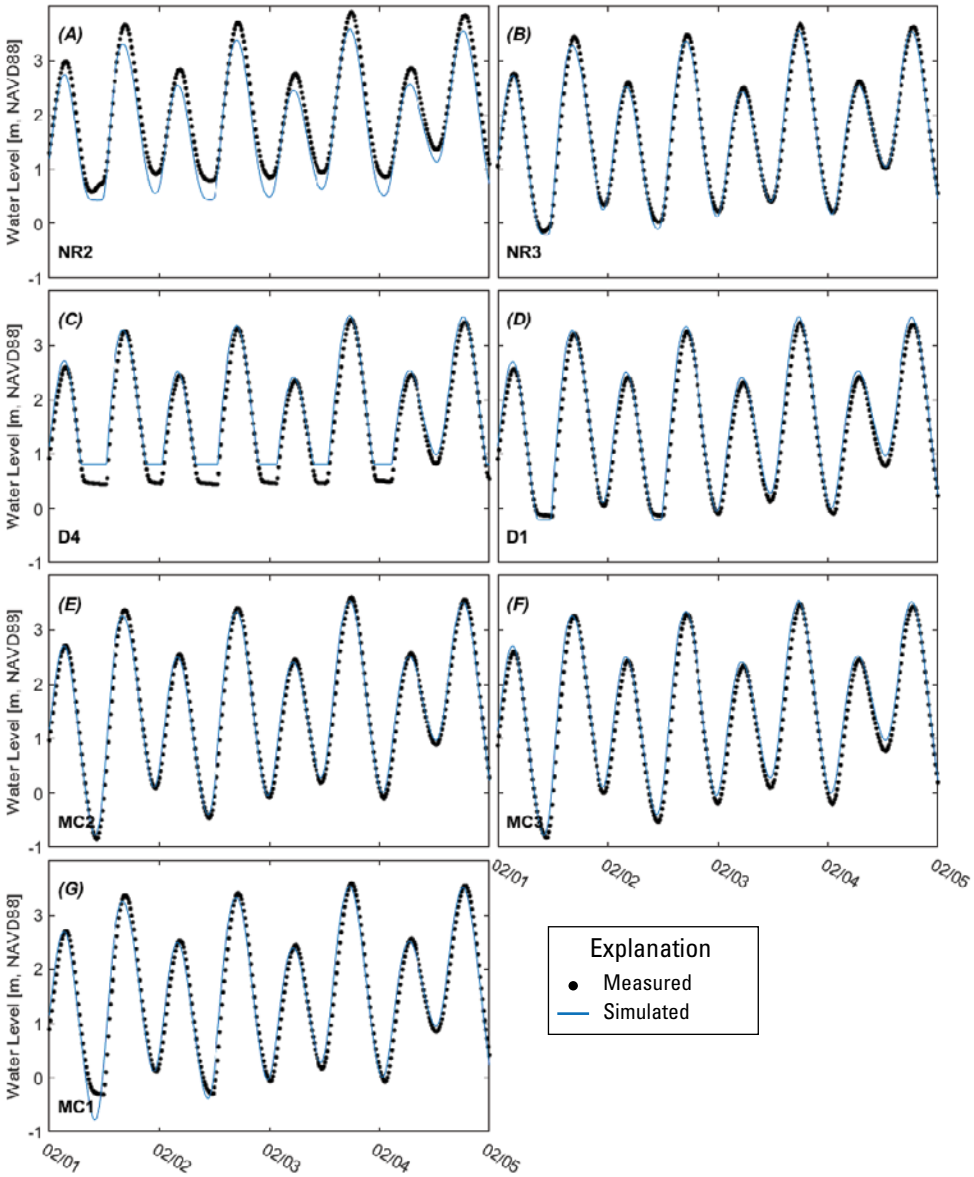

Figure 15. Graphs showing measured and simulated water-level elevations versus time at sites used for validation. m, meter; NAVD88, North American Vertical Datum of 1988.

Table 5. Simulated water-level elevation root-mean-square-error (RMSE), bias, bias-removed root-mean-square error (RMSE-br), and coefficient of determination (R^2).

[See figure 3 for location of sites used for validation. cm, centimeter; --, no data]

Validation site	RMSE [cm]	Bias [cm]	RMSE-br [cm]	R^2
NR2	30.8	26.5	15.6	0.9
NR3	35.1	−7.1	34.4	0.89
D1	22.3	−15.5	16	0.96
D2	31.8	−24.5	20.4	0.83
D4	24.8	−19.3	15.5	0.92
MC2	25.1	−14.8	20.3	0.96
MC3	19.4	--	19.4	0.98
MC1	32.4	−1.0	32.4	0.93

Table 6. Simulated current velocity root-mean-squared-error (RMSE), bias, bias-removed root-mean-square error (RMSE-br), and coefficient of determination (R^2).

[See figure 3 for location of sites used for validation. cm/s, centimeter per second]

Site	RMSE [cm/s]	Bias [cm/s]	RMSE-br [cm/s]	R^2
NR2	35.9	−30.4	19.2	0.2
D4	21.1	−2.6	20.9	0.43
D2	14.6	−0.3	14.6	0.63
D1	13.5	−0.1	13.5	0.72
MC3	16.1	−3.1	15.8	0.83

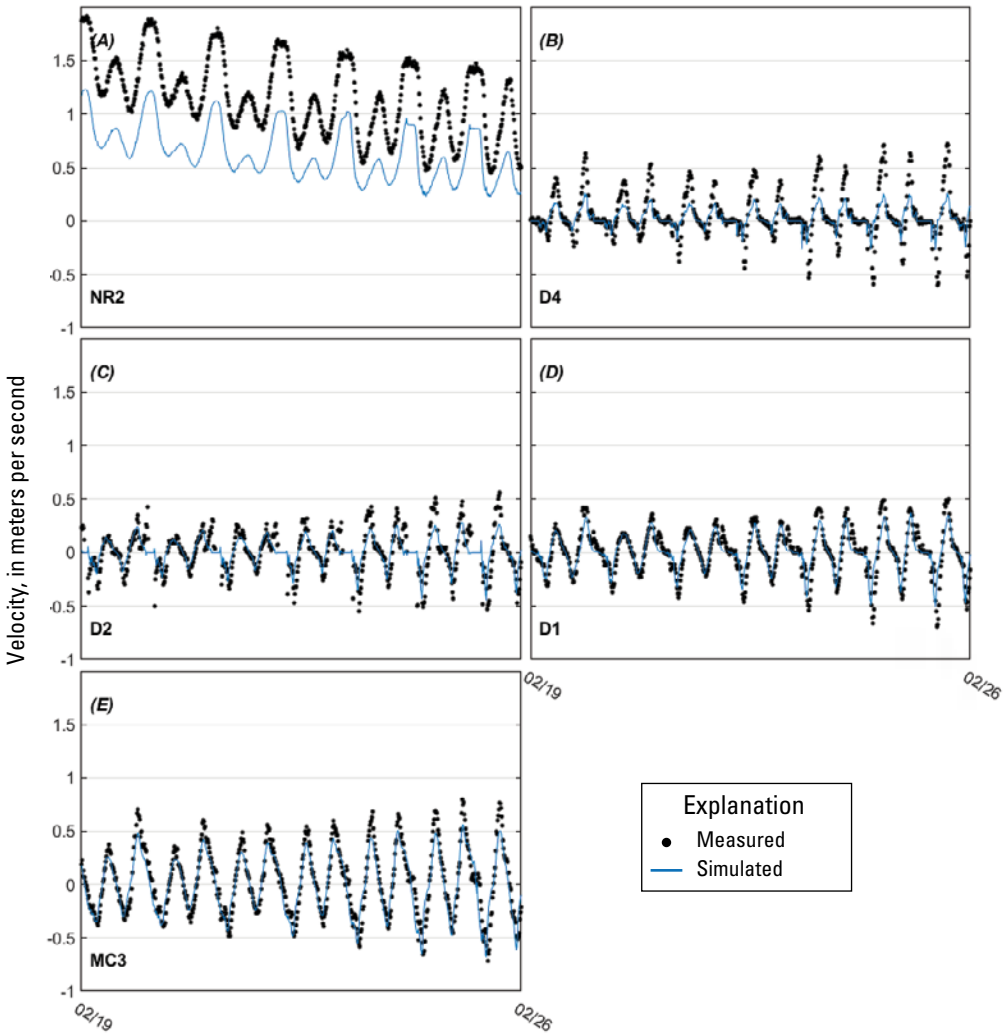

Figure 16. Graphs showing measured and simulated along channel velocities over time at sites used for validation.

velocity structure in narrow channels (for example, site D4). Narrow channels are smeared in the averaging of bathymetry in comparatively coarse model cells resulting in wider, shallower flow compared to reality.

Suspended-Sediment Concentrations

Simulated and measured suspended-sediment concentrations (SSC) were compared at sites D4 and MC3 (figs. 17–20).

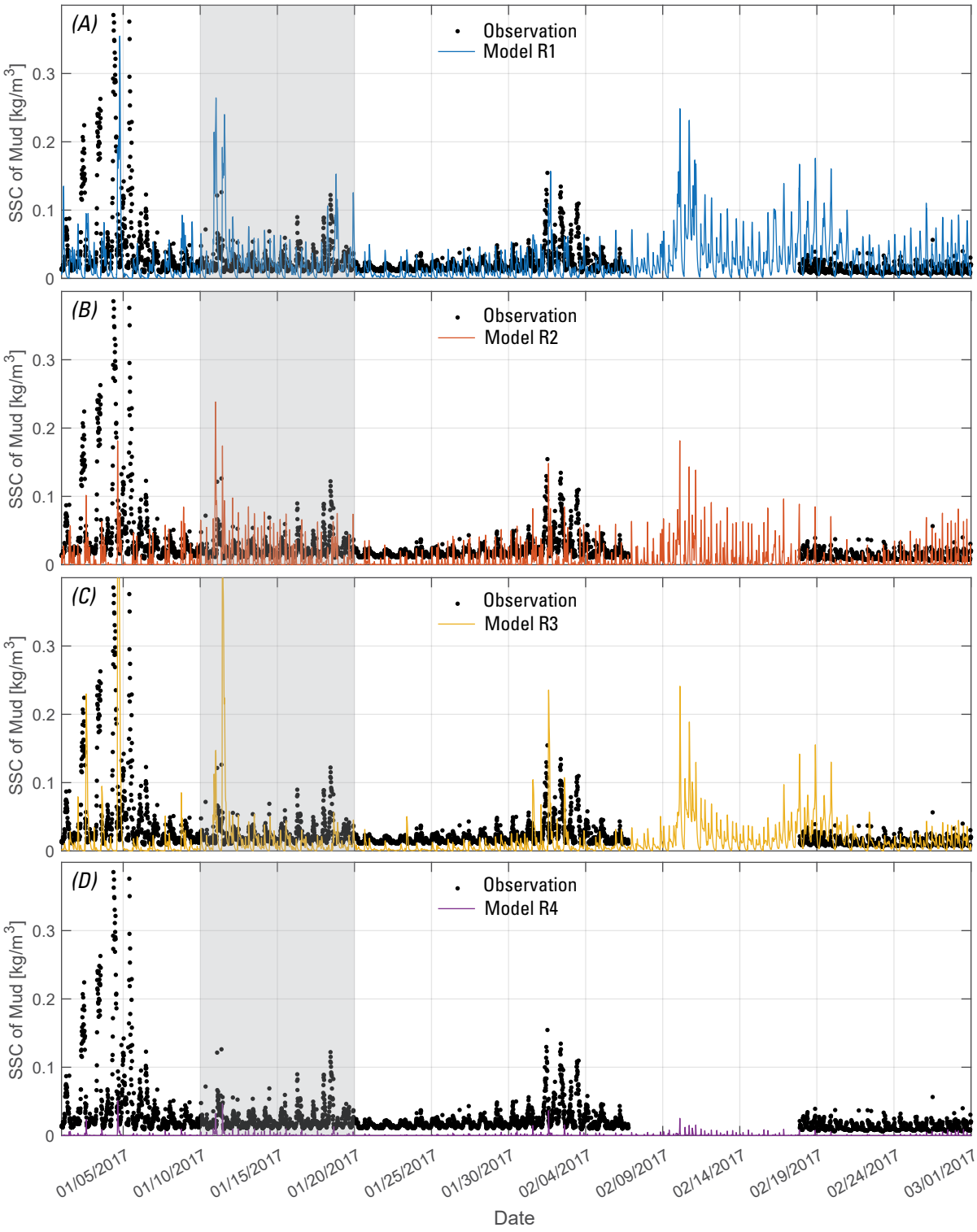

Figure 17. Graphs showing simulated and measured suspended-sediment concentrations (SSC) at site D4 for the four model sediment configurations, R1 (*A*), R2 (*B*), R3 (*C*), R4 (*D*), with highlighted 10-day representative period (gray) shown in figure 18. kg/m^3, kilogram per cubic meter.

Simulated SSC shows overall similar tidal patterns with higher concentrations during wind or discharge events. At site D4, during low tide the simulated SSC decreases to zero while measured SSC peaks (fig. 18). This discrepancy is believed to result from turbulent mixing of suspended sediment in ponds formed at the inlets as ebb flow cascades down and forms small erosional headwall scarps. The inlets and ponds are only partly resolved by the comparatively coarse model grid. Overall, tidal

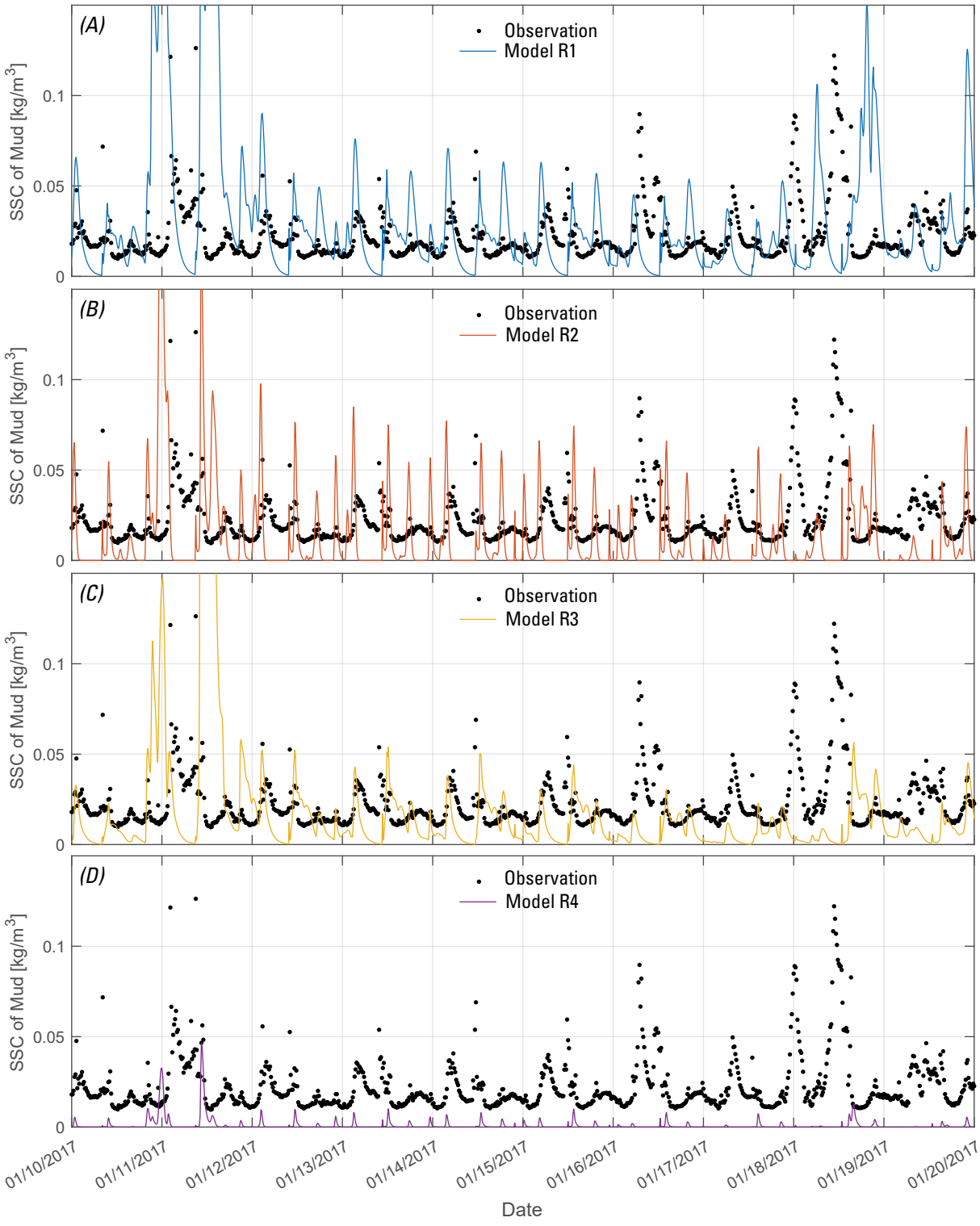

Figure 18. Graphs showing simulated and measured suspended-sediment concentrations (SSC) at site D4 for the 10-day period shown in figure 17 for the four model sediment configurations, R1 (*A*), R2 (*B*), R3 (*C*), R4 (*D*). kg/m^3, kilogram per cubic meter.

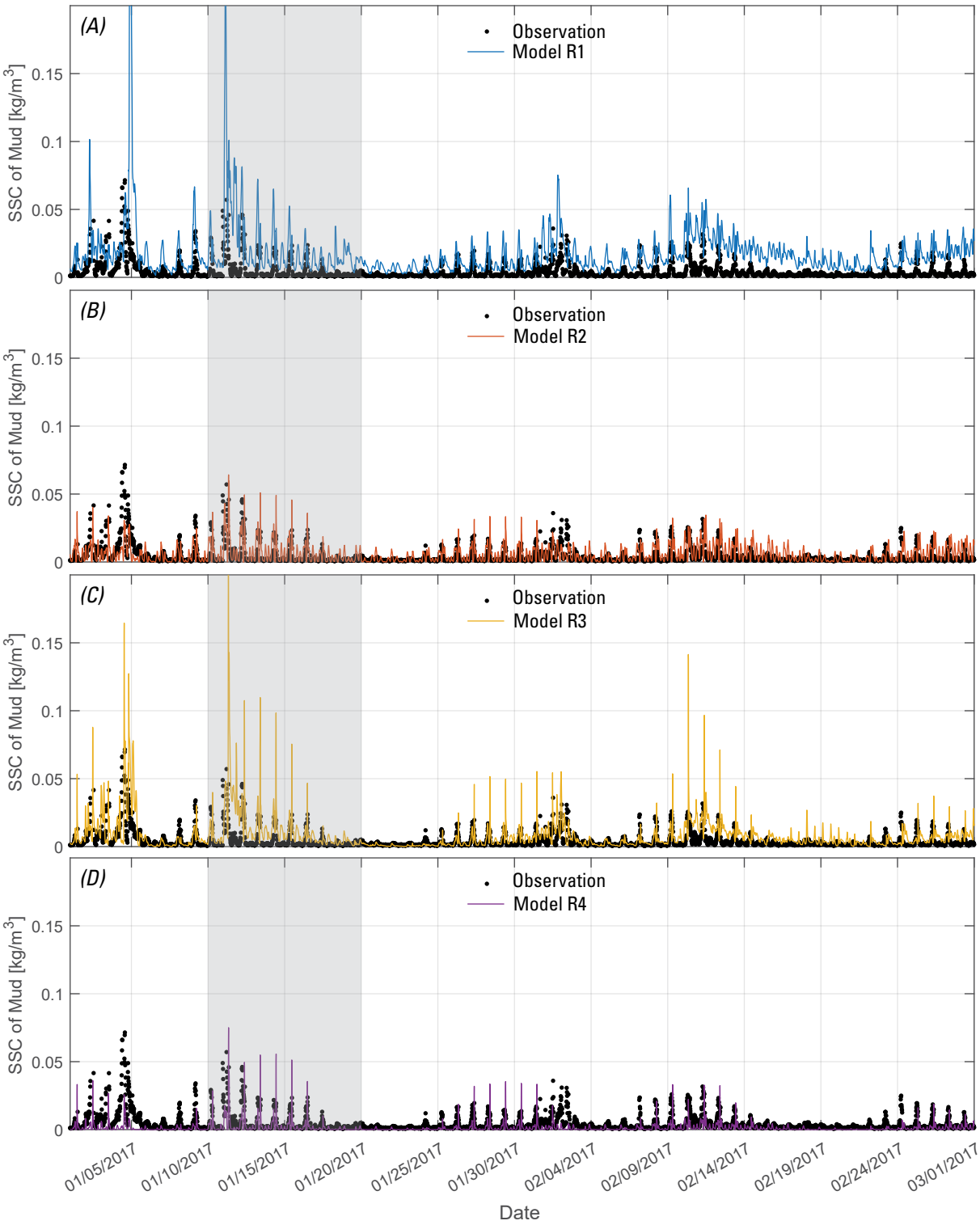

Figure 19. Graphs showing simulated and measured suspended-sediment concentrations (SSC) at site MC3 for the four model sediment configurations, R1 (*A*), R2 (*B*), R3 (*C*), R4 (*D*) with highlighted 10-day representative period (gray) shown in figure 20. kg/m^3, kilogram per cubic meter.

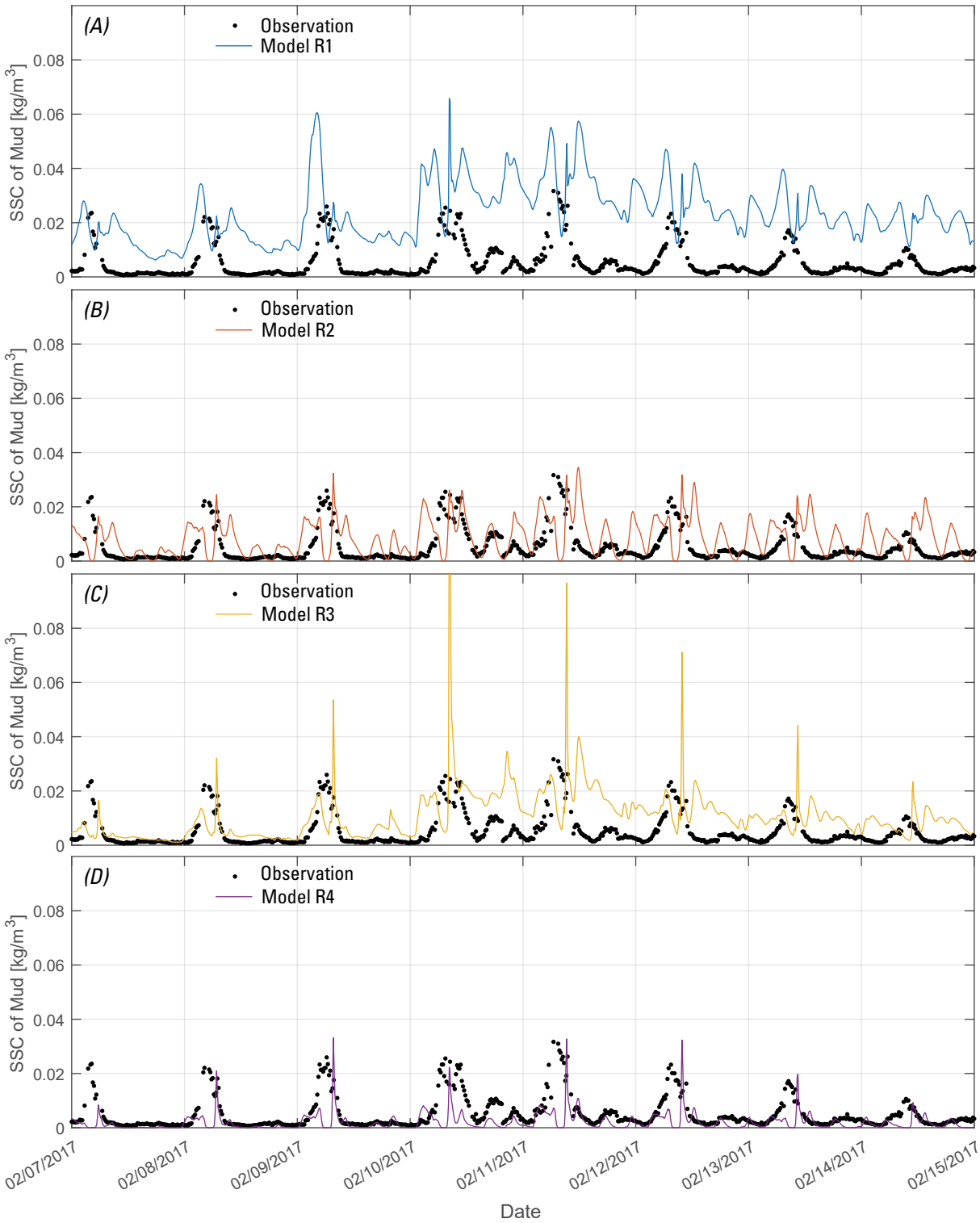

Figure 20. Graphs showing simulated and measured suspended-sediment concentration (SSC) at site MC3 for the 10-day period shown in figure 19 for the four model sediment configurations, R1 (*A*), R2 (*B*), R3 (*C*), R4 (*D*). kg/m³, kilogram per cubic meter.

variability in SSC was greater in simulations than in measurements. Comparisons across model sensitivity tests (R1–R4) suggest SSC is generally simulated best with the R2 and R3 model sediment configurations at site D4 (fig. 17). This is particularly clear during a shorter 10-day time series detailing the timing and magnitudes of SSC fluctuations (fig. 18). Model configuration R4 with the highest settling velocity and bed shear may approximate the measured SSC characteristics at site MC3 better, where a sand is more prominent on the McAllister Creek channel bed (figs. 19 and 20).

Modeled Hydrodynamics and Residual (Mean) Circulation

Simulated water levels and depth-averaged current velocities illustrate the influence of ebb and flood tides on the connectivity and flow paths of the Nisqually River across the delta. At peak high tide, flow is directed into the restoration area along the left bank at site NR2 and through McAllister Creek (fig. 21*A*). During high tide, transport along the northern boundary of the

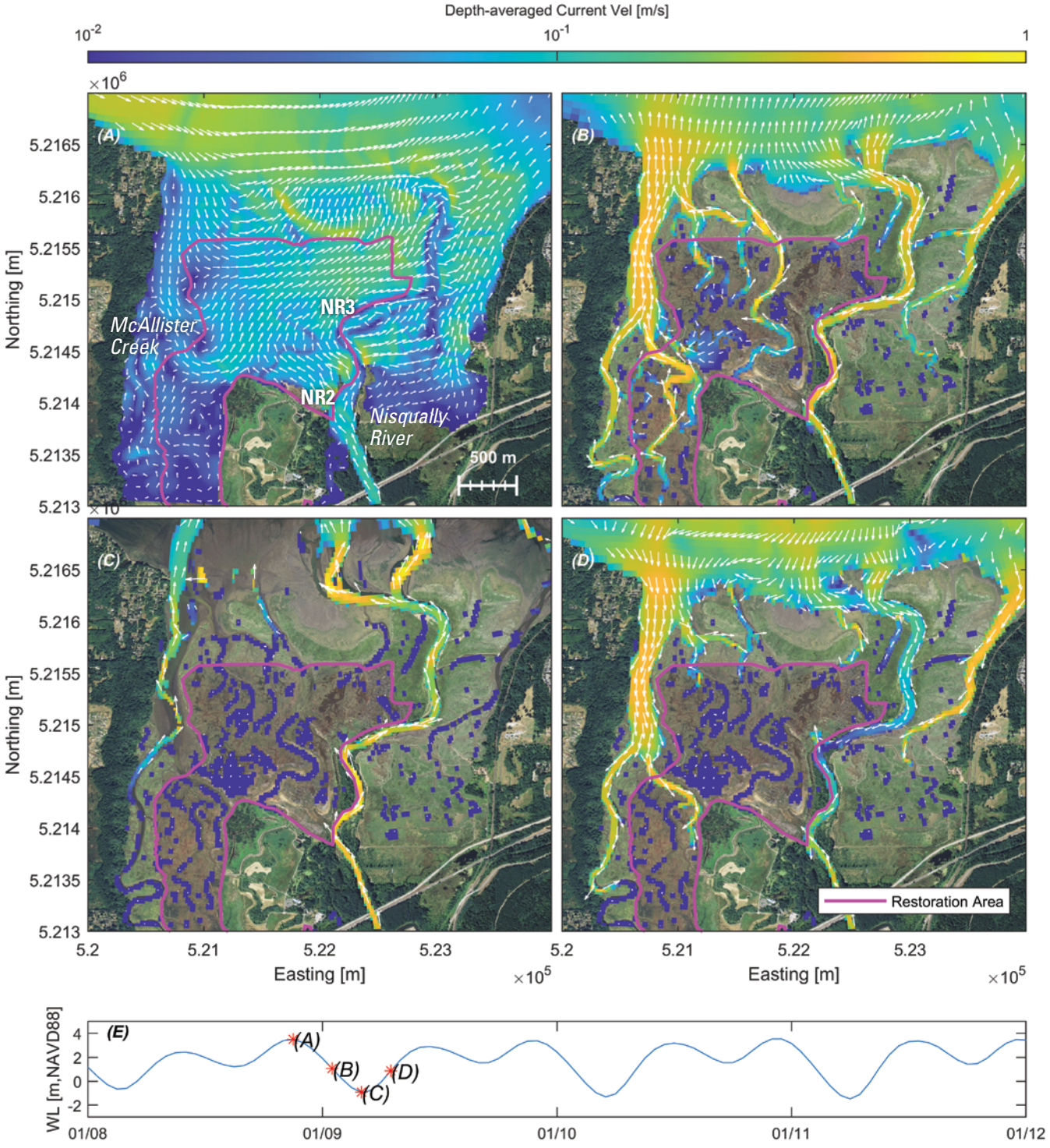

January 2017

2009 restoration area is increasingly directed offshore (north) closer to the river mouth and downstream from site NR3, presumably as a result of greater river influence. With the ebbing tide, transports are directed offshore across the entire delta and are increasingly confined to the narrow channels as the water levels decline (fig. 21*B*). At low tide, the delta is mostly exposed with transport from McAllister Creek and the Nisqually River directing water offshore (fig. 21*C*). With the rising tide, velocities are highest in McAllister Creek and eventually water levels impede the river discharge and force flow into the restoration at site NR3 (fig. 21*D*).

The modeled inundation frequency during a spring-neap tidal cycle was 25–65 percent over the bare marsh platform and as much as 100 percent in the deeper tidal channels (fig. 22*A*). Modeled spring-neap current velocities show strong offshore-directed flow out of the river and across most of the northern boundary of the restoration area and predominant on-shore flow through McAllister Creek (fig. 22*B*). The influence of river discharge on flow in the restoration area is clear, with river flow routed partially across the lower left bank near site NR3, where the levee elevation is lowest. A general counter-clockwise circulation pattern across the central region of the restoration was observed where weak landward residual flow through McAllister Creek appears balanced by offshore flow through the narrow D1–D4 channels. A similar pattern observed in summer suggests the residual flow is in part driven by the river flow and tidal exchange, the latter of which favors strong flood flow through the larger and deeper McAllister Creek channel than the four smaller D1–D4 inlet channels with shallower sills (fig. 22*B*).

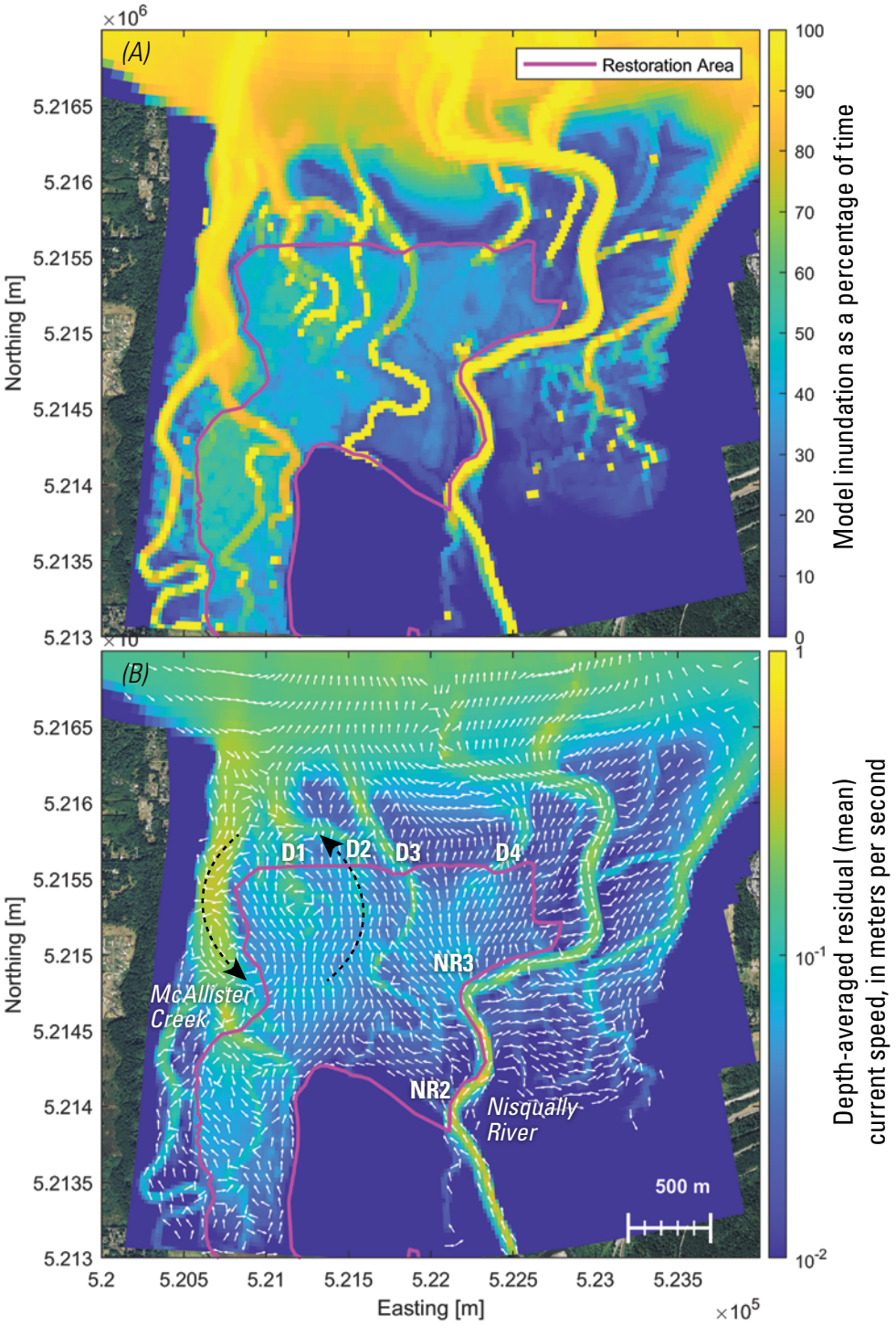

Figure 22. Maps showing modeled inundation as a percentage of time (*A*) and depth-averaged residual (mean) current speed (log-scale colors) and direction (small arrows) over an average spring-neap tidal cycle (14.5-days) showing river flow through the restoration area near site NR3 and out through the four D1–D4 channels balanced by flow in through McAllister Creek, which sets up counterclockwise circulation (dashed arrows) inside the restoration area. m, meter.

Figure 21. Maps showing modeled instantaneous depth-averaged current velocity (log-scale colors) and directions (arrows) near the restoration area for points in tide (high tide [*A*], max ebb [*B*], low tide [*C*] and max flood [*D*]) noted with stars in (*E*). m, meter; m/s, meter per second; NAVD88, North American Vertical Datum of 1988; WL, water level.

Modeled Sediment Transport—Current Conditions

Sediment Accumulation

The patterns of modeled sediment accumulation from IS simulations accounting for all processes examined and sediment on the bed were relatively similar among the R2–R4 sediment configurations that best fit measured SSC relations (figs. 18 and 19) with more accumulation in winter (fig. 23) than in summer (fig. 24). Winter simulations of mud for model configuration R1 projected widespread erosion and only a few areas of accumulation at high elevations (fig. 23*A*). In contrast, model configurations R2–R4 resulted in mud accumulation near site NR3 and along distributary channel levees in the restoration area (fig. 23*C*, *E*, *G*, arrows in 23*E*). More mud accumulation (2.0–2.5 centimeters [cm]) was predicted with model configuration R2 than with R3 (0.5–1.0 cm) but R2 accumulation was much patchier between large areas of erosion (fig. 23*C*). In contrast, accumulation was widely distributed with configuration R3 (fig. 23*E*). Model configuration R4 predicted mud accumulation near site NR3 and at high elevations near McAllister Creek (fig. 23*G*). Winter simulations predicted much lower accumulation of sand in the restoration area than mud and only fine sand showed any notable accumulation (fig. 23*B*, *D*, *F*, *H*). Configuration R3 predicted the greatest accumulation of fine sand which was primarily restricted along channel edges and in the outer reach of McAllister Creek (arrows in fig. 23*F*). Differences in sand accumulation and erosion are due to the interactions of mud and sand as parameters governing sand transport were not changed. Variation in sand transport also may be due to the varying initial bed thickness that was derived from the bed generation simulations.

Simulations of summer sediment transport showed considerably lower accumulation than winter but similar final spatial patterns of mud and sand deposition (fig. 24). Less mud accumulation in summer than in winter for R2–R4 (fig. 24*C*, *E*, *G*) is consistent with lower mud delivery in summer than in winter. Less erosion of mud in summer than in winter for all configurations, especially R1 (fig. 24*A*) points to reduced fluvial delivery and lower wave energy.

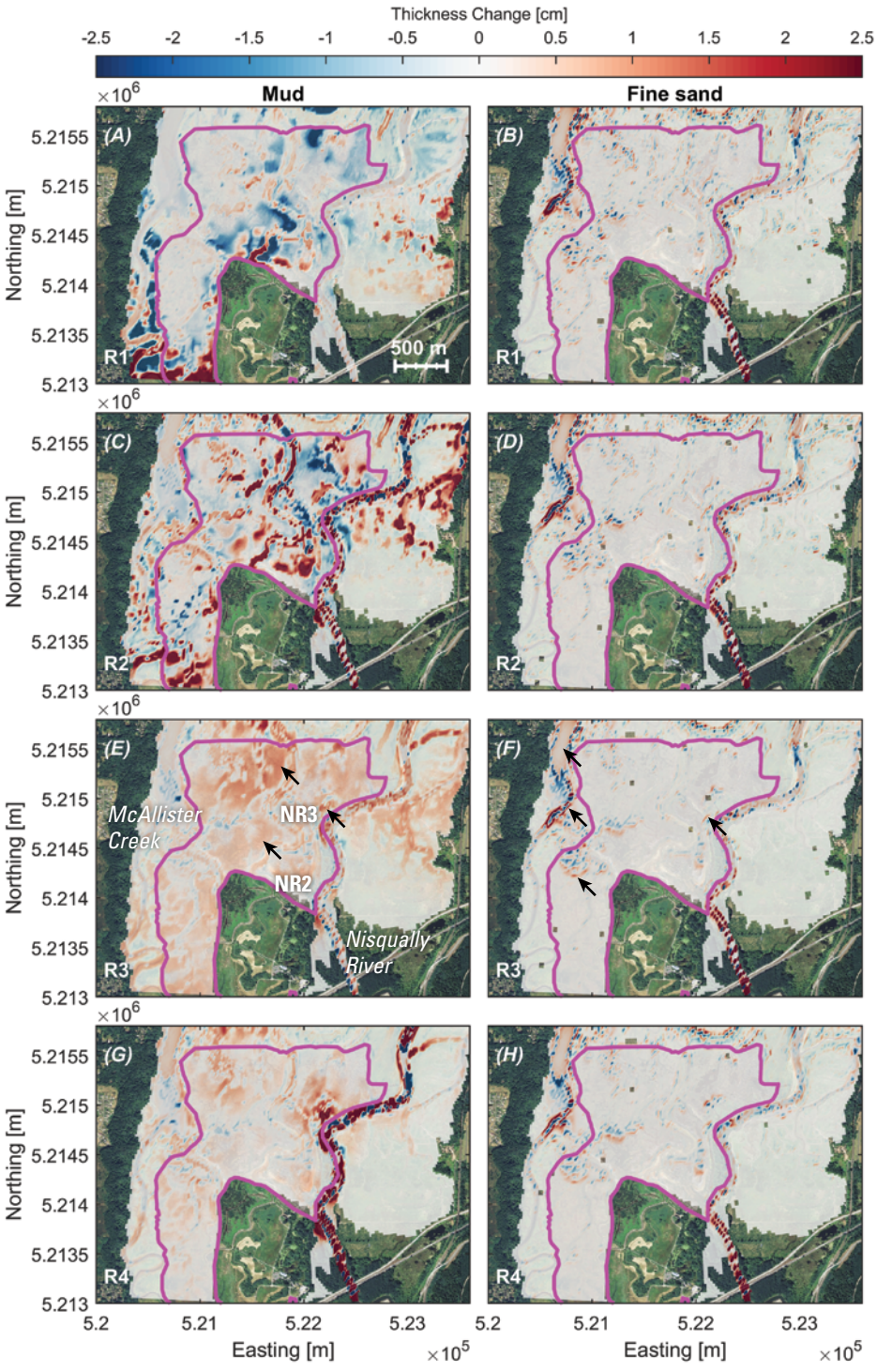

Figure 23. Maps showing modeled mud and fine sand accumulation/erosion for initial sediment on the bed (IS) winter simulations R1 (*A*, *B*), R2 (*C*, *D*), R3 (*E*, *F*) and R4 (*G*, *H*) with examples of accumulation near site NR3 and along levees (arrows). cm, centimeter; m, meter.

Similar restoration-area patterns of sand accumulation with slight reduced magnitudes of accumulation in summer than in winter for all configurations suggest that despite greater fluvial sediment input in winter, direct delivery has minimal influence on coarse material dynamics in the restoration area (fig. 24*B*, *D*, *F*, *H*). Sand accumulation and erosion patterns in McAllister Creek were consistent with those elsewhere in the restoration area, suggesting they are more closely aligned with hydrodynamic processes operating throughout the year than seasonal variations in river sediment delivery.

Mean Sediment Transport

Mean sediment transport and transport during discrete events including stream floods, storms, and waves were examined in terms of direct and indirect transport pathways that reflect different physical transport processes.

Direct transport is sediment transported directly from the river to the nearshore and restoration. Direct transport into the restoration occurs along the left (east) riverbank (fig. 5) and predominantly during high tides when the lower portions of riverbank are breached (fig. 25). Indirect transport is sediment transported into the restoration from the tidal flats across the northern restoration boundary (fig. 5). Indirect transport occurs with the tidal flood as sediments in suspension and those resuspended by currents and waves are transported southward to the restoration area (fig. 25).

The model indicates that the mean trajectory of sediment is directed down the Nisqually River to the tidal flat (fig. 25). Direct transport of mud or sand into the restoration area from the river primarily occurs near site NR3 and along the left bank of the river downstream from site NR3. Minimal sand transport to the restoration area was simulated in NIS runs and therefore is not shown in figure 25. NIS simulations of mean mud transport show most direct input to the restoration area via the left bank near and downstream of site NR3 and substantial transport across and out of the restoration area along the northern boundary (fig. 25*A*–*D*), particularly for simulations of low settling velocity (fig. 25*A*, *C*). Mean NIS mud transport also is predicted to enter the restoration area from McAllister Creek for R1–R3 simulations (fig. 25*A*–*C*).

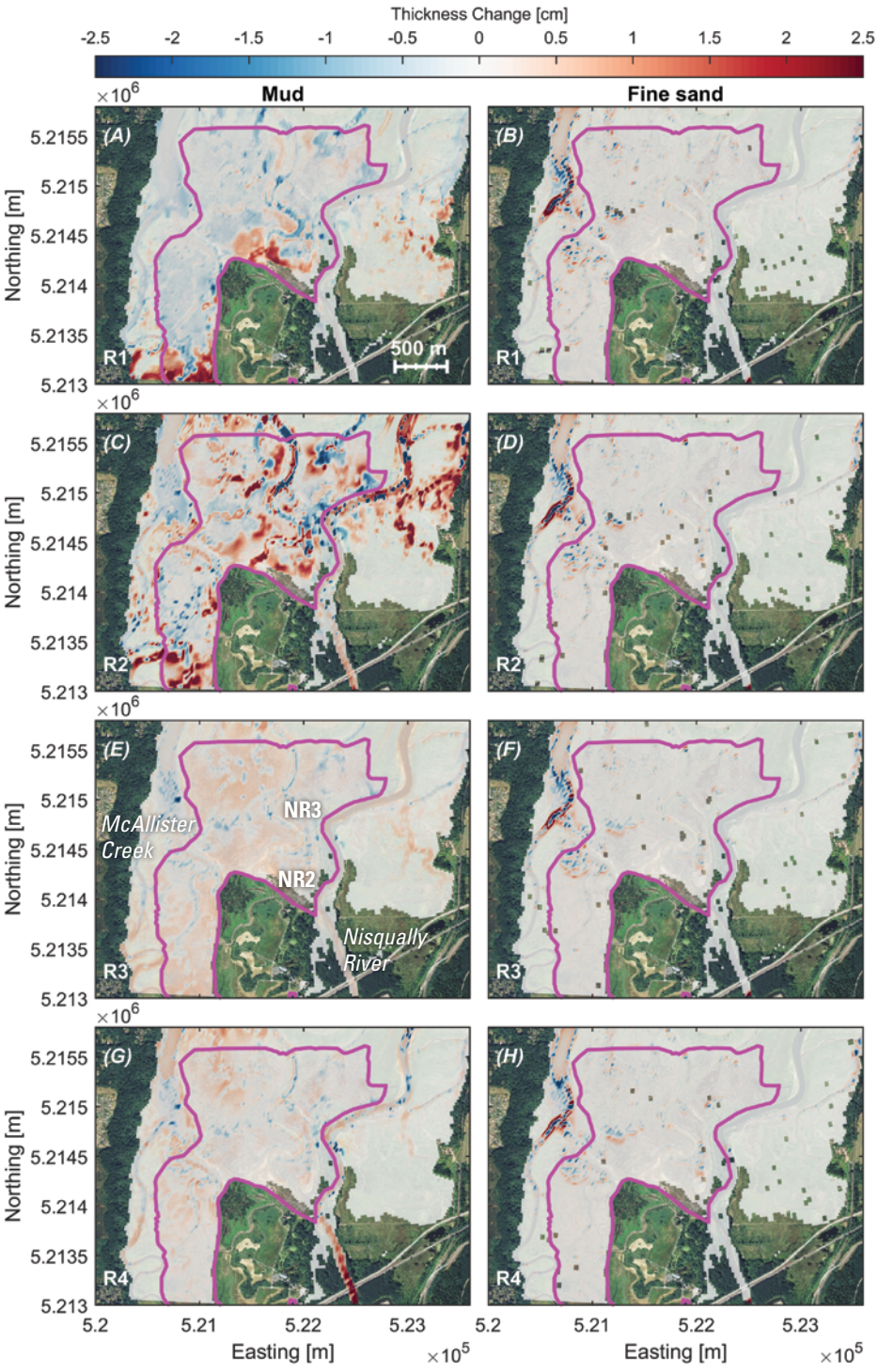

Figure 24. Maps showing modeled mud and fine sand accumulation/erosion for initial sediment on the bed (IS) summer simulations R1 (*A*, *B*), R2 (*C*, *D*), R3 (*E*, *F*) and R4 (*G*, *H*). cm, centimeter; m, meter.

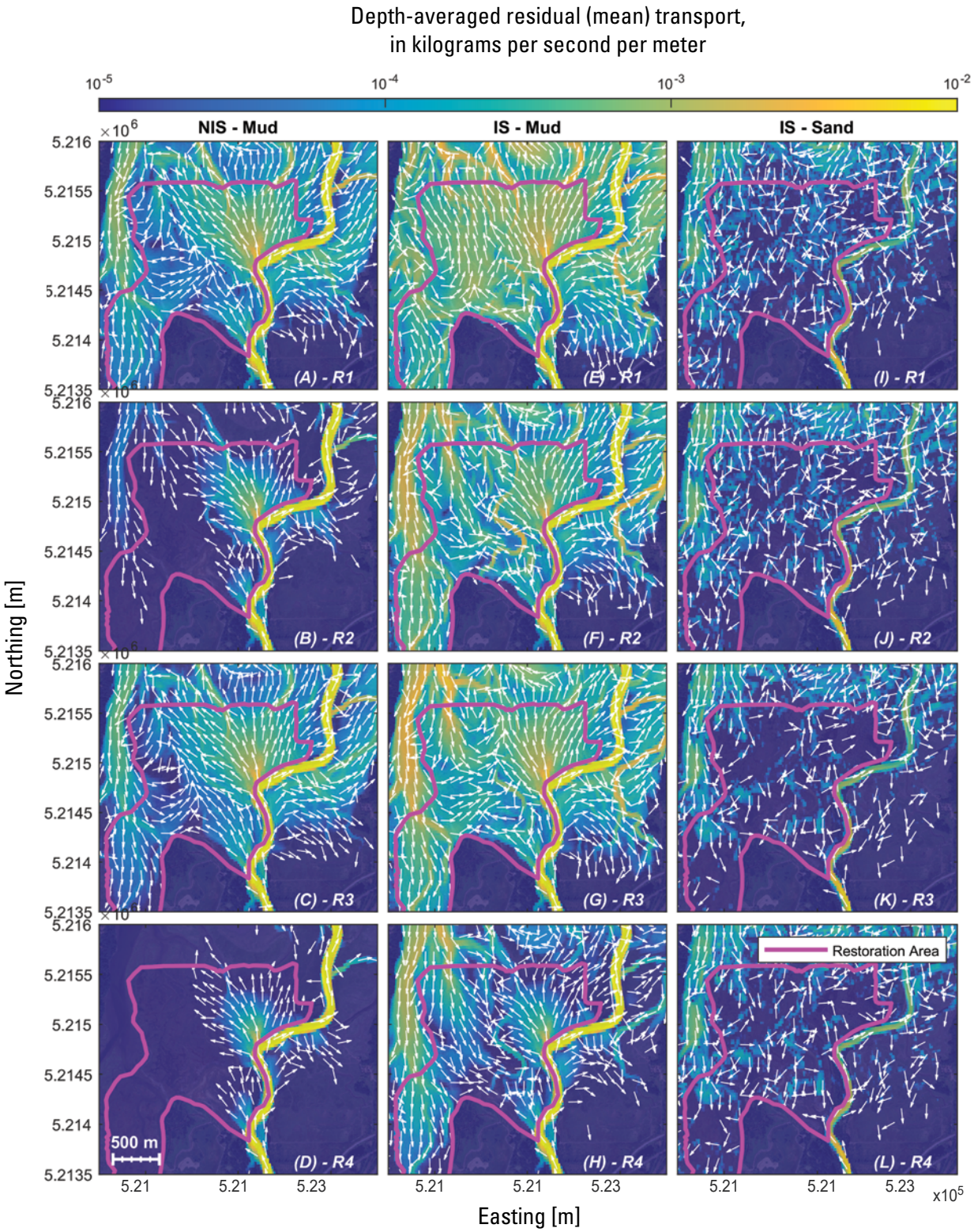

Figure 25. Maps of residual (mean) transport (log-scale colors) and directions (arrows) for winter no sediment on the bed (NIS) simulations of mud for model sediment configurations, R1 (*A*), R2 (*B*), R3 (*C*), R4 (*D*); initial sediment on the bed (IS) simulations of mud for model sediment configurations, R1 (*E*), R2 (*F*), R3 (*G*), R4 (*H*); and initial sediment on the bed (IS) simulations of sand for model configurations, R1 (*I*), R2 (*J*), R3 (*K*), R4 (*L*), with respect to the restoration area. m, meter.

Mean IS mud and sand transport revealed considerably more material moving into, across, and out of the restoration area than in NIS simulations (fig. 25*D–L*). The overall greater amount of transport in IS simulations suggests that the hydrodynamics are sufficiently great to resuspend, entrain, and move bed material and add it to existing fluvial delivery. The patterns of mud transport were similar among IS and NIS simulations including transport directed into the restoration near site NR3 and McAllister Creek and out of the restoration area along most of the northern boundary (fig. 25*A–H*).

Sand transport into the restoration area was 2–3 percent of the total sediment delivered to the delta by the river. Direct and indirect IS simulations of riverine fine-sand transport was principally to the tidal flats and offshore (fig. 25*I–L*). Sand transport was directed into McAllister Creek and relatively high along the entire creek channel. Sand transports were similar across simulations R1–R4 because sand transport parameters remained unchanged while only the initial availability of sand on the bed varied.

Fluvial Sediment Routing

The contributions of different sediment sources and transport processes was evaluated by isolating fluvial sediment delivery across the left bank "direct" boundary from the total owing to redistribution of fluvial and existing bed sediment across the northern boundary (fig. 5). The total mass of mud delivered to the delta from the Nisqually River for the winter 2017 NIS simulation was about 14,000 metric tons (fig. 26). Except for R1 simulations, most of this mud (8,000–14,000 metric tons) settled within the model domain and delta. During R1–R4 simulations, from 1,900 to 2,300 metric tons of mud, equivalent to about 14–16 percent of the fluvial load, settled in the restoration area (fig. 26). The variability in mud delivery to the restoration area among the four model configurations was lower than the variability in delivery predicted for the rest of the delta, perhaps as a result of its proximity and smaller area. Very little sand settled in the restoration area in the NIS simulations for all configurations (fig. 25).

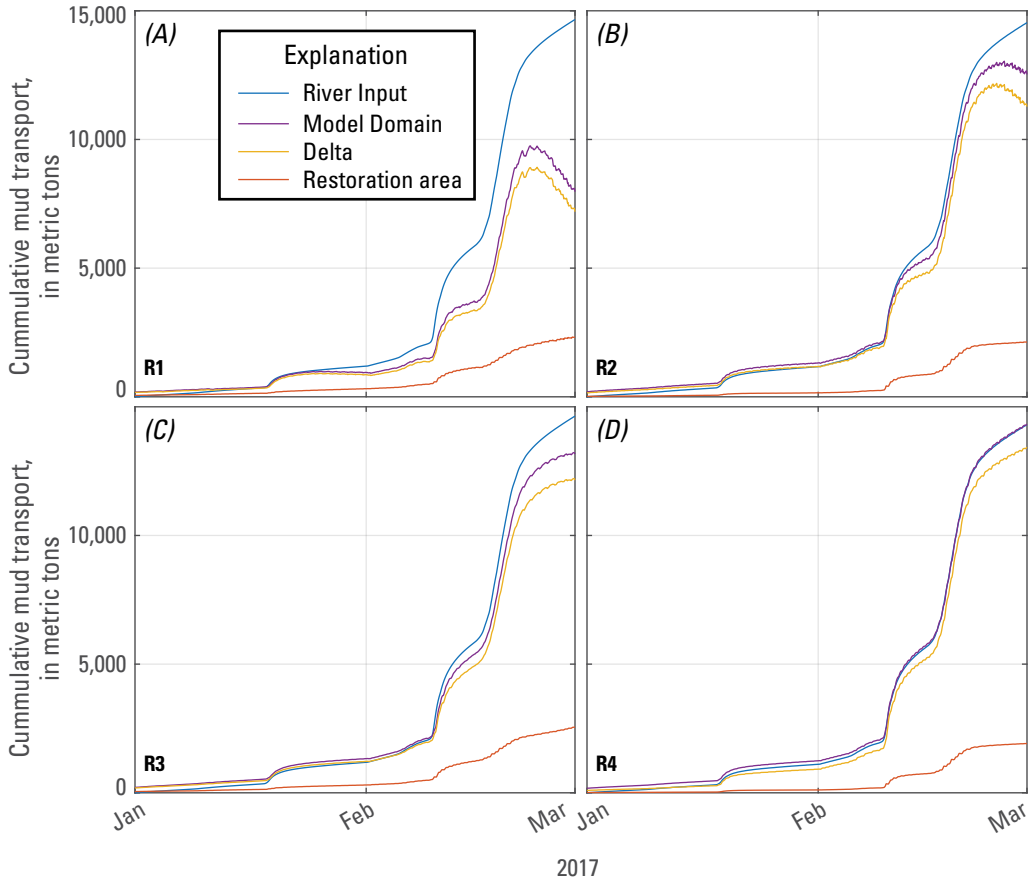

Figure 26. Graphs showing simulated cumulative mud transport by the river, across the entire model domain, delta, and into the restoration area during winter 2017 with no initial sediment on the bed (NIS) for the four model sediment configurations, R1 (*A*), R2 (*B*), R3 (*C*), R4 (*D*).

Total Sediment Flux and Net Delivery

Initial sediment on the bed (IS) simulations provide insight into indirect transport sediments into and out of the restoration area during periods of resuspension. Whereas the direct fluvial transport of mud into the restoration area was relatively insensitive to model sediment configurations (R1–R4), the indirect transports varied with some results showing net export (for example, R1, fig. 27*A*, *E*). Net sediment export simulated by model configuration R1 is consistent with it serving as an endmember of low settling velocity and low critical bed shear that are suspected to under-represent the entire distribution of sediment across the Nisqually River estuary. In contrast, model configurations R2–R4 were associated with indirect transport equivalent to or greater than direct transport into the restoration area leading to a net input of mud over winter and summer simulations (fig. 27*B–D*, *F–H*). IS simulations show that in addition to much greater fluvial sediment delivery in winter than in summer, indirect delivery of mud to the restoration area can be equivalent or greater than direct delivery.

The variability in indirect import for simulations R2–R4 is considered here to best bracket the settling velocity and critical bed shear values across the study area based on simulated and measured SSC (figs. 17–20) and was relatively low. Net sediment flux into the restoration area for simulations R2–R3 was 3,000–5,700 metric tons in winter and 2,300–2,500 metric tons in summer. The predicted export of about 7,000 metric tons under simulation R1 is consistent with excessively low settling velocities and critical bed shear values for the varied sediment composition of the entire system and overpredicted the measured suspended-sediment concentrations (figs. 17–20). Such low settling velocities lead to extended periods of time in suspension for transport away from the restoration area, and low critical bed shear values inflate potential scour and erosion that have not been observed (fig. 9)

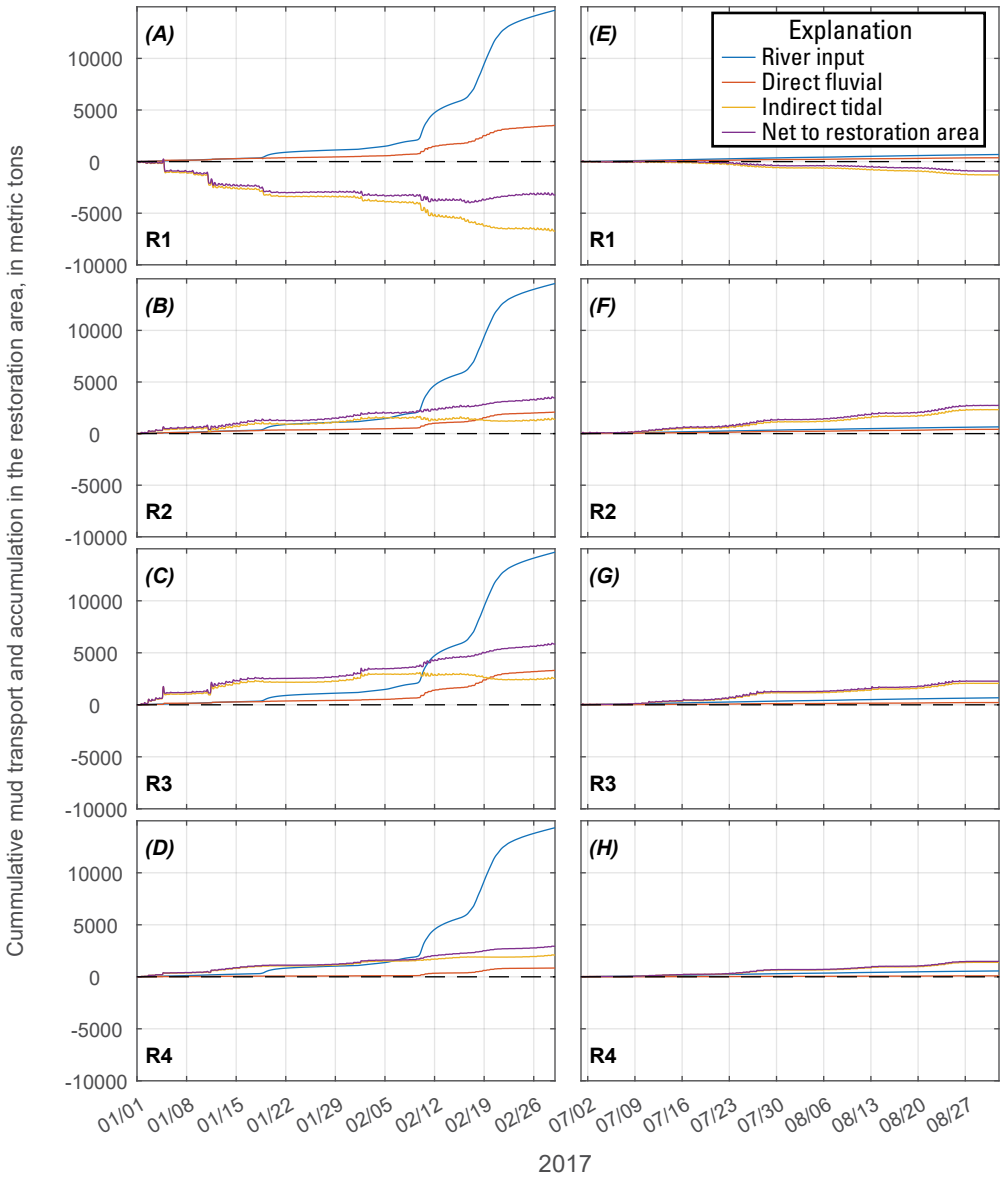

Figure 27. Graphs showing simulated cumulative mud transport from the river into the restoration area by direct (fluvial) and indirect (tidal) pathways with initial bed sediment (IS) for the four model sediment configurations, R1–R4 during winter 2017 (*A–D*) and summer 2017 (*E–H*). Positive values indicate import while negative values indicate export from the restoration area.

Model configuration R4, with higher critical bed shear and settling velocity effects on SSC than measured (figs. 17–20), showed accuracy in areas dominated by sand and is considered here to underestimate mud transport. Summer flux results likely represent maximum values, as they may be biased high by an initial bed sediment configuration that reflects high winter mud input.

Principal Sediment Transport Processes

Variations in the direct and indirect transport of sediment to the restoration area are the result of interactions among fluvial sediment loading, existing nearshore geomorphology and substrate, and the processes associated with river flow, winds, waves, tides, and circulation. Fluvial sediment influence on the restoration area is best observed during winter—two prominent river discharge events on February 10 and 19, 2017, increased direct transport into the restoration area by 400–500 percent in response to four-fold increases in flow (fig. 28*B*, *E*). In contrast, indirect transport during these events was small relative to periods of high waves associated with northern winds capable of redistributing bed sediment and low river flow (for example, January 4 and 10, 2017, fig. 28*D*, *F*). Direct mud transport was an order of magnitude lower in summer than in winter; indirect transport was an order of magnitude higher in summer than direct transport, indicating the importance of waves in redistributing sediment and affecting accumulation when fluvial sediment input is low (fig. 28*K*, *L*).

In addition to fluvial sediment loading and wave-driven resuspension, the model shows strong spring–neap variability of sediment transport into the restoration area. Although obscured in winter by large discharge events, peak daily sediment transport in summer almost always occurred during spring tides (fig. 28*G*, *K*, *L*). Whereas peak direct transport correlated most strongly with maximum daily water-level

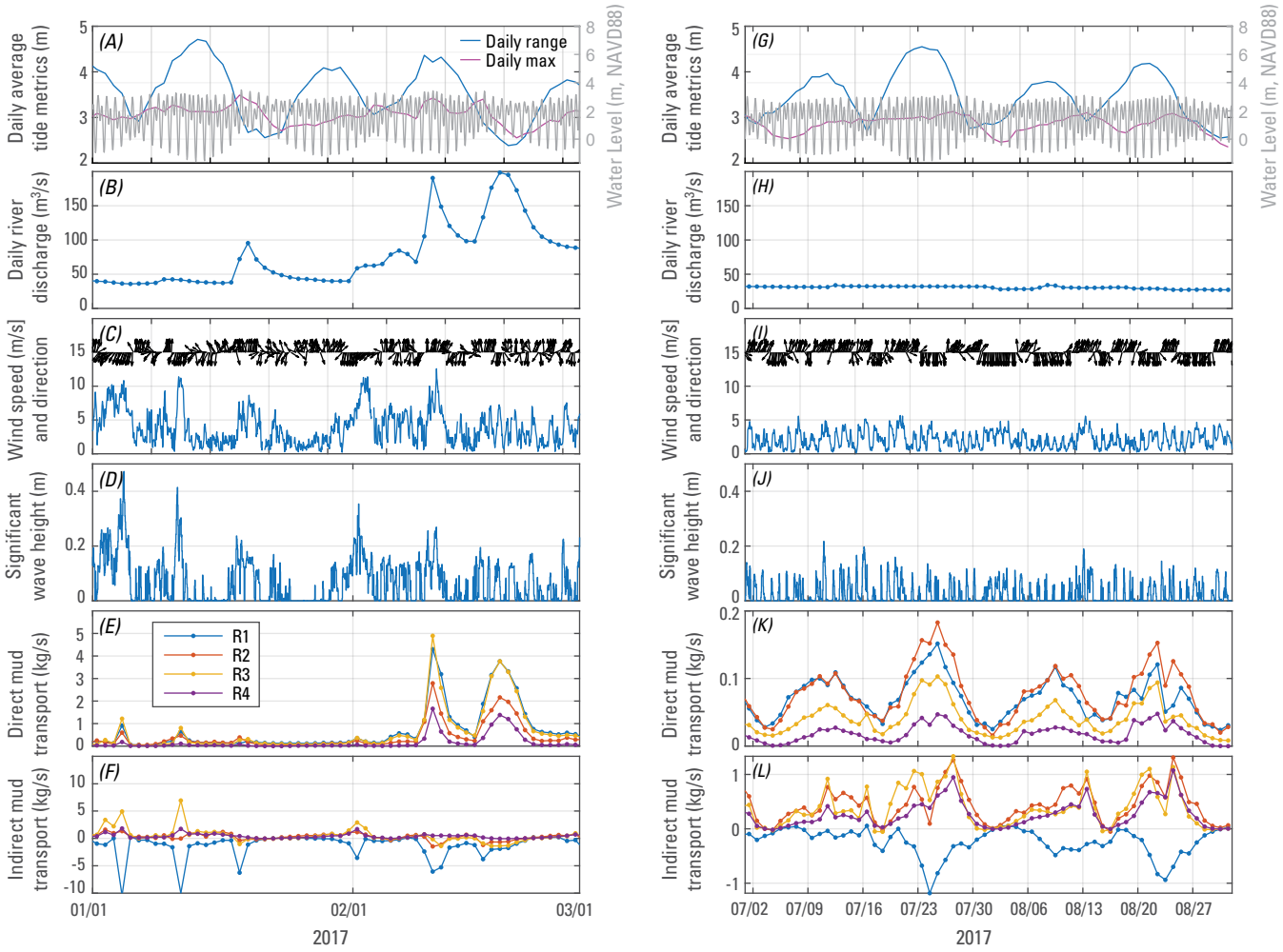

Figure 28. Graphs showing daily tide water-level elevations and ranges (*A*, *G*), daily river discharge (*B*, *H*), wind speed (line) and direction (arrows) (*C*, *I*), significant wave height (*D*, *J*), and resulting mud transport associate with direct (*E*, *K*) and indirect (*F*, *L*) pathways for the four model sediment configurations for January–February 2017 (*A*–*F*) and July–August 2017 (*G*–*L*). kg/s, kilogram per second; m, meter, m/s, meter per second; m³/s, cubic meters per second; NAVD88, North American Vertical Datum of 1988.

elevations (fig. 28*G, K*), indirect mud delivery, particularly during summer, corresponded with or immediately followed peak daily tidal range (fig. 28*G*, *L*). Peak direct mud transport into the restoration area during maximum water-level elevations may be related to tidal backwatering effects on fluvial sediment routing that retard downstream flow and help direct suspended fines through site NR3 and over the left (west) streambank. The greater indirect transport lagging the maximum spring range and occasionally the highest spring water-level elevation may be related to the larger spatial extent of resuspension during maximum inundation and subsequent trapping on the ebb. Tide-range effects were less important during winter compared to high fluvial sediment delivery and high wave events generated by strong winds (fig. 28*B*, *C*, *D*).

Model Uncertainty

Realistic sediment transport and morphodynamic models are challenged by complex spaciotemporal variability and uncertainty in sediment-size distribution, bed composition and stratigraphy, sediment transport properties, and non-linear morpho-hydrodynamic feedbacks that influence sediment fate as the system changes. The limitations posed by these uncertainties and computational constraints to resolve geomorphic processes operating across large regions by sensitive to site-specific factors require numerical sediment transport modeling to simplify physics and reduce resolution and simulation times. The impacts of the inherent simplifications and unknowns of this model study, however, are believed, in general, to be smaller than the modeled uncertainty for varying cohesive parameters. For example, the dimension reduction of the depth-averaged framework used, greatly simplifies computation and likely captures transports well, as prior observations show depth uniform current and SSC during high flows that drive most of the sediment movement (Curran and others, 2016a, b) when the shallow environment is well-mixed. Whereas the morphostatic assumption overlooks important sedimentation feedbacks to morphological change, the potential for substantially higher sediment accumulation is unlikely given the strong influence of waves in redistributing sediment (fig. 27) and recent studies of low accommodation space for sedimentation in similar river-delta settings (Grossman and others, 2020). The models here capture the uncertainty in sediment parameters that are often poorly known and, as shown, result in transport estimates varying by a factor of 2–3. Such uncertainty is expected to dwarf other unknowns and simplifications such as model resolution. Despite the range of predictions, all simulations indicate a general sediment deficiency within the system.

Sediment Budget of the Nisqually River Delta Marshes

Modeled annual to decadal sediment delivery, accumulation and predicted changes in bed elevation were used to evaluate the sediment budget of the Nisqually River Delta and model accuracy. Model results from 1984 to 2019 were used to derive an annual average budget of potential sediment input and accumulation within the restoration area prior to 2009, and for direct comparisons to measured changes since 2009. Model accuracy was evaluated by comparing simulated accumulation to (1) radioisotope-derived sedimentation rates from sediment cores representative of the last several decades, and (2) measured bed-elevation changes derived from repeat high-resolution lidar surveys conducted in 2011 and 2014 (fig. 9). The flux for 2016–17 was evaluated to place the results of our study into the context of long-term natural variability.

Modeled direct transport of mud to the restoration area during winter was well predicted by daily averaged Nisqually River mud discharge with R^2 values of 0.90–0.94 (fig. 29). The relation was poorer in summer, but overall flux in summer was extremely low and relatively insignificant. Direct transport of sand to the restoration showed a similar although comparatively less significant relation to fluvial delivery with R^2 ranging from 0.15 to 0.35. However, the delivery of sand was less than 1 percent of river input and so comparatively insignificant.

Wave energy and tidal range anomalies were observed to have the strongest correlations with indirect sediment (mud) transport to the 2009 restoration area (fig. 30), likely because waves enhance resuspension on the bed and tidal range is correlated with tidal currents enhancing transport. The resulting correlations between modeled and parameterized indirect mud transport ranged in skill, with the role of waves and tide range explaining from 31 to 64 percent of the variance (fig. 30). Results were similar for indirect sand transport regressions (not shown) with an explained variance of 43–47 percent.

The standard error associated with the regression fits between modeled and parameterized transport was evaluated as standard deviation of the coefficient (table 7). The regression uncertainty of the regression coefficients was similar to the range of coefficients in model configurations R2–R4. We therefore considered the range of fluxes and associated error of the model configurations in our calculations to account for the uncertain range and sensitivity to sediment properties in the system.

The regression relations for direct (fig. 29) and parameterized indirect transports (fig. 30) were used to estimate the annual direct and indirect sediment delivery to the restoration area over the 35-year period (1984–2019). The mean, minimum, and maximum annual delivery reflect the range of outputs from sediment configurations R2–R4; R1 was not included given the over-estimated SSC and net export was inconsistent with independent data from elevation change and sediment core accretion chronologies. Estimated sediment delivery to the restoration area was analyzed for (1) 2011–14 to compare measured change from repeat lidar, (2) water years 2016–17 of this study to place our

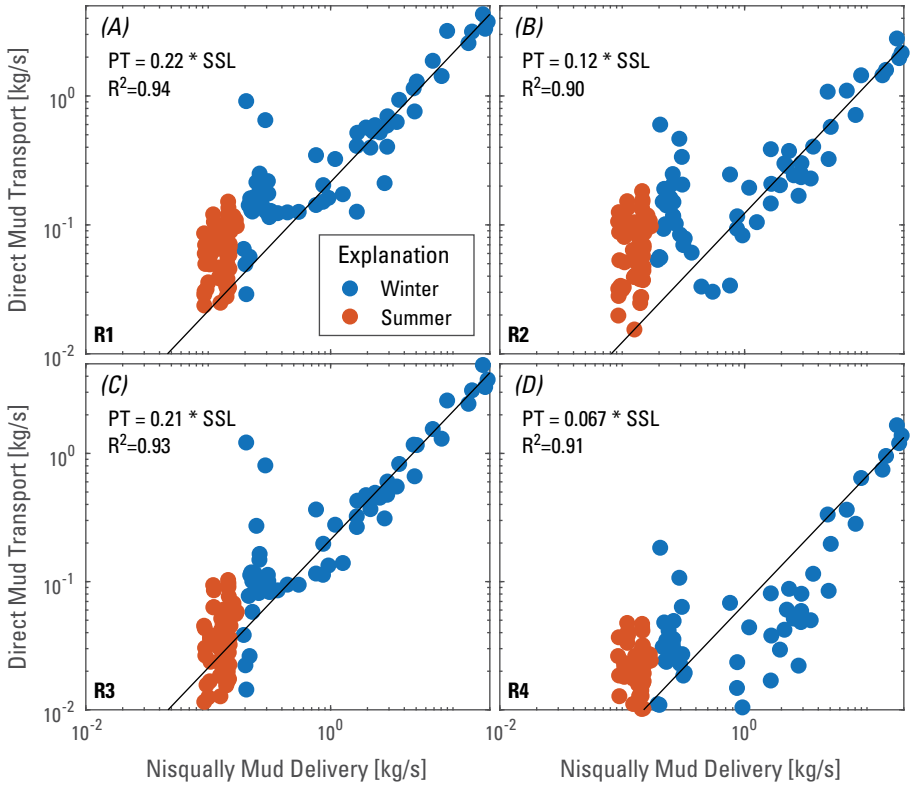

Figure 29. Graphs showing fits between modeled daily averaged direct mud transport rate or parameterized transport (PT) into the restoration area and daily averaged suspended mud delivery rate by the Nisqually River in winter and summer for the four model sediment configurations, R1 (*A*), R2 (*B*), R3 (*C*), R4 (*D*). kg/s, kilogram per second; PT, parameterized transport; SSL, suspended-sediment load.

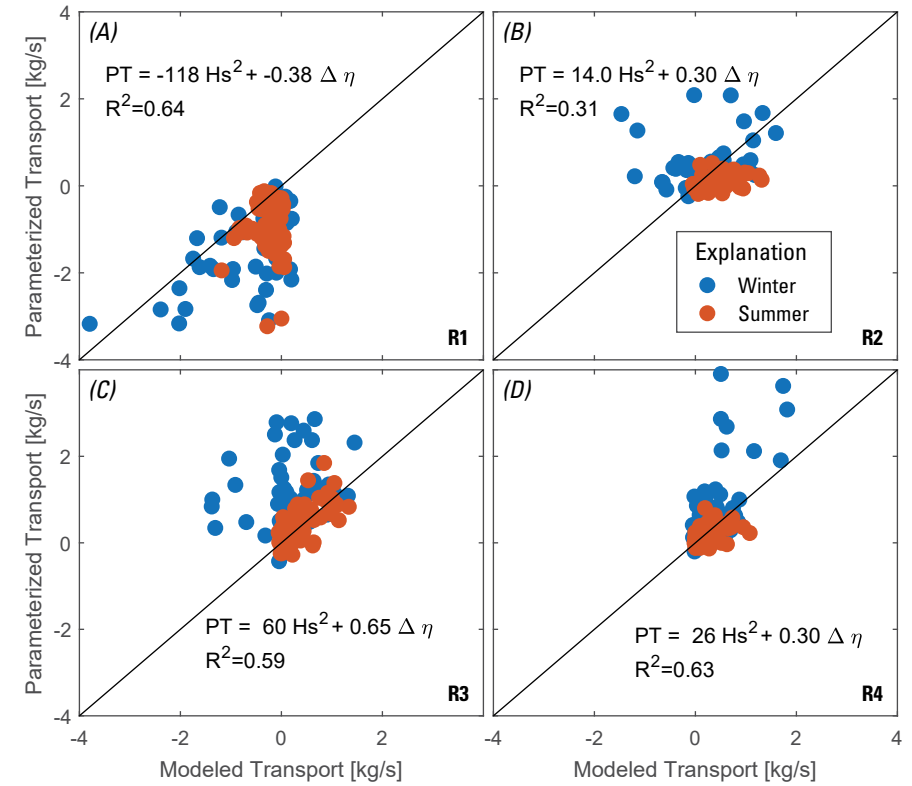

Figure 30. Graphs showing parametrized transport versus modeled transport of mud fluxing indirectly into the restoration for the four model sediment configurations, R1 (*A*), R2 (*B*), R3 (*C*), R4 (*D*). The regression equations show the estimated relation between parameterized transport (PT) and significant wave height squared (Hs^2) and tidal range ($\Delta\eta$).

Table 7. Standard error expressed as the standard deviation of the modeled to parameterized mud transport regressions for the four model sediment configurations.

[Hs^2, waves; $\Delta\eta$, tidal range]

Sediment configuration	Indirect regression for mud			
	Hs^2 coefficient	Standard error	$\Delta\eta$ coefficient	Standard error
R1	−118	7.8	−0.38	0.16
R2	14	4.1	0.30	0.09
R3	60	5.1	0.65	0.17
R4	26	2.4	0.30	0.05

Table 8. Estimated sediment delivery by the Nisqually River and transport to the restoration by direct river breaching and indirect tidal forcing across the delta for the minimum, maximum, and mean of sediment configurations R2, R3, and R4.

[max, maximum; min, minimum]

Time period (water years)	Fluvial sediment delivery (metric tons)			Range	Mud transport to restoration area (metric tons)			Sand transport to restoration area (metric tons)		
	Total	Mud	Fine sand		Direct	Indirect	Total	Direct	Indirect	Total
2011–2014	362,520	181,260	90,630	Min	11,300	9,920	21,220	170	2,970	3,140
				Mean	22,320	25,640	47,960	390	3,730	4,120
				Max	35,430	46,820	82,250	590	4,360	4,950
2016–2017	292,230	146,110	73,060	Min	9,790	5,740	15,530	150	1,800	1,950
				Mean	19,340	15,410	34,750	340	2,260	2,600
				Max	30,680	28,330	59,010	510	2,650	3,160
Yearly average	92,400	46,200	23,100	Min	3,100	1,340	4,430	50	370	420
				Mean	6,110	3,240	9,350	110	460	570
				Max	9,700	5,850	15,550	160	540	700

results into context of longer-term variability, and (3) 1984–2019 to develop a long-term average of potential sediment flux (table 8).

The results indicate that higher flows measured in 2016–17 and 2011–14 led to about 58 percent and about 6 percent greater total and mud fluvial sediment delivery, respectively, than the estimated long-term average of 1984–2019 potential delivery had the 2009 restoration area been in place. Whereas the proportion of annual direct delivery to the restoration area of fluvial inputs was similar among time periods, annual indirect delivery varied and was higher in 2011–14 and 2016–17 than in 1984–2019, indicative of the greater influence of winds and waves. The fraction of mud directly delivered by the river over these longer time spans is estimated at 12–21 percent with a mean of 13 percent. Indirect mud transport to the restoration area as a percentage of mud delivered by the river is estimated to be 6–26 percent with a mean of 14 percent for 2011–14 (fig. 31*A*), 4–19 percent with a mean of 11 percent for water years 2016–17 (fig. 31*B*), and 3–13 percent with a mean of 7 percent for 1984–2019 (fig. 31*C*). The mean total sediment delivery to the restoration area including mud and sand as a percentage of the total river input is estimated to be 19 percent for 2011–14, 17 percent for water years 2016–17, and 14 percent for the long-term average 1984–2019. This variability is driven largely by differences in the influence of tidal and wind-related processes among the three time periods.

Comparison of Modeled Sediment Flux to Observed Change

The modeled magnitude of sediment flux is lower than observed by lidar change but in closer agreement with radioisotope-derived sediment accumulation rates in sediment cores (Drexler and others, 2019). The estimated annual average sediment flux into the delta and into the 2009 restoration area agree well with the spatial patterns of changes derived from lidar elevation differencing between 2011 and bias-corrected 2014 lidar data (fig. 9). The modeled spatial distribution of sediment accumulation over the more elevated

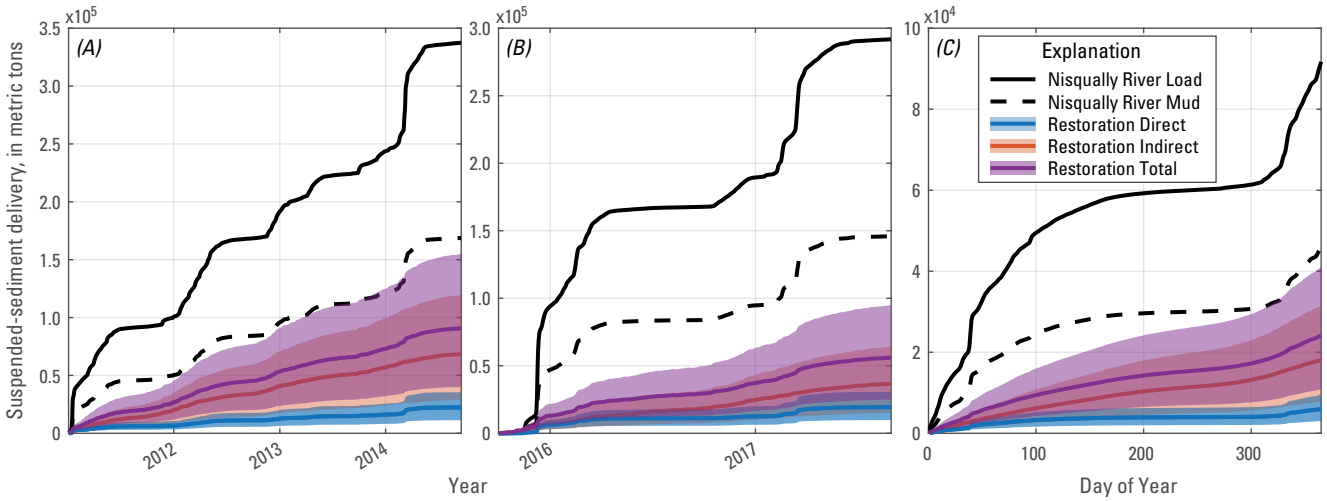

Figure 31. Graphs showing cumulative fluvial sediment delivery, fraction of fluvial mud delivery, and accumulation in restoration area from direct, indirect, and total sources during 2011–14 water years (*A*), 2016–17 water years (*B*), and 1984–2019 average (*C*). Shaded areas represent the range of simulated transport associated with the R1–R4 model sediment configurations.

regions of the restoration area and focused deposition along channel levees and site NR3, agree well with patterns in 3-year accumulation observed from lidar change (fig. 32), particularly for model configuration R3 (fig. 23). The discrepancy between land surface lowering and modeled accumulation near the mouth of the Nisqually River downstream from site NR3 may be related to vegetation bias adjustment, channel bank erosion and wetland retreat (Ballanti and others, 2017), and/or the morphostatic assumption of the model.

The lidar elevation difference between 2011 and 2014 suggests a volume increase of 253,000 cubic meters (m^3). This is equivalent to a total of 8.7 cm of sediment accumulation over the 2,600,409 square meters (m^2) of the restoration and an annual rate of 2.5 centimeters per year (cm/yr) assuming a density of 500 kilograms per cubic meters (kg/m^3) for mud and 1,600 kg/m^3 for sand. The modeled sediment accumulation of 98,000 m^3 represents about 40 percent of the amount derived from lidar differencing for the same period and lies within our modeled uncertainty in the range of estimates owing to variability in critical bed shear and settling parameters for mud. Even so, we interpret this difference to remaining bias in the lidar based results, which produce rates substantially greater than rates derived from sediment core accumulation.

The modeled sediment fluxes agree more closely with vertical sediment accumulation rates ranging from 0.31 to 1.23 cm/yr across the restoration area and outside previously diked marsh (Drexler and others, 2019). Mean accumulation rates of 0.79 cm/yr inside the restoration area were nearly double the rates outside the restoration area (0.42 cm/yr) (Drexler and others, 2019). The accumulation rates inside the restoration area also were higher closer to the old ring dike than at site NR3, consistent with our modeled results. Although spatial patterns of modeled accumulation are relatively consistent using the lidar approach, validation of the magnitude is limited by bias and inherent vertical error in both the lidar and our model results. Comparisons of modeled and core-based accumulation, however, agreed within 18–56 percent. Greater modeled accumulation compared to the cores may be explained by compaction affecting the core sediments and not accounted for in the model. Lastly, additional sources of sediment flux into the restoration area from processes like erosion of channel banks and marsh are not accounted for by the model.

Sea-Level Rise Vulnerability and Implications for Marsh Recovery Time and Restoration

Historical subsidence, restricted sediment delivery, and impending sea-level rise leave the Nisqually River Delta and restoration area investments vulnerable. The volume of subsided marsh platform within the 2009 restoration area below the 3-m elevation suitable for marsh development is estimated to be 2,352,000 m^3. Under the observed rates of sediment delivery and current rate of about 2.5 millimeters per year (mm/yr) of sea-level rise (Miller and others, 2018), 85–200 years are needed to fill the subsided platform to the elevation for marsh development (fig. 33). This estimate assumes uniform sedimentation across the subsided platform and accounts for the effects that sea-level rise will have on increasing the volume deficit to reach the 3-m grade of mean marsh occurrence. More than 18 years would be required to fill the subsided grade if 100 percent of the river sediment supply was directed to and retained in the restoration area. This scenario, however, would compromise the resilience of marshes surrounding the delta that also rely on Nisqually

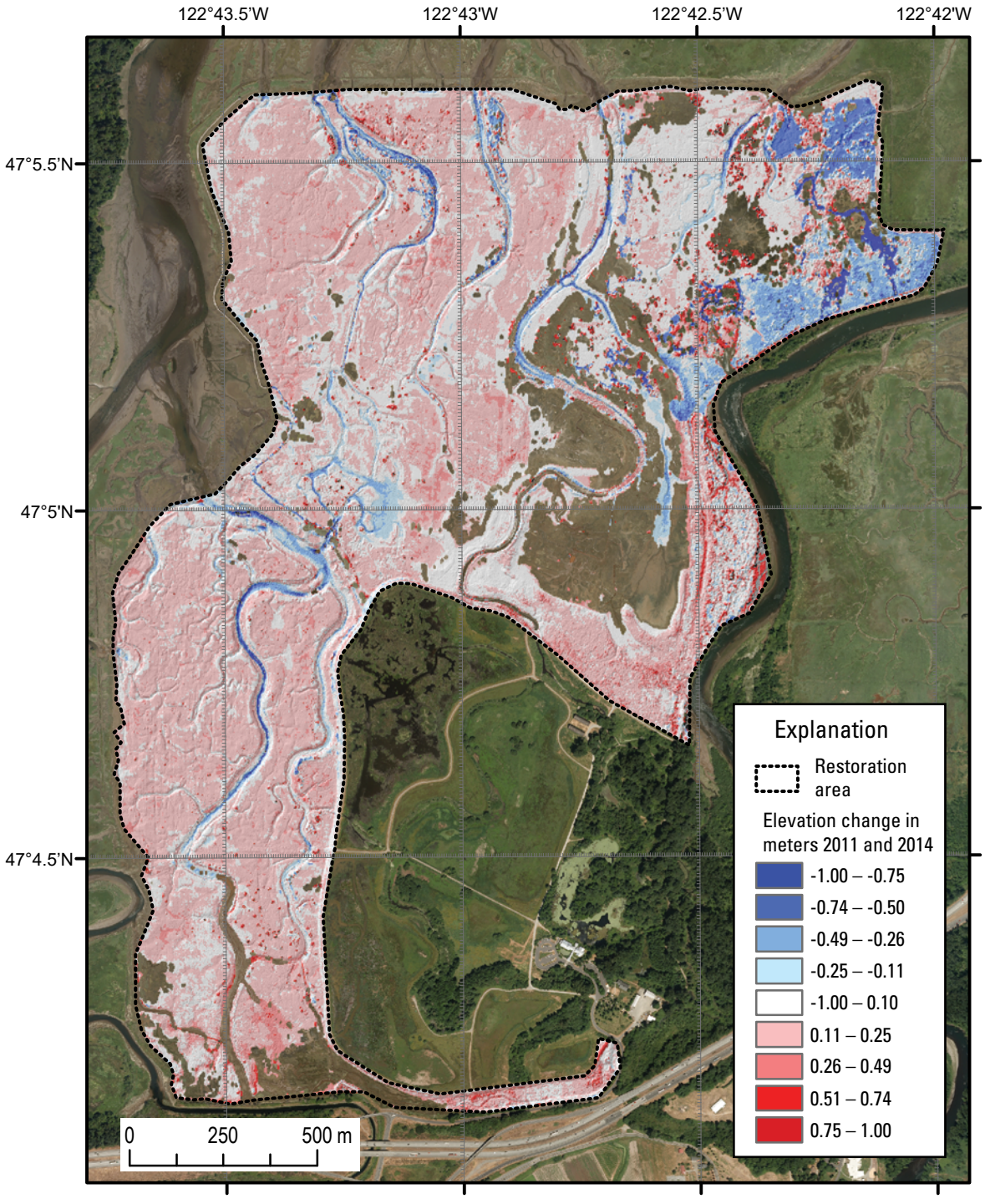

Figure 32. Map showing elevation change based on differencing the bias-corrected 2014 and raw 2011 lidar surveys. m, meter.

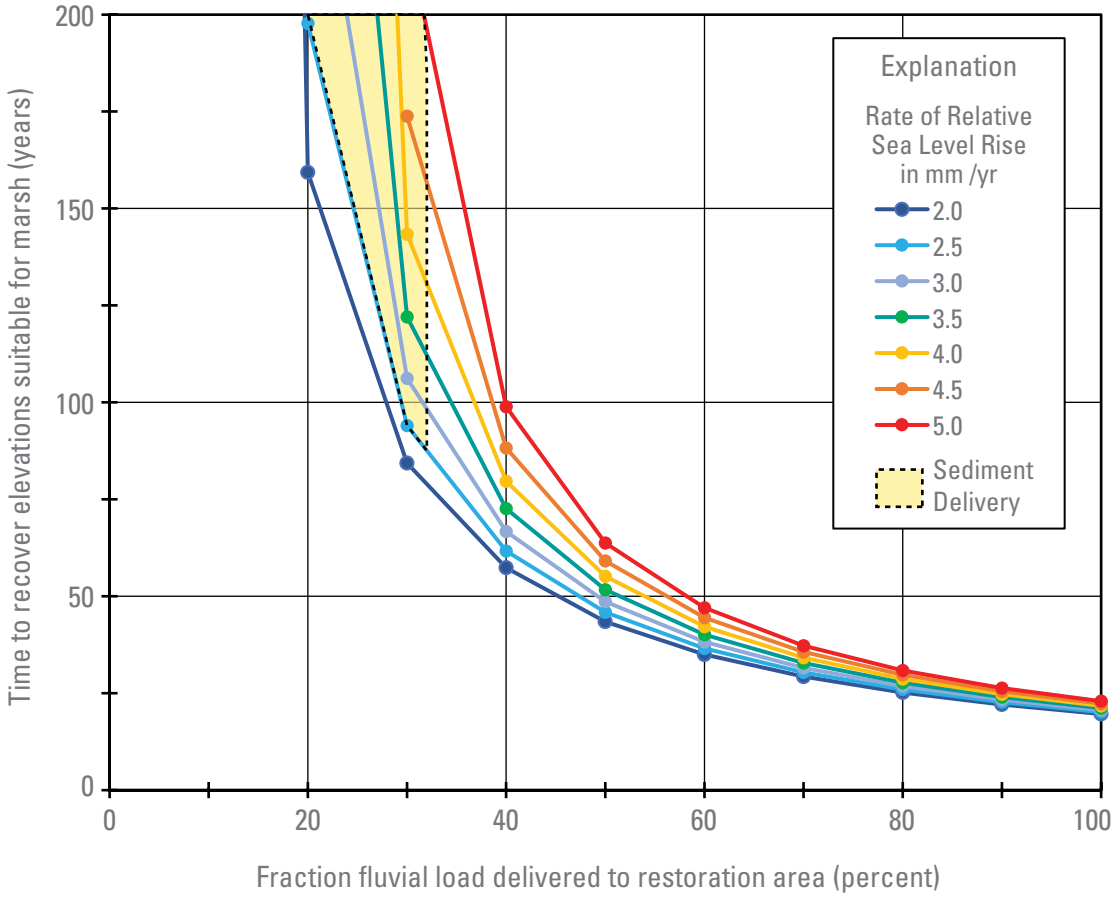

Figure 33. Graph showing time required to fill subsided marsh platform areas suitable for marsh with projected rates of sea-level rise (in millimeters per year [mm/yr]) given the fraction of the Nisqually River sediment load delivered to the restoration area. The estimate from this study implies that it will take 85–200+ years to re-establish marsh across the entire 305 hectares of restoration area with 14–32 percent of the fluvial sediment supply reaching the restoration area.

River sediment and are important to the overall functioning of the delta and goals of recovery.

Opportunities to Recover Sediment Supply

Schematized Model of Alternatives to Recover Additional Sediment

Four metrics derived from the schematized model were used to evaluate the relative potential of the identified restoration alternatives at site NR2 to enhance sediment delivery over existing conditions (fig. 7). These included (1) hydrodynamics, (2) sediment accumulation, (3) sediment routing efficiency, and (4) sediment transport efficiency. These metrics were evaluated for each combination of alternative, stream discharge, and sea level to inform how the alternatives may perform today and in the future. The schematized transports based on non-cohesive sediment transport formulations are comparable to the NIS "direct river delivery" modeling approach and evaluate the relative difference in alternative configuration to convey sediment to the restoration area in 2009.

Potential to Restore Additional Sediment Supply

The three channel alternatives showed an increase in sediment transport to the restoration area relative to today; channel alternative C (composed of a deeper and continuous gradient) was the most effective among the alternative geometries. No matter the channel alternative, an appreciable increase in flow and sediment delivery to the central subsided area requires larger flows at the 2-year or greater recurrence interval (fig. 34). The limited transport potential is likely controlled by the low elevation of the NR2 region within the tidal prism and low hydraulic gradient between the river at

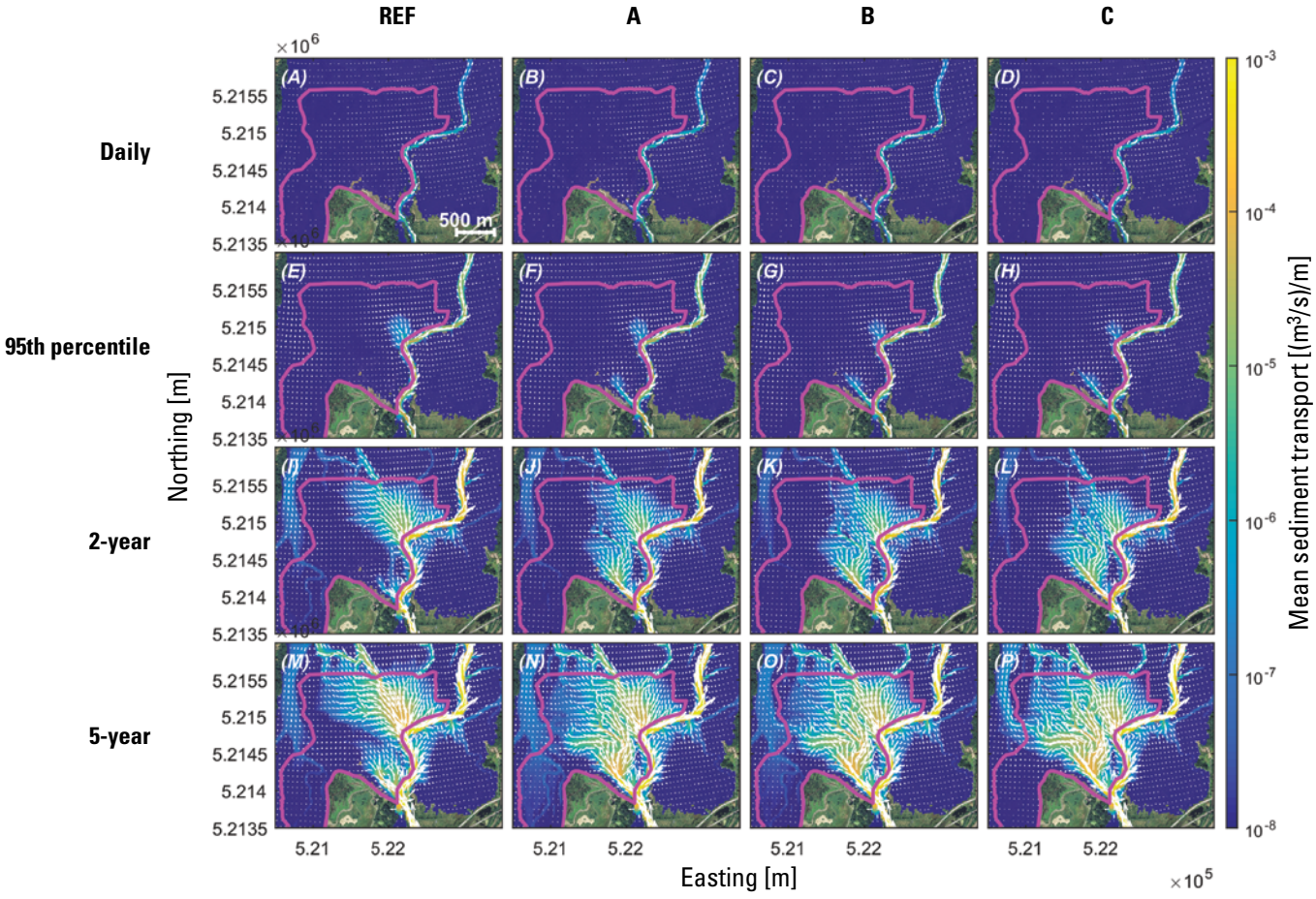

Figure 34. Maps showing mean sediment transport with a log scale for daily mean flow (*A*, *B*, *C*, *D*), 95th percentile daily flow (*E*, *F*, *G*, *H*), 2-year flood (*I*, *J*, *K*, *L*), and 5-year flood (*M*, *N*, *O*, *P*). Columns show results for the current reference condition (*A*, *E*, *I*, *M*) and three channel alternatives A (*B*, *F*, *J*, *N*), B (*C*, *G*, *K*, *O*), and C (*D*, *H*, *L*, *P*). m, meter; (m³/s)/m, cubic meters per second per meter.

site NR2 and downstream end of each channel alternative. As a result, only high streamflows during infrequent high tides (fig. 21) drive flow across the restoration area. During lower tides, configurations A and B—lacking connectivity to Leschi Slough—flow was limited to the channel. Only alternative C, with a continuous connection to Leschi Slough, promoted conveyance beyond high tide, and that was only appreciable during flows equal to or larger than the 2-year flood.

The modeled sediment accumulation across the restoration area indicates that the identified distributary restoration alternatives would add a nominal amount of sediment to the restoration area. Scaling the results for the frequency of each discharge class occurrence showed that the potential annual sediment delivery through these alternatives today would be about 800–1,000 m^3 when summing across the four discharge classes and their frequency of occurrence (fig. 35, table 9). Sand represented about 15–25 percent of the estimated total routed through the alternatives whereas silts comprised 75–85 percent. These are likely maximum estimates, given the large proportion of sediment delivery associated with 2- and 5-year flood events, which may or may not occur in any given 2- or 5-year period because of Alder Lake operations. The resulting potential for additional sediment accretion across the restoration area was 0.04–0.25 mm/yr (table 9). Although these accretion rates are averages assuming even distribution over the restoration area, the model suggests that sedimentation

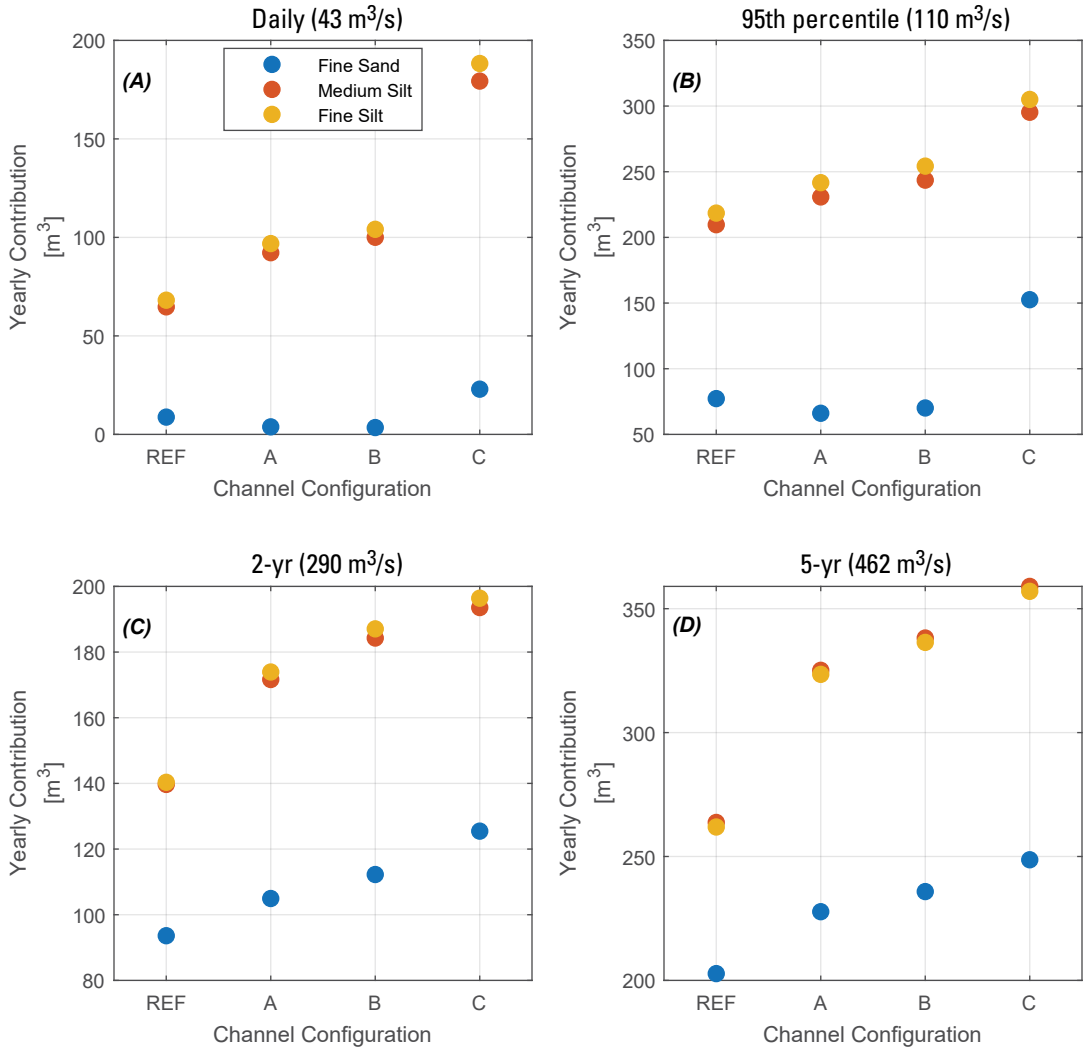

Figure 35. Graphs showing estimates of potential yearly sediment contribution (in cubic meters [m³]) to the restoration area from the identified alternatives and reference conditions for discharges of 43 (*A*), 110 (*B*), 290 (*C*) and 462 cubic meters per second (m³/s) (*D*). yr, year.

Table 9. Annual sediment routing and marsh accretion potential under present sea-level position for alternative C associated with the frequency of occurrence of modeled discharge class per year.

[Accretion potential is estimated assuming sediment transported evenly across 80 percent of the non-channel area of 2009 Browns Farm (308 hectares) restoration area. days/yr, days per year; m³, cubic meters; m³/yr, cubic meters per year; mm/yr, millimeters per year]

Discharge class	Occurrence (days/yr)	$<S_{Entrance}>$ (m³)	$S_{Entrance}$, year (m³/yr)	Accretion potential (mm/yr)
1	182.5	Max. 0.53 (C1_SL0)	94	0.04
2	18.3	Max. 14.5 (C2_SL0)	255	0.11
3	0.48	Max. 550.6 (C3_SL0)	264	0.11
4	0.19	Max. 3150 (C4_SL0)	599	0.25

resulting from the alternatives would be focused closer to the NR2 entrance and channel levees (fig. 34), similar to patterns observed near site NR3 (fig. 32).

Sediment Conveyance and Transport Efficiency of Channel Alternatives

To evaluate the capacity of the channel alternatives to convey sediment to the restoration area, the magnitude and composition of sediment transport through each alternative geometry were evaluated with the model. Metrics of channel routing and transport efficiency also were derived. In addition to varying amounts of sediment routed into each of the alternatives, the modeled sediment conveyance through each channel alternative varied greatly and each showed a rapid decrease with distance from the entrance of the channel at the Nisqually River (fig. 36). Tidally averaged sediment routed into each alternative increased from alternative A to C and increased an order of magnitude with each sequentially larger discharge class. With greater streamflow, sediment conveyance increased but even the highest flow of the 5-year event resulted in a steep decrease in transport between the middle and end of the restored channel, likely related to the potential for sediment aggradation along the pathway (fig. 36*C*).

Tidally averaged sediment transport through each channel alternative ranged from less than 1 m^3 for alternative A to about 1,000 m^3 for alternative C and was higher with greater discharge (fig. 37). Sediment transport was slightly higher under +1 m sea-level rise than for present sea level. The composition moved through each alternative was almost entirely silt. Only the 5-year flow was projected to transport appreciable amounts of sand (10–18 percent of the total), which was higher under current sea level than +1 m (fig. 37).

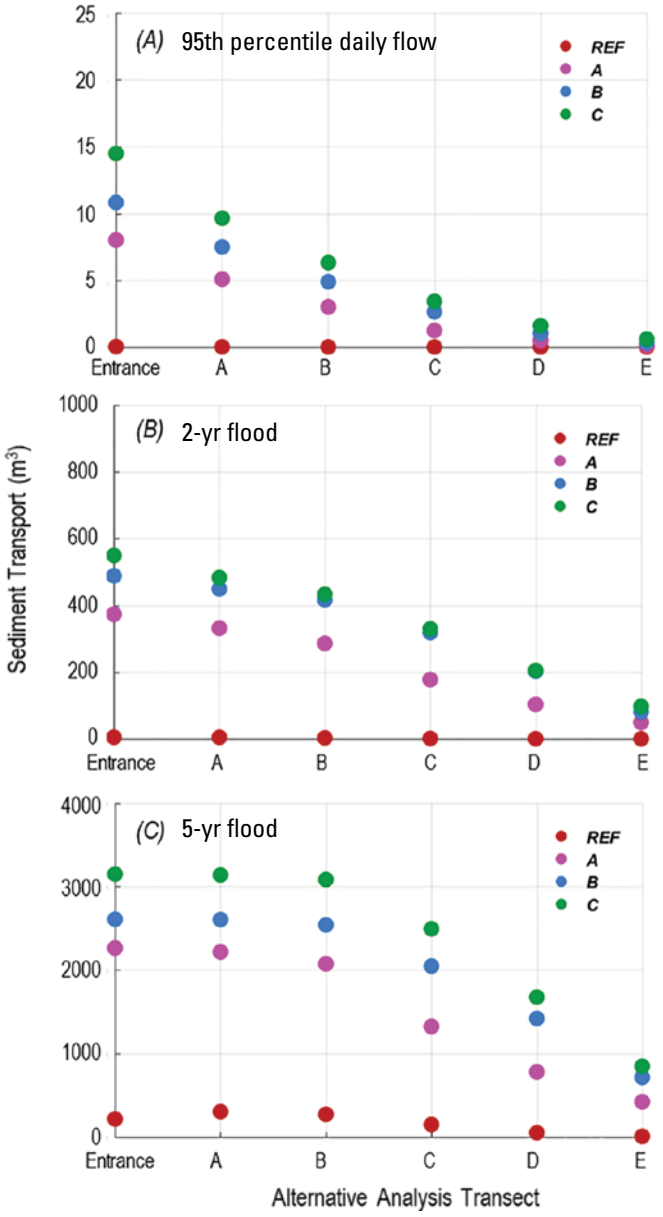

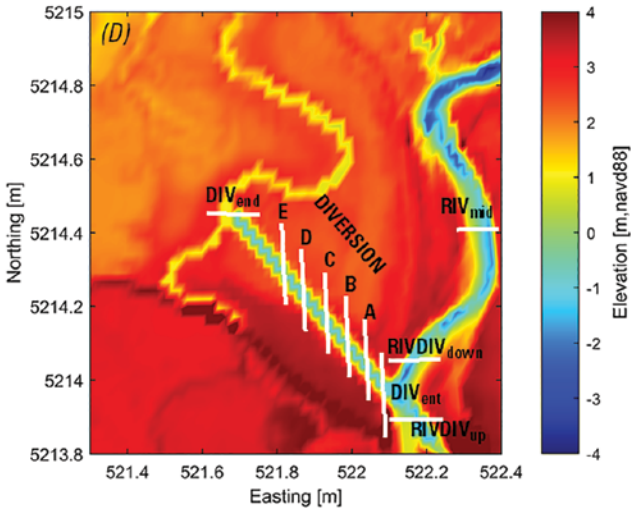

Figure 36. Graphs showing predicted sediment transport (in cubic meters [m^3]) across the five-channel analysis transects for the three identified alternatives A, B, and C for the 95th percentile daily flow (*A*), 2-year (*B*) and 5-year flood (*C*) along the alternative "diversion" shown in *D* (alternative C displayed). m, meter; NAVD88, North American Vertical Datum of 1988; yr, year.

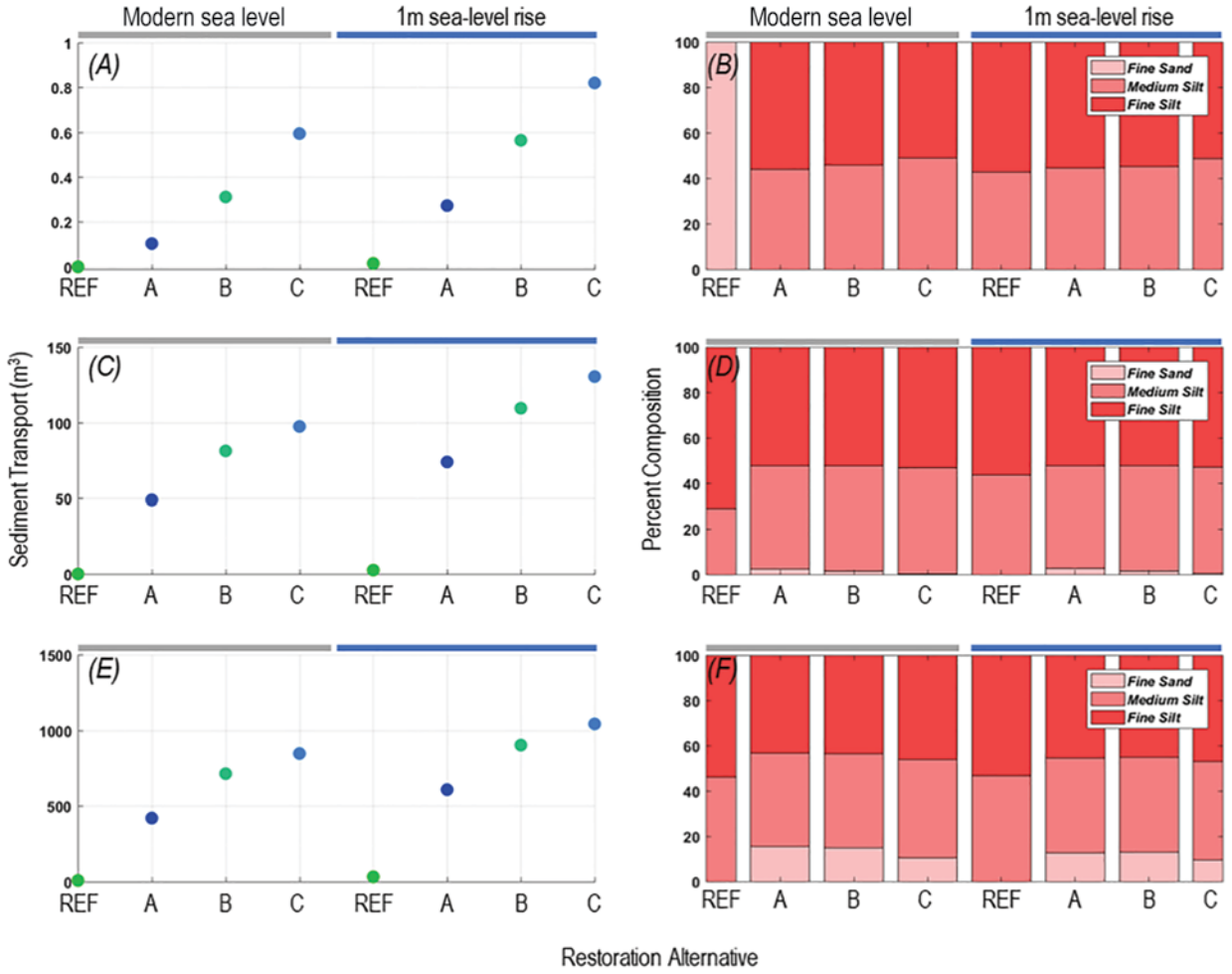

Figure 37. Graphs showing tidally averaged transport and percentage of composition of sediment through each identified alternative for modern sea level and with +1 m sea-level rise for discharges of the 95th daily percentile (*A*, *B*), 2-year (*C*, *D*), and 5-year flood flows (*E*, *F*). m, meter; m^3, cubic meters.

Relating the modeled transports into and through the channel alternatives to the amount of sediment delivered by the river is used to evaluate the routing and transport efficiency of each alternative. The model suggests that the routing efficiency of the identified channel alternatives are modest, ranging from 10 to 28 percent under high flows of the 2- and 5-year floods, but insignificant for lower daily and annual mean flows. Under the 2-year flood, the model suggests that from 10 to about 22 percent of the river sediment load can be routed into the restoration area via alternatives A, B, and C today and under +1 m of sea-level rise (fig. 38*A*). Similarly, for a 5-year flood simulation, about 2 to 30 percent of the river load is routed by the alternatives (fig. 38*C*). The overall low conveyance, however, revealed the transport efficiency of the alternatives is low and likely limiting to recovering sediment to the subsided restoration area. Modeled sediment transported through each alternative was less than 3 percent of the load delivered by the river for a 2-year flood today and up to 5 percent under 1 m of sea-level rise. Transport efficiency for the 5-year flood was marginally higher ranging from 4 to 8 percent for modern sea level and 5 to 10 percent under +1 m higher sea level (fig. 38*B*, *D*). The low overall sediment transport efficiency of these alternatives is consistent with the low hydraulic gradient near site NR2. The modest routing efficiency but low overall transport efficiency of the alternatives also suggests that most of the routed material would be retained in the channel and lead to sedimentation and aggradation. It remains uncertain and a goal of additional modeling to assess whether the hydrodynamics and sediment transport associated with proposed restoration alternatives would lead to steady filling of these low gradient channels or sufficient geomorphic change to maintain conveyance.

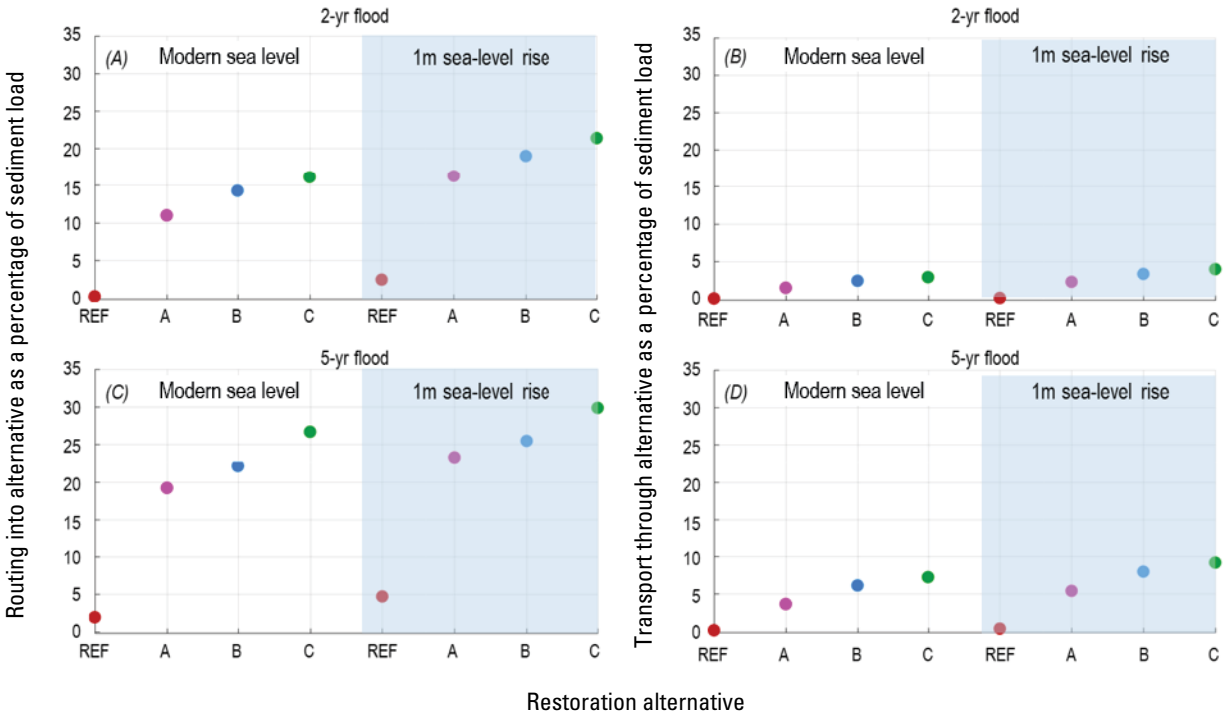

Figure 38. Graphs showing routing (*A*, *C*) and transport (*B*, *D*) efficiency of each channel alternative as a percentage of the sediment delivery for the 2-year (yr) flood (*A*, *B*) and 5-year flood (*C*, *D*) for modern sea level and with +1 meter (m) sea-level rise.

Implications for Restoration—Siting, Extent, Phasing, and Strategies

Guidance for estuary habitat recovery (for example, Clancy and others, 2009) rests on a paradigm of restoring historical habitats and connectivity by simply removing or lowering levees assuming sediment delivery and accumulation will occur. The sediment budget and routing modeling assessment of this study shows that restoring "opportunity" for sediment delivery may not be sufficient to achieve full recovery of the Nisqually River Delta or in a reasonable time frame. The study highlighted the sensitivity of estuary restoration outcomes to sediment availability and transport which are in turn affected by modified hydrodynamics and sediment dynamics in the drainage basin, coastal processes offshore, sediment properties, and the siting and extent of restoration. This study has important implications for estuary restoration including (1) siting within the tidal prism and with respect to sediment transport potential, (2) extent required to recover sediment supply given the geomorphic context, and (3) concerns related to phasing strategies to achieve marsh and estuary recovery efficiently and effectively.

Siting Restoration to Increase Sedimentation

This study indicates that restoration siting with respect to sediment transport potential is critical to achieve outcomes. The 2009 Brown's Farm Restoration area and identified adaptive management alternatives near site NR3 were located relatively low in elevation within the tidal range. As a result, sediment transport to the subsided marshes and broader 2009 restoration area with these alternatives relies significantly on tidal transport to move needed sediment onshore and higher in elevation. The limited frequency and capacity for flood tide transport of sediment upslope and the compounding effect of wave resuspension that contributes to sediment export significantly constrains sediment delivery and retention. The low potential to recover sediment supply with the existing and identified alternatives equate to long recovery time to build grade suitable for marsh succession which may add additional risk to recovery goals given the increasingly uncertain behavior but accelerating rate of sea level rise in the region.

The findings of this study suggest that a restoration sited higher in the system at the head of the delta (for example, along the I-5 Causeway) may be a more effective approach and investigations into the potential for more direct and greater routing of sediment from the Nisqually River are underway. Delivery of a larger proportion of the fluvial sediment load and at a higher rate would more effectively compensate for transport processes out of the restoration area and promote greater retention. Routing sediment to the head of the delta is expected to promote delta progradation into the area of maximum subsidence and delivery of additional coarser material given the higher hydraulic gradient that can withstand the bed shear stresses that lead to redistribution and export. Higher accumulation and lower recovery time are expected (fig. 33). The exponential nature of the recovery curve in figure 33 suggests that a greater amount of sediment recovered sooner can

help achieve full system recovery more effectively by restoring the subsided grade for marsh succession before sea-level rise accelerates. Restored marsh is suspected to also provide positive feedback to sedimentation (Lacy and others, 2020).

The findings of this study are corroborated by recent studies of estuary channel reconnections sited low in the tidal range like the 2012 Port Susan Bay estuary restoration that may promote sufficient sediment flux to maintain marsh today but not in the future, given the area's subsidence and projected increase in sea-level rise (Nowacki and Grossman, 2020). Similar to the elevation siting concerns of the 2009 Nisqually River and 2012 Port Susan Bay estuary restorations, location of such projects with respect to the ebb tidal flow path of the lower river are important. At Nisqually River, Port Susan Bay, and the 2015 Qwuloolt estuary restoration in the lower Snohomish (http://salishsearestoration.org/wiki/Qwuloolt_Restoration), the direction of ebb flow transport of potential fluvial sediment is away from the project areas instead of flowing through or across the project areas. The orientation of these types of restoration projects requires consideration in projects occurring on the updrift side of the ebb tidal transport pathway, which routes sediment away from the project area.

Extent of Restoration—To Breach or Notch and Role of Geomorphic Context

The extent of restoration and re-engineering required is critical to restoration success, recovery time, and cost. A question raised for this study was whether and to what extent restoration of sediment supply to recover marshes required full channel breach or partial notching. Partial notching is often preferred to reduce cost required to fully breach (for example, excavate levee to channel floor) and may reduce or retard the full brunt of large floods. Partial notching may only serve marsh recovery where it can affect sufficient sediment delivery; therefore, understanding the extent and relative variability in suspended sediment availability may be important. Hypothetically, full breach enhances desired sediment delivery by promoting greater conveyance of sediment to locations of interest for accumulation. Full breach also may facilitate a greater flux of coarser material to be transported in suspension or via bed load. Coarser sediment is important to build grade rapidly and be retained longer under post-depositional erosion processes than fine material because of its lower susceptibility to mobility and compaction. To address these concerns, in addition to the load of sediment delivered by the Nisqually River, focus was placed on evaluating the extent that suspended-sediment concentration and fraction of fines vary with depth. Improved understanding of the geomorphic context, in terms of the distribution of sediment in the water column, would help assess whether and to what extent sufficient sediment of suitable composition could be recovered via partial notching of a channel reconnection rather than full breach.

Depth Variability in Fluvial Sediment Availability

On three occasions during higher than normal river flows that ranged from 63 to 183 m^3/s, suspended-sediment samples were collected in multiple sets using the Equal Discharge Increment (EDI) method at 100, 50, and 10 percent depths (fig. 39*A*, *B*) to clarify if any notable difference exists in suspended sediment availability for notching to be an effective and sufficient sediment recovery approach. Although slight variability in suspended-sediment concentration and size was observed with depth, the system generally was well-mixed and more sensitive throughout the water column to hydrodynamic conditions (flows, tides) than to depth. Given that recovery time of at least 18 years is required even if 100 percent of the sediment available downstream from Alder Lake could be routed to the 2009 restoration area under existing conditions and the most effective alternatives (for example, alternative C), partial notching would further limit potential sediment conveyance. Notching may work in settings of sufficient sediment delivery and retention and where it can reduce redistribution during high flows that full breach may exacerbate.

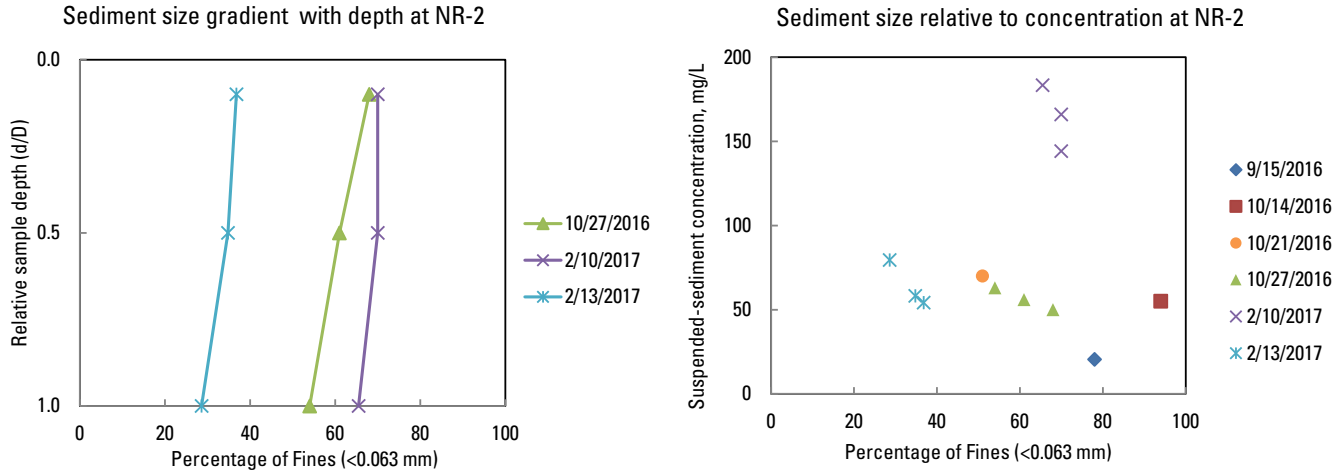

Figure 39. Graphs showing percentage of fine suspended sediment (silt and clay size <0.063 millimeter [mm]) of suspended-sediment samples collected at varying depths and times (*A*); percentage of fines relative to the suspended-sediment concentration of samples at varying depths and times (*B*). d/D, depth per total depth; mg/L, milligram per liter.

Phasing and Strategies for Restoration Effectiveness

The lengthy recovery times estimated to re-establish marsh habitat at the restoration site associated with low sediment flux and availability downstream from Alder Lake raise questions as to whether full ecosystem recovery could have been more efficiently achieved or now might benefit with alternative strategies or phasing actions. Adaptive management actions could include combinations of (1) additional distributary reconnections to fluvial sources higher in the system, (2) nourishment from external sources (for example, Thorne and others, 2019), and (3) erosion reduction or sediment trapping mechanisms in the form of added roughness, fencing, vegetation or berms (National Research Council, 2007). The latter would be especially important along the northern restoration boundary to reduce loss of sediment offshore of the restoration area, where similar features (for example, the outer ring dike) were removed in 2009. Although immediate ecosystem recovery gains in the form of tidal reconnection have led to increased salmon habitat use and productivity in the 2009 restoration area (David and others, 2014), the marsh habitat has not recovered as quickly or extensively as expected, leaving these gains vulnerable in the long term to erosion and sediment export through the northern part of the outer ring dike area.

In contrast to the removal of the entire outer ring dike in 2009 to restore tidal connectivity and fish access, a question remains as to what extent retaining the northern part or the entire outer ring dike would have promoted more efficient system recovery by reducing sediment export and enhancing retention for marsh development. The removal of the entire "outer" ring dike in 2009 was intended to demonstrate process-based restoration; however, the processes changed markedly since the dike was built in the late 1800s in response to the construction of the Alder Lake and the I-5 Causeway that restrict sediment flux. An extreme alternative might have included reconnection of the restoration area to the river only leaving most of the ring dike to trap as much sediment as possible. This may have taken 10–20 years and at the expense of early fish access but could have been expedited by sediment nourishment for a delay in full tidal connectivity of only a few years. An intermediate alternative may have been to restore connectivity for water, sediment, and fish between the restoration area and Nisqually River and McAllister Creek along the eastern and western boundaries, respectively, promoting greater net sediment retention balanced by moderate fish access and estuarine influence for tidal marsh development. Integrating our estimates of marsh recovery time and required sediment supply (fig. 33) with models of fish production by habitat area and type (for example, Beamer and others, 2005) may inform trade-off decisions and benefits associated with a range of potential ecosystem recovery trajectories.

Benefits of Restoration for Flood Hazard Reduction

The sensitivity of simulated water levels in the lower Nisqually River to restoration alternatives suggests that distributary channel reconnections may have benefits to reducing flood stage near the action and upstream. During moderate flows of 290 m^3/s, simulated water-level elevations declined as far as 0.5 km upstream from site NR2 with alternative C than for current conditions over a spring-neap tidal cycle (fig. 40*A–D*). Across this portion of the lower Nisqually River, water flow through alternative C led to a mean water-level elevation decline of 0.20–0.45 m for flows of 290 and 462 m^3/s, respectively, and a maximum water-level reduction of 0.25–0.55 m for a discharge of 462 m^3/s (fig. 40*E*). The results also suggest that restoration alternatives higher in the system (for example, through the I-5 causeway) also may decrease flood stage water levels given that tidal inundation extends above the modeled domain (fig. 22).

Summary

Refining our understanding and predictive models of sediment budgets, transport, and accumulation are important for determining the complex interactions of sediment in estuaries and potential outcomes of climate and land-use change, including ecosystem restoration. Through modeling and measurements, we evaluated the amount of sediment that is delivered by the Nisqually River to the Nisqually River Delta and the Billy Frank Jr. Nisqually National Wildlife Refuge and recently restored marshes important for salmon habitat and recovery. The study also examined the extent to which distributary channel restoration alternatives may help recover additional sediment accounting for variations in projected sea-level rise and streamflows. The model and measurements were used to evaluate the estuary sediment transport dynamics and the relative contributions of principal transport processes to sediment accumulation. We qualified elements of existing estuary restoration guidance and identified potential opportunities to enhance sedimentation where restoration efforts are challenged by land uses (for example, dams, levees) that limit sediment delivery and accelerating sea-level rise. Sufficient sediment delivery is important to ensure marshes keep up with sea-level rise and to realize investments in the 2009 Nisqually River Delta restoration.

Our findings indicate that the amount of sediment available downstream from Alder Lake and reaching the Nisqually River Delta is insufficient to recover the recently restored marshes, as about 20 years would be needed to fill subsided grade for marsh development and redirection and attenuation of the entire annual fluvial sediment load. Model results instead indicate that 7–32 percent of the annual fluvial sediment load accumulates in the restored marshes and that recovery time will likely be 85–200+ years depending on the rate of sea-level rise. The predicted sediment accumulation within the 2009 restoration area

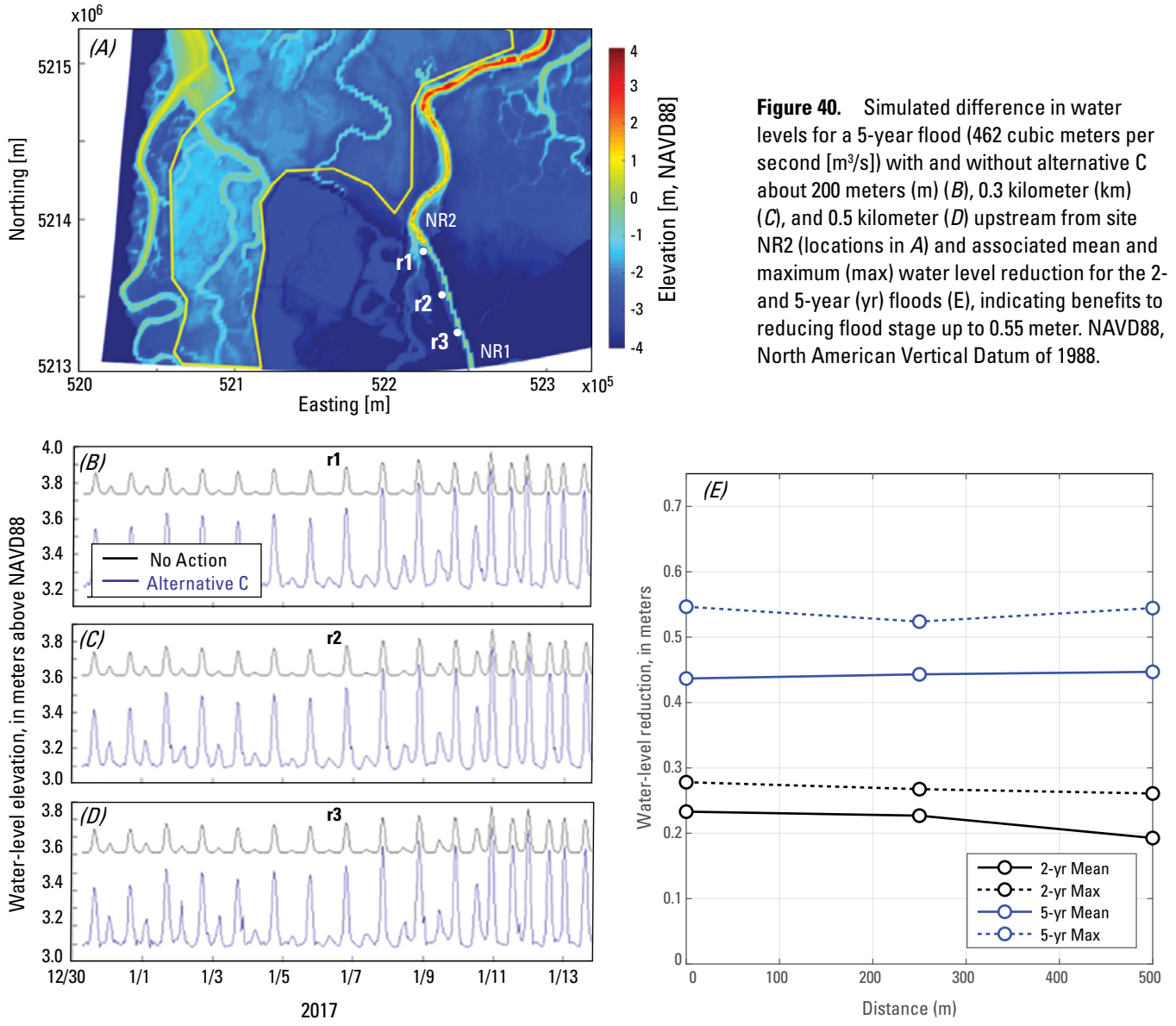

Figure 40. Simulated difference in water levels for a 5-year flood (462 cubic meters per second [m³/s]) with and without alternative C about 200 meters (m) (*B*), 0.3 kilometer (km) (*C*), and 0.5 kilometer (*D*) upstream from site NR2 (locations in *A*) and associated mean and maximum (max) water level reduction for the 2- and 5-year (yr) floods (E), indicating benefits to reducing flood stage up to 0.55 meter. NAVD88, North American Vertical Datum of 1988.

is consistent with recent independent sediment accumulation rates. The model results of three identified distributary channel restoration alternatives show that an additional 5–8 percent of the annual sediment supply could be delivered to the restoration area under present sea level and about 10–12 percent under 1 meter (m) higher sea level. The overall low potential for sediment flux of existing and proposed restoration alternatives suggests a need for adaptive management strategies focused on sediment recovery to achieve the investment goals made in the Nisqually River Delta.

The model showed that transport and accumulation of sediment is sensitive to fluvial sediment delivery, coastal processes, sediment properties, and siting and configurations of channels and restoration alternatives. Because the physical and transport properties of sediment are extremely variable and uncertain in coastal environments like the Nisqually River estuary, models bracketing the range of sediment properties were used to provide an envelope of uncertainty surrounding estimates of sediment flux, accumulation, and channel conveyance. The endmembers of the modeled sediment configurations were qualified for their suitability to predict the fate of fine sediment in the system. One model configuration (R1), suggesting extreme sediment export, is suspected to inaccurately characterize higher settling velocities and bed shear stress values of a large fraction of sediment in the estuary whereas a less mobile configuration (R4) showed moderate accuracy in areas dominated by sand. The model helped qualify the importance of fluvial sediment delivery relative to coastal processes, including winds, waves, and tidal currents, which redistribute sediment both into and out of the restoration area. Fluvial sediment input was the primary source of sediment to the delta and marshes, and winds and waves generally doubled the flux of sediment into the restored marshes in winter when fluvial sediment input is high. During summer, winds and waves can

drive 2–4 times more sediment into the marshes than delivered by the river, but summer river delivery represents only less than 5–10 percent of the annual delivery.

The study has important implications for estuary restoration in general and especially the Pacific Northwest where sediment runoff to the coast is high but compromised by land use in many watersheds and critical for the functioning and resilience of coastal ecosystems subject to a wide gradient in subsidence. The low overall sediment transport to and retention within the restored Nisqually River marshes is largely a result of implementing restoration low in the system relative to the tide range. This study showed that sediment recovery strategies sited low in the estuary tide range depend strongly on flood tide transport to move sediment upslope and can result in sediment deposition in settings frequently exposed to winds and waves that erode and export material. These findings suggest that siting distributary channel restoration higher in the system, where delivery to the head of the delta can promote progradation over subsided areas, is likely more effective to establish higher supply and potentially coarser material for added retention. In settings of low sediment delivery, distributary channel restoration strategies of partial notching are not favored over full breaching, which can convey more sediment. The importance of coastal processes in exporting sediment also indicates that adaptive management alternatives that enhance sediment supply from external sources (including nourishment) and that reduce export through trapping may be needed.

The considerable recovery times spanning 85–200+ years to recover lost grade and marshes raised the question as to whether full ecosystem recovery may be achieved more quickly by phasing efforts to first restore sufficient sediment supply to fully re-establish subsided grade and maintain lost marsh, before introducing tidal connectivity for fish, which exposes the area to winds, waves, and sediment export that prolong recovery. The modeling here suggests that increasing the delivery and retention of fluvial sediment to 50–80 percent of the annual river load could hasten marsh recovery to subsequently provide more comprehensive services to salmon and estuary productivity. Our modeling also indicates that restoration of delta distributary channels for enhancing conveyance and connectivity of water, sediment, and fish also provides benefits to reducing flood exposure by decreasing flood stage. The extent of this benefit with the identified alternatives ranged from 0.25 to 0.50 m along at least 1 river kilometer but was not entirely resolved and is the focus of a subsequent study with an expanded model.

References Cited

Allen, R.M., Lacy, J.R., and Stevens, A.W, 2021, Cohesive Sediment Modeling in a Shallow Estuary: Model and Environmental Implications of Sediment Parameter Variation: Journal of Geophysical Research Oceans, v. 126, no. 9, https://doi.org/10.1029/2021JC017219.

Ballanti, L., Byrd, K.B., Woo, I., and Ellings, C., 2017, Remote sensing for wetland mapping and historical change detection at the Nisqually River delta: Sustainability, v. 9, 1919, https://doi.org/10.3390/su9111919.

Barnhardt, W.A., and Sherrod, B.L., 2006, Evolution of a Holocene delta driven by episodic sediment delivery and coseismic deformation, Puget Sound, Washington, USA: Sedimentology, v. 53, no. 6, p. 1211–1228, https://doi.org/10.1111/j.1365-3091.2006.00809.x.

Barnosky, A.D., Hadly, E.A., Bascompte, J., Berlow, E.L., Brown, J.H., Fortelius, M., Getz, W.M., Harte, J., Hastings, A., Marquet, P.A., Martinez, N.D., Mooers, A., Roopnarine, P., Vermeij, G., Williams, J.W., Gillespie, R., Kitzes, J., Marshall, C., Matzke, N., Mindell, D.P., Revilla, E., and Smith, A.B. 2012, Approaching a state shift in Earth's biosphere: Nature, v. 486, p. 52–58, https://doi.org/10.1038/nature11018.

Beamer, E., Bernard, R., Hayman, B., Hebner, B., Hinton, S., Hood, G., Kraemer, C., McBride, A., Musslewhite, J., Smith, D., Wasserman, L., and Wyman, K., 2005, Skagit Chinook recovery plan: Burlington, Washington, Skagit River System Cooperative, 304 p., accessed June 13, 2022, at http://www.skagitcoop.org/.

Bortleson, G.C., Chrzastowski, M.J., and Helgerson, A.K., 1980, Historical changes of shoreline and wetland at eleven major deltas in the Puget Sound region, Washington: U.S. Geological Survey Hydrologic Investigations Atlas HA–617, 11 sheets, scale 1:24,000.

Clancy, M., Logan, I., Lowe, J., Johannessen, J., MacLennan, A., Van Cleve, F.B., Dillon, J., Lyons, B., Carman, R., Cereghino, P., Barnard, B., Tanner, C., Myers, D., Clark, R., White, J., Simenstad, C., Gilmer, M., and Chin, N., 2009, Management measures for protecting and restoring the Puget Sound nearshore: Washington Department of Fish and Wildlife, prepared in support of the Puget Sound Nearshore Ecosystem Restoration Project, Technical Report 2009-01, 307 p., accessed June 13, 2022, at https://wdfw.wa.gov/publications/02188.

Collins, B.D., and Montgomery, D.R., 2011, The legacy of Pleistocene glaciation and the organization of lowland alluvial process domains in the Puget Sound region: Geomorphology, v. 126, no. 1–2, p. 174–185, https://doi.org10.1016/j.geomorph.2010.11.002.

Curran, C.A., Grossman, E.E., Magirl, C.S., and Foreman, J.R., 2016a, Suspended sediment delivery to Puget Sound from the lower Nisqually River, western Washington, July 2010–November 2011: U.S. Geological Survey Scientific Investigations Report 2016–5062, 17 p., https://doi.org/10.3133/sir20165062.

Curran, C.A., Grossman, E.E., Mastin, M.C., and Huffman, R.L., 2016b, Sediment load and distribution in the lower Skagit River, Skagit County, Washington: U.S. Geological Survey Scientific Investigations Report 2016–5106, 24 p., https://doi.org/10.3133/sir20165106.

Czuba, J.A., Magirl, C.S., Czuba, C.R., Grossman, E.E., Curran, C.A., Gendaszek, A.S., and Dinicola, R.S., 2011, Sediment load from major rivers into Puget Sound and its adjacent waters: U.S. Geological Survey Fact Sheet 2011–3083, 4 p., https://doi.org/10.3133/fs20113083.

Czuba, J.A., Magirl, C.S., Czuba, C.R., Curran, C.A., Johnson, K.H., Olsen, T.D., Kimball, H.K., and Gish, C.C., 2012, Geomorphic analysis of the river response to sedimentation downstream of Mount Rainier, Washington: U.S. Geological Survey Open-File Report 2012–1242, 134 p., https://doi.org/10.3133/ofr20121242.

David, A.T., Ellings, C.S., Woo, I., Simenstad, C.A., Takekawa, J.Y., Turner, K.L., Smith, A.L., and Takekawa, J.E., 2014, Foraging and growth potential of juvenile Chinook salmon after tidal restoration of a large river delta: Transactions of the American Fisheries Society, v. 143, no. 6, p. 1515–1529, https://doi.org/10.1080/00028487.2014.945663.

Davis, B.E., 2005, A guide to the proper selection and use of federally approved sediment and water-quality samplers: U.S. Geological Survey Open-File Report 2005–1087, 26 p., https://doi.org/10.3133/ofr20051087.

Deltares, 2010, Delft3D-Flow User Manual (version 3.14): Deltares, Delft, The Netherlands.

Drexler, J.Z., Woo, I., Fuller, C.C., and Nakai, G., 2019, Carbon accumulation and vertical accretion in a restored versus historic salt marsh in southern Puget Sound, Washington, United States: Restoration Ecology, v. 27, no. 5, p. 1117–1127.

Ellings, C.S., Davis, M.J., Grossman, E.E., Woo, I., Hodgson, S., Turner, K.L., Nakai, G., Takekawa, J.E., and Takekawa, J.Y., 2016, Changes in habitat availability for outmigrating juvenile salmon (*Oncorhynchus* spp.) following estuary restoration: Restoration Ecology, v. 24, no. 3, p. 415–427.

ENSR International, 1999, Nisqually National Wildlife Refuge—Habitat management and restoration project—hydrodynamic and sediment transport model development: Redmond, Washington, ENSR International document no. 2334-011-800 [report prepared for Ducks Unlimited], 131 p.

Fresh, K.L., Dethier, M.N., Simenstad, C.A., Logsdon, M., Shipman, H., Tanner, C.D., Leschine, T.M., Mumford, T.F., Gelfenbaum, G., Shuman, R., and Newton, J.A., 2011, Implications of observed anthropogenic changes to the nearshore ecosystems in Puget Sound: Washington Department of Fish and Wildlife, prepared for the Puget Sound Nearshore Ecosystem Restoration Project, Technical Report 2011-03, 34 p., accessed July 20, 2021, at https://wdfw.wa.gov/sites/default/files/publications/02183/wdfw02183.pdf.

Glysson, G.D., 1987, Sediment-transport curves: U.S. Geological Survey Open-File Report 87–218, 47 p.

Grossman, E.E., Stevens, A.W., Dartnell, P., George, D., and Finlayson, D., 2020, Sediment export and impacts associated with river delta channelization compound estuary vulnerability to sea-level rise, Skagit River Delta, Washington, USA: Marine Geology, v. 430, https://doi.org/10.1016/j.margeo.2020.106336.

Lacy, J.R., Foster-Martinez, M.R., Allen, R.M., Ferner, M.C., and Callaway, J.C., 2020, Seasonal variation in sediment delivery across the bay-marsh interface of an estuarine salt marsh: Journal of Geophysical Research Oceans, v. 125, no. 1, https://doi.org/10.1029/2019JC015268.

Lesser, G.R., Roelvink, J.A., van Kester, J.A.T.M., and Stelling, G.S., 2004, Development and validation of a three-dimensional morphological model: Coastal Engineering, v. 51, nos. 8–9, p. 883–915.

Levesque, V.A., and Oberg, K.A., 2012, Computing discharge using the index velocity method: U.S. Geological Survey Techniques and Methods, book 3, chap. A23, 148 p. [Also available at http://pubs.usgs.gov/tm/3a23/]

Miller, I.M., Morgan, H., Mauger, G., Newton, T., Weldon, R., Schmidt, D., Welch, M., and Grossman, E., 2018, Projected sea-level rise for Washington State—A 2018 assessment: A collaboration of Washington Sea Grant, University of Washington Climate Impacts Group, Oregon State University, University of Washington, and U.S. Geological Survey, prepared for the Washington Coastal Resilience Project, accessed June 13, 2022, at https://cig.uw.edu/resources/special-reports/sea-level-rise-in-washington-state-a-2018-assessment/.

Miller, I.M., Yang, Z., vanArendonk, N., Grossman, E., Mauger, G.S., and Morgan, H., 2019, Extreme coastal water level in Washington State—Guidelines to support sea level rise planning. A collaboration of Washington Sea Grant, University of Washington Climate Impacts Group, Oregon State University, University of Washington, Pacific Northwest National Laboratory, and U.S. Geological Survey. Prepared for the Washington Coastal Resilience Project. accessed June 13, 2022, at https://cig.uw.edu/publications/extreme-coastal-water-level-in-washington-state-guidelines-to-support-sea-level-rise-planning/.

Mueller, D.S., Wagner, C.R., Rehmel, M.S., Oberg, K.A., and Rainville, F., 2013, Measuring discharge with acoustic Doppler current profilers from a moving boat (ver. 2.0, December 2013): U.S. Geological Survey Techniques and Methods, book 3, chap. A22, 95 p. [Also available at https://dx.doi.org/10.3133/tm3A22/]

National Research Council, 2007, Mitigating shore erosion along sheltered coasts: Washington, DC, The National Academies Press, https://doi.org/10.17226/11764.

Nelson, L.M., 1974, Sediment transport by streams in the Deschutes and Nisqually River basins, Washington, November 1971–June 1973: U.S. Geological Survey Open-File Report 74–1078, 33 p.

Nowacki, D.J., and Grossman, E.E., 2020, Sediment transport in a restored, river-influenced Pacific Northwest estuary: Estuarine, Coastal and Shelf Science, v. 242, https://doi.org/10.1016/j.ecss.2020.106869.

Oberg, K.A., Morlock, S.E., and Caldwell, W.S., 2005, Quality assurance plan for discharge measurements using acoustic doppler current profilers: U.S. Geological Survey Scientific Investigations Report 2005–5183, 35 p.

Opatz, C.C., Curran, C.A., Tecca, A.E., and Grossman, E.E., 2019, Stage, water velocity and water quality data collected in the Lower Nisqually River, McAllister Creek and tidal channels of the Nisqually River Delta, Thurston County, Washington, February 11, 2016 to September 18, 2017 (ver. 1.1, December, 2019): U.S. Geological Survey data release, https://doi.org/10.5066/F7GF0SG7.

Partheniades, E., 1965, Erosion and deposition of cohesive soils: Journal of the Hydraulics Division, v. 91, no. 1, p. 105–139.

Porter, S.C., and Swanson, T.W., 1998, Radiocarbon age constraints on the rates of advance and retreat of the Puget Lobe of the Cordilleran Ice sheet during the last Glaciation: Quaternary Research, v. 50, no. 3, p. 205–213, https://doi.org/10.1006/qres.1998.2004.

Porterfield, G., 1972, Computation of fluvial-sediment discharge: U.S. Geological Survey Techniques of Water-Resource Investigations, book 3, chap. C3, 66 p.

Puget Sound Lidar Consortium, 2021, Public-domain high-resolution topography for the Pacific Northwest: Web page, accessed July 29, 2021, at https://pugetsoundlidar.ess.washington.edu/.

Rasmussen, P.P., Gray, J.R., Glysson, G.D., and Ziegler, A.C., 2009, Guidelines and procedures for computing time-series suspended-sediment concentrations and loads from in-stream turbidity-sensor and streamflow data: U.S. Geological Survey Techniques and Methods, book 3, chap. C4, 52 p.

Simenstad, C.A., Ramirez, M., Burke, J., Logsdon, M., Shipman, H., Tanner, C., Toft, J., Craig, B., Davis, C., Fung, J., Bloch, P., Fresh, K., Myers, D., Iverson, E., Bailey, A., Schlenger, P., Kiblinger, C., Myre, P., Gerstel, W., and MacLennan, A., 2011, Historical change of Puget Sound shorelines: Puget Sound Nearshore Ecosystem Project Change Analysis, Puget Sound Nearshore Report No. 2011-01, Washington Department of Fish and Wildlife, Olympia, Washington, and U.S. Army Corps of Engineers, Seattle, Washington, accessed June 13, 2022, at https://wdfw.wa.gov/sites/default/files/publications/02186/wdfw02186.pdf.

Steffen, W., Richardson, K., Rockström, J., Cornell, S.E., Fetzer, I., Bennett, E.M., Biggs, R., Carpenter, S.R., de Vries, W., de Wit, C.A., Folke, C., Gerten, D., Heinke, J., Mace, G.M., Persson, L.M., Ramanathan, V., Reyers, B., and Sörlin, S., 2015, Planetary boundaries—Guiding human development on a changing planet: Science, v. 347, no. 6223, p. 1–10.

Thorne, K.M., Freeman, C.M., Rosencranz, J.A., Ganju, N.K., and Guntenspergen, G.R., 2019, Thin-layer sediment addition to an existing salt marsh to combat sea-level rise and improve endangered species habitat in California, USA: Ecological Engineering, v. 136, p. 197–208, https://doi.org/10.1016/j.ecoleng.2019.05.011.

Tyler, D.J., Danielson, J.J., Grossman, E.E., and Hockenberry, R.J., 2020, Topobathymetric model of Puget Sound, Washington, 1887 to 2017: U.S. Geological Survey data release, https://doi.org/10.5066/P95N6CIT.

U.S. Environmental Protection Agency, 2005, National Coastal Condition Report II: U.S. Environmental Protection Agency, Office of Research and Development/Office of Water, Washington, DC 20460, EPA-620/R-03/002, December 2004.

U.S. Geological Survey, 2022, USGS water data for the Nation: U.S. Geological Survey National Water Information System database, http://dx.doi.org/10.5066/F7P55KJN, accessed May 25, 2022, at https://waterdata.usgs.gov/nwis.

van der Wegen, M., Jaffe, B.E., and Roelvink, J.A., 2011, Process-based, morphodynamic hindcast of decadal deposition patterns in San Pablo Bay, California, 1856–1887: Journal of Geophysical Research, v. 116, no. F2, 22 p.

van Rijn, L.C., 2007a, Unified view of sediment transport by currents and waves—I: Initiation of motion, bed roughness, and bed-load transport: Journal of Hydraulic Engineering, v. 133, no. 6, p. 649–667.

van Rijn, L.C., 2007b, Unified view of sediment transport by currents and waves—II: Suspended transport: Journal of Hydraulic Engineering, v. 133, no. 6, p. 668–689.

van Rijn, L.C., and Walstra, D.J.R., 2004, Description of TRANSPOR2004 and Implementation in Delft3D-Online (Report Z3748): Deltares WL, Delft Hydraulics, Delft, The Netherlands, accessed July 17, 2021, at https://repository.tudelft.nl/islandora/object/uuid%3Aea12eb20-aee3-4f58-99fb-ebc216e98879.

Webster, K.L., Ogston, A.S., and Nittrouer, C.A., 2013, Delivery, reworking and export of fine-grained sediment across the sandy Skagit River tidal flats: Continental Shelf Research, v. 60S, p. S58–S70.

Woo, I., Davis, M.J., Ellings, C.S., Nakai, G., Takekawa, J.Y., De La Cruz, S. 2018, Enhanced invertebrate prey production following estuarine restoration supports foraging for multiple species of juvenile salmonids (*Oncorhynchus* spp.): Restoration Ecology, v. 26, no. 5, p. 964–975, https://doi.org/10.1111/rec.12658.

Moffett Field Publishing Service Center
Manuscript approved September 26, 2022
Edited by Kathryn Pauls
Illustration support by JoJo Mangano
Layout by Cory Hurd

USGS

Grossman and others—Assessment of Vulnerabilities and Opportunities to Restore Marsh Sediment Supply at Nisqually River Delta—Open-File Report 2022–1088

ISSN 2331-1258 (online)
https://doi.org/10.3133/ofr20221088